

Regulation Mechanisms of the Ubiquitin C-terminal Hydrolases UCH-L5 and BAP1

Danny D. Sahtoe

ISBN/EAN: 978-94-6233-075-7.

Publisher: Het Nederlands Kanker Instituut - Antoni van Leeuwenhoek Ziekenhuis.

Printing: Gildeprint.

Cover & layout: Danny D. Sahtoe.

Copyright © 2015 by Danny D. Sahtoe. All rights reserved.

This thesis was printed with financial support from Erasmus University Rotterdam and the Netherlands Cancer Institute.

Regulation Mechanisms of the Ubiquitin C-terminal Hydrolases UCH-L5 and BAP1

Regulatie mechanismen van de ubiquitine C-terminale hydrolasen
UCH-L5 en BAP1

Thesis

to obtain the degree of Doctor from the
Erasmus University Rotterdam
by command of the
rector magnificus

Prof.dr. H.A.P. Pols

and in accordance with the decision of the Doctorate Board.

The public defence shall be held on
Wednesday the 4th of november 2015 at 09:30 hrs
by

Danny Dinesh Sahtoe
born in Den Haag

Doctoral Committee:

Promotor: Prof.dr. T.K. Sixma

Other members: Dr. H. Van Attikum

Prof.dr. R. Kanaar

Prof.dr. C.P. Verrijzer

Table of contents

Chapter 1	General introduction	7
Chapter 2	Layers of DUB regulation	21
Chapter 3	Mechanism of UCH-L5 activation and inhibition by DEUBAD domains in RPN13 and INO80G	43
Chapter 4	BAP1/ASXL1 recruitment and activation for H2A deubiquitination	81
Chapter 5	Characterization of the oligomeric state of the BAP1/ASXL1 complex	113
Chapter 6	General discussion	127
Addendum	Summary	136
	Samenvatting	138
	Curriculum vitae	140
	PhD Portfolio	141
	List of publications	142
	Dankwoord	143

chapter | ONE

General introduction

Ubiquitin conjugation

A defining feature of eukaryotic life is regulation of molecular processes. In many cases these regulatory effects are mediated through post-translational modifications (PTMs). One of these PTMs is ubiquitination. Ubiquitin is a small 76 aa protein that is highly conserved in eukaryotes differing only by three amino acids between yeast and humans. The molecular structure of ubiquitin is compact and features a globular β -grasp fold followed by an extended C-terminal tail ending with a Gly-Gly motif.

During the process of ubiquitination the C-terminal Gly76 residue of ubiquitin is covalently attached to the ϵ -amino group of a lysine residue on target proteins forming a stable isopeptide bond. The modification is reversible and can be cleaved off by deubiquitinating enzymes (DUBs)^{1,2}. This seemingly simple PTM has far reaching ramifications in cells. It can mediate signal transduction, change the stability of target proteins, their enzymatic activity, their subcellular localization and can even serve as a seed for the assembly of new macromolecular complexes. Examples of ubiquitination and their effects are mono-ubiquitination of PCNA as a signal for DNA damage, ubiquitination of the DUB ATXN3 increases its rate, and the assembly of the BRCA-A complex to sites of DNA damage as a result of ubiquitination events³⁻⁵. The ubiquitin mark is pervasive in cells, and has been observed in systems ranging from the cell cycle and gene regulation to DNA repair and endocytosis⁵⁻⁸.

Mechanistically ubiquitin conjugation proceeds via a three-step enzymatic cascade that has been extensively studied in the past decades (Figure 1)⁹. Because the C-terminal Gly76 of ubiquitin is unreactive as such, it first requires activation by E1 activating enzymes Uba1 or Uba6 through adenylation of the C-terminus at the expense of one ATP molecule. Subsequently the reactive ubiquitin-adenylate moiety is transferred to the active site cysteine of the E1 resulting in an E1-ubiquitin thioester intermediate. In the second major step, one of several dozens of E2 ubiquitin conjugating enzymes binds the E1 after which ubiquitin is transferred to the active site cysteine of the E2 in a transthioesterification reaction forming a E2-ubiquitin thioester.

Ubiquitin E3 ligases catalyze the transfer of ubiquitin from E2-ubiquitin thioesters to the target protein via three divergent mechanisms. The RING/U-box class of E3 ligases allosterically promotes ubiquitin transfer from E2's to targets. This class of proteins were long thought to merely function as scaffolds that bridge the E2-ubiquitin thioester and target. In recent years it has become clear however that they are active catalysts that bind the E2-ubiquitin thioester and stabilize a reactive conformation to allow efficient attack by the lysine residue on the target protein¹⁰⁻¹⁴. In the HECT class of E3 ligases, ubiquitin is first transferred to the active site cysteine of the HECT enzyme in another transthioester-

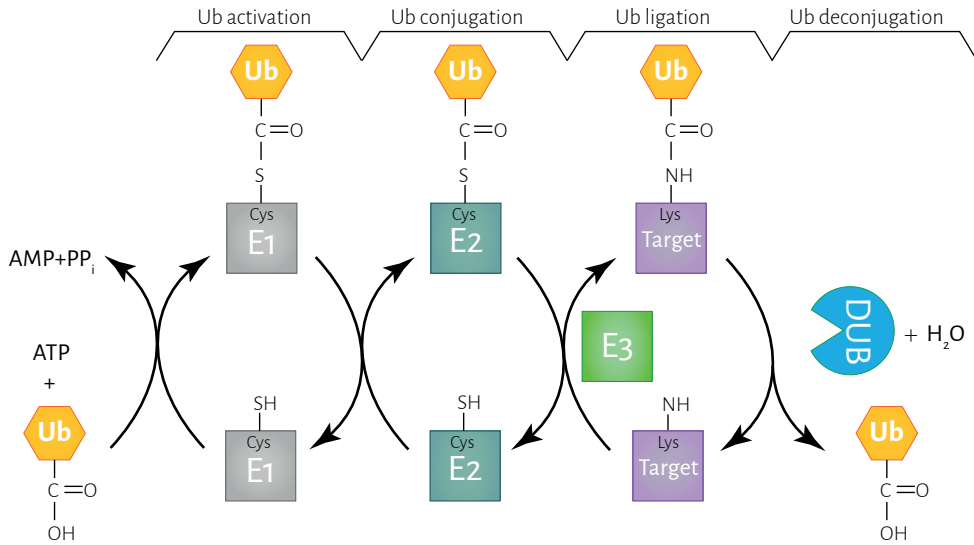


Figure 1 | The ubiquitin system. Ubiquitin conjugation to a target protein is an ATP dependent three-step process requiring an E1 activating enzyme, E2 conjugating enzyme and E3 ligase. Deubiquitinating enzymes (DUBs) reverse the modification.

ification reaction before being ligated to the target protein¹⁵. The RBR class of E3 ligases employ a hybrid RING/HECT mechanism to ubiquitinate targets¹⁶⁻¹⁸.

Thousands of different target proteins are ubiquitinated. In mono-ubiquitination a single ubiquitin is attached to a target, while in polyubiquitination, multiple mono-ubiquitins or polymeric ubiquitin chains are conjugated to targets (Figure 2). Polyubiquitin chains arise when ubiquitin itself is ubiquitinated. This occurs on one of the seven lysines or on the N-terminal amino group of ubiquitin. In this way, eight different linkages of ubiquitin chains can be formed. Recent research indicates that “mixed” chains, consisting of different linkage types in the same polymer, can also be generated¹⁹. All chain types form distinct structures and are associated with specific cellular processes. Most famously, proteins modified with ubiquitin chains linked through lysine 48 (K48 chains) destined them for proteasomal destruction while K63 and ‘linear’ Met1 linked chains have potent signaling functions^{20,21}. Mixed K48/K11 chains enhance proteasomal degradation of some targets¹⁹.

The formation of polyubiquitin chains makes ubiquitination more versatile but also more complex than for example phosphorylation since different signals can be generated with the same molecule. To be able to decode these ubiquitin signals, cells use a multitude of ubiquitin binding domains that can specifically bind different ubiquitin-conjugates and thus “read” the signal (Figure 2). Among them are ubiquitin binding-in-ABIN-and-NEMO domains (UBAN), ubiquitin interacting motifs (UIM), ubiquitin associated domains (UBA) and some zinc fingers²². They generally bind free ubiquitin with low affinity but have high-

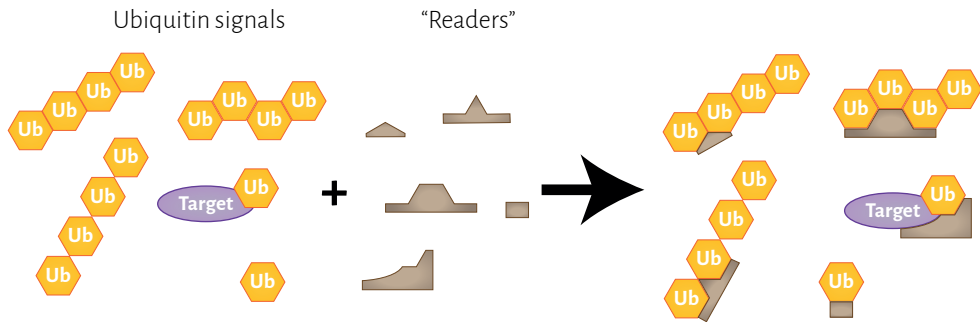


Figure 2 | Ubiquitin signals and readers. Ubiquitin can be conjugated non-ubiquitin proteins (magenta) or to itself giving rise to different polyubiquitin chain types. These different chains represent distinct signals. Several ubiquitin binding domains (brown) can specifically “read” the different ubiquitin signals.

er affinities for polyubiquitin chains through avidity effects. These domains can be very specific and discriminate between different chain types²².

Polyubiquitin chains are of great importance in ubiquitin biology as they are responsible for the assembly and localization of important complexes. The DNA double strand break response for example depends on K63 polyubiquitin chains and binding domain recognizing them²⁰. Similarly NF- κ B completely depends on “reading” of linear Met1-linked polyubiquitin²³.

Ubiquitin deconjugation

Ubiquitin signals can be dampened or completely reversed by DUBs (Figure 1) enabling these isopeptidases to control all aspects of the ubiquitin-system. Being able to deubiquitinate proteins is useful for cells as it allows for rapid response to challenges and allows recycling of proteins instead of resynthesizing unmodified proteins. The importance of proper DUB function is evident from the high incidence of DUB deregulation in various neurological diseases and cancers^{2,24}. Also, in certain infectious diseases, pathogens hijack host DUBs or encode their own DUBs to disable host defense systems and promote infection²⁵. Because of these roles, DUBs are currently pursued as potential drug targets.

The human genome encodes around 100 DUBs and based on the structure of their catalytic domains DUBs are subdivided in five families: the ubiquitin C-terminal hydrolase (UCH), ubiquitin specific protease (USP), ovarian tumor protease (OTU), Machado-Joseph disease (MJD) and jab1/mov34/mpn (JAMM) families^{1,2} (Figure 3). While the first four are cysteine proteases the JAMM family members are metallo-isopeptidases that depend on Zinc ions for catalysis.

The JAMM domain DUBs are structurally related to JAB domains found in bacteria, which are hypothesized to function as deconjugating enzymes for ancient ubiquitin-like

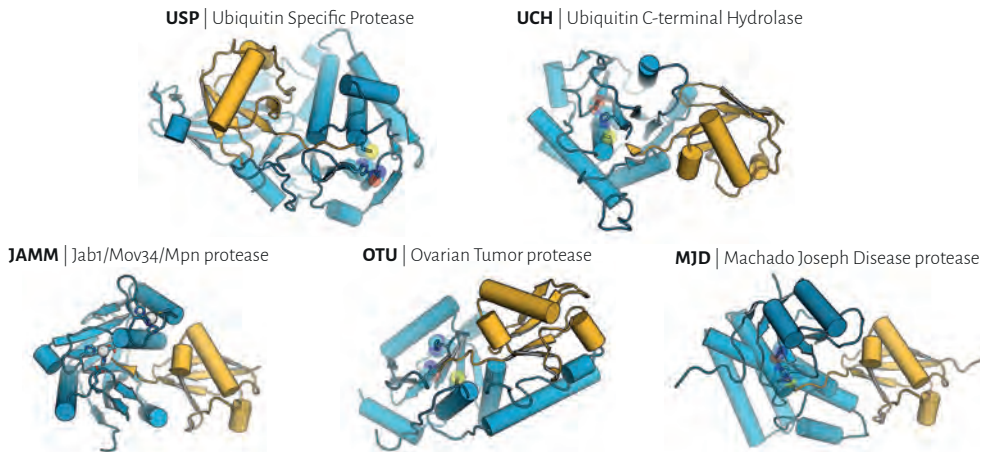


Figure 3 | The deubiquitinating enzymes (DUBs). Representatives (blue) for each DUB family bound to ubiquitin (gold) are depicted. We distinguish five sub families of DUBs: UCH, USP, MJD, OTU and JAMM. The first four are cysteine proteases while the JAMM family has metallo-protease activity.

pathways²⁶. A common characteristic of the cysteine dependent DUBs is that all of these bear structural resemblance to papain-like proteases and are hence thought to share their catalytic mechanism with papain-like enzymes.

Chemically, all DUBs are hydrolases that utilize a water molecule in conjunction with an active site to break the isopeptide bond between ubiquitin and the target. The actual catalytic mechanism is different between metallo and cysteine dependent DUBs. In case of the UCH class, the enzymes that are the focus of this thesis, the reaction is initiated by deprotonation of the active site cysteine (Figure 4). This is achieved by a histidine general base that is coordinated by an asparagine or aspartic acid and gives rise to cysteine thiolate. This increases the reactivity of the cysteine for a nucleophilic attack on the carbonyl carbon of the scissile bond resulting in a tetrahedral oxyanion transition state. The negative charge of the transition state is stabilized by an “oxyanion hole” that facilitates the collapse of the transition state releasing the formerly ubiquitinated substrate as the leaving group. At this point the DUB is still covalently linked to ubiquitin and a second nucleophilic attack is required by a water molecule to regenerate the enzyme as well as free ubiquitin (Figure 4).

The general functions of DUBs are diverse^{1,2}. An important one is ubiquitin processing. Since ubiquitin is produced as a head to tail polyprotein DUBs are required to hydrolyze polyubiquitin into free ubiquitin ready for use in cells. DUBs are also necessary for ubiquitin recycling of K48 polyubiquitin chains that were attached to proteins that are degraded by the proteasome. Similarly, DUBs can liberate ubiquitin from the numerous of small polyamines in cells that can be adventitiously conjugated to ubiquitin. Aside from these

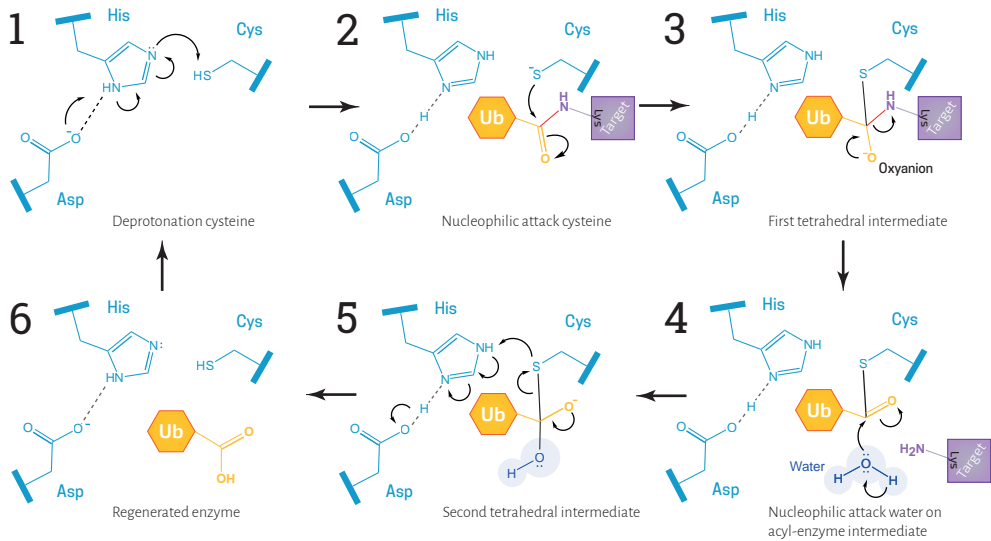


Figure 4 | Proposed reaction mechanism of cysteine protease DUBs. The hydrolysis of an isopeptide bond between ubiquitin (gold) and a target lysine (magenta) requires a catalytic triad consisting of a cysteine, histidine and aspartic acid or asparagine (blue). The reaction is initiated by the abstraction of a hydrogen from the cysteine by the histidine general base (1) increasing the nucleophilicity of the cysteine. After the nucleophilic attack of the cysteine on the scissile bond (red line), a tetrahedral intermediate forms featuring an oxyanion (2,3) that soon collapses to give rise to an acyl-enzyme intermediate (4) while releasing the formerly ubiquitinated substrate. The enzyme is regenerated by nucleophilic attack of a water molecule (4,5,6).

general house-keeping roles DUBs have more specific functions by controlling ubiquitination events in almost all cellular pathways including endosomal sorting, DNA repair, gene regulation, RNA processing and the cell cycle.

Regulation of DUBs

Most DUBs are multi-domain proteins that in addition to the catalytic domain contain a large variety of other domains. *In vitro* studies comparing the activity of CD's to full length DUBs have uncovered that these additional domains can sometimes allosterically modulate the catalytic activity of the CD²⁷⁻³¹. In most cases, these domains activate the CD. Besides this type of intramolecular regulation, the catalytic activity of DUBs is also often directly governed by external proteins. Regulation does not always necessarily directly impinge on catalysis but may also guide DUBs to the correct cellular compartments or substrates. This can also be achieved by either intramolecular domains or external factors.

Because DUBs are generally considered to be relatively unspecific enzymes their tight regulation may be regarded as a safeguard mechanism for the cell that protects it from aberrant deubiquitination. As such, the DUB regulators are powerful accessory components of the ubiquitin-system. In chapter 2, different layers of DUB regulation are discussed in depth. A clear understanding of these mechanisms can assist in identifying

crucial elements of DUB activity and in the development of targeted therapy.

The central theme in this thesis is to understand the molecular mechanisms that underlie these regulatory processes, particularly in the UCH family of DUBs.

UCH-L5

UCH-L5 (UCH37) is a member of the UCH family of DUBs. The protein is 329 aa and consists of an N-terminal catalytic UCH domain followed by an extended helical domain called the ULD³². UCH-L5 knock-out is embryonically lethal in mice and its function is perturbed in a number of different human cancers such as esophageal and hepatocellular carcinomas³³⁻³⁶.

UCH-L5 functions in several cellular systems. In TGF- β signaling it has been reported to deubiquitinate TGF- β receptor type I through association with SMAD7³⁷. In addition to this, UCH-L5 is part of two very different large molecular assemblies, the proteasome and the INO80 chromatin remodeling complex where its activity is tightly regulated³⁸⁻⁴¹.

In the proteasome, UCH-L5 is a non-essential component that resides in the 19S regulatory particle and associates with the RPN13 subunit. This interaction activates UCH-L5 on minimal substrates^{42,43} and is thought to be important for K48 polyubiquitin hydrolysis by UCH-L5. This activity is proposed to rescue some poorly ubiquitinated substrates from proteasomal degradation⁴⁴. RPN13 consists of an N-terminal Pru domain that is responsible for polyubiquitin binding while its C-terminal domain binds UCH-L5^{45,46}.

In animals UCH-L5 is present in an animal-specific sub-module of the INO80 chromatin remodeling complex along with YY1 and INO80G (NFRKB)³⁸. However, in this complex, UCH-L5 is inhibited by association with an N-terminal fragment of the INO80G subunit. This complex has an important role in the DNA damage response (DDR) by regulating DNA end resection⁴⁷. The inhibition of UCH-L5, when it is bound to INO80G, stands in stark contrast to the activation of UCH-L5 in the proteasome. INO80G itself has furthermore been identified as an important determinant for stem cell identity⁴⁷⁻⁴⁹.

BAP1

BRCA-1 associated protein 1 (BAP1) is a 729 aa UCH enzyme that was originally identified as a BRCA-1 interactor in a yeast-2-hybrid screen⁵⁰. It is closely related to UCH-L5. Together with the N-terminal UCH domain, BAP1 and UCH-L5 also share the ULD domain that is located at the C-terminus of BAP1. BAP1 however also contains an approximately 350 aa insert relative to UCH-L5 situated between the CD and ULD domains. This insert is predicted to be disordered and bears no sequence resemblance to annotated conserved domains.

In recent years, BAP1 has risen to prominence due to its frequent disruption in several cancers such as renal, pleural mesothelioma's and uveal cancers⁵¹⁻⁵⁷. In many of these cancers BAP1 strongly correlates with poor survival. Moreover families have been described with germline BAP1 mutations where affected members are predisposed to a variety of cancers that are described collectively as the BAP1 cancer syndrome⁵⁸. BAP1 is a tumor suppressor but little is currently known about the molecular carcinogenesis of BAP1 de-regulation.

Several studies in the past years have started to shed some light on BAP1's tumor suppressor activity. In these studies, BAP1 has emerged as a pivotal regulator of chromatin associated processes including DNA repair, DNA replication and gene expression. In these processes BAP1 is often present in large multi-protein complexes with proteins such as ASXL1, ASXL2, KDMB1B, HCF-1, YY1, MBD5, MBD6, OGT and FOXK2^{54,59-63}.

A recent DNA repair screen identified BAP1 as one of a select subset of DUBs that both localizes to DNA damage sites and gives DNA repair defects if perturbed⁴⁷. Although BAP1's role in this pathway has not been clearly resolved, another study indicates that BAP1 is necessary for the assembly of RAD51 and BRCA1 at damage foci⁶⁴. BAP1 knock-out led to a variety of defects including increased frequency of chromosomal breaks after DNA damage⁶⁴.

In addition to DNA repair BAP1 also has roles in DNA replication. For instance, BAP1 prevents proteasomal degradation of Ino80, a key chromatin remodeler required for the progression of DNA replication⁶⁵. The importance of this function is highlighted by the low Ino80 protein levels in BAP1 defective mesothelioma cells⁶⁵. Similar to Ino80, BAP1 also stabilizes the transcriptional regulator HCF-1 by deubiquitinating it through the formation of a ternary complex that also includes the transcription factor YY1. This complex increases the expression of COX7C, an essential mitochondrial protein^{59,62}. As HCF-1 is known as an important factor controlling cell cycle progression, BAP1 may also contribute to this process⁶⁶.

BAP1 also functions in Polycomb gene repression. In *Drosophila*, BAP1 associates with the Polycomb group protein ASX (ASXL1 in humans) to form the evolutionarily conserved Polycomb Repressive DUB⁶³. In this complex, ASX activates BAP1 to deubiquitinate mono-ubiquitinated H2A at lysine 119, an epigenetic mark for gene repression. Paradoxically, both the generation of K119 mono-ubiquitination, by the E3 ligase RING1B/BMI1, and removal of this repressive mark by BAP1 are required for the repression of genes.

In general, to what extent the different BAP1 functions are intertwined is unclear. In some cases though, there may be functional connections. For instance the recruitment of BAP1

to certain genomic loci by transcription factor FOXK2 locally stimulates H2A deubiquitination suggesting that ASXL1 is also involved⁶⁰. Similarly deubiquitination of HCF-1 by BAP1 has been suggested to occur in a multi-protein complex also including activator ASXL1 or ASXL2 and OGT⁵⁴.

Common ancestry of UCH-L5 and BAP1 regulators

The UCH-L5 and BAP1 regulators, RPN13, INO80G and ASXL1 are large and diverse proteins consisting of different domains. A common feature between them is, however, that all three contain a conserved stretch of about 150 residues. This stretch was identified through sensitive sequence analysis approaches and was subsequently named DEUbiquitinase ADaptor domain (DEUBAD)⁶⁷. Before this discovery, it was experimentally shown that fragments that include the DEUBAD domains of INO80G and RPN13 bind UCH-L5's ULD³⁸⁻⁴¹, but it was not yet noticed that they were related. Since BAP1 also contains a ULD and regulator ASXL1 a DEUBAD domain, it was proposed that the general role of these domains was to bind ULD domains of their cognate DUB and thereby regulate their activity⁶⁷. In chapter 3 and 4 we show that this prediction was correct.

Relevance of DUB regulation

Because the ubiquitin system is crucial for normal cellular physiology and often deregulated in disease, it has held a promise as a potentially "druggable" system. But unlike the phosphorylation system where some successes have been achieved, the ubiquitin system has proven a difficult target. Targeting the conjugation machinery especially presents some practical difficulties. There are only two E1 enzymes and these are vital for normal physiology potentially making E1 inhibitors highly toxic for healthy cells. E2's and E3's are more numerous but lack distinct active site clefts that are in general more amendable for the development of small molecule inhibitors. Because of these reasons, focus has shifted to DUBs. DUBs contain defined active site clefts but despite this the development of inhibitors is progressing slowly. Currently, only one high affinity compound is known that specifically inhibits USP1 but so far none are available on the market or in clinical trials.

Since the catalytic states of DUBs differ in the presence of regulator, a key question for drug design is what the molecular characteristics are for each state. Most of the available structures of DUBs are in absence of regulators making this question more pressing. Understanding how the different activity states of DUBs look like on an atomic scale would aid in the development of specific therapeutic compounds. Additionally, since DUBs can have multiple substrates and multiple regulators that recruit them to relevant cellular systems, elucidating the structure of unique DUB-regulator complexes may in the future allow hitting specific pathways with therapeutics.

But aside from possible therapeutical applications, the work described in this thesis

will also contribute to a more thorough understanding of the fundamentals of enzyme mechanism. Particularly, this thesis provides insights into the relation between enzyme structural plasticity and catalysis as described in chapter 3.

Outline of the thesis

In **chapter 2** an outline is provided for DUB activity regulation. We identify, classify and describe the different layers of DUB regulation that have been reported in the literature. What will become apparent is the large diversity of regulatory modes that exist between different DUBs but also within a DUB.

Chapter 3 explores how the UCH-L5 is activated by regulatory protein RPN13 and inhibited by INO80G, a protein related to RPN13. Using crystal structures of the activated and inhibited complexes we highlight how conformational plasticity in UCH-L5 is exploited by these regulatory proteins to tune the affinity for substrates and consequently regulate DUB activity.

In **chapter 4** we examine the mechanism of H2A deubiquitinating by the important tumor suppressor BAP1. We demonstrate how ASXL1 activates BAP1 in a two-step process that also requires the BAP1 C-terminal extension. **Chapter 5** delves into aggregation state of BAP1 and the BAP1/ASXL1 complex and the possible consequences for DUB activity.

We conclude with **chapter 6** that presents a general discussion about the findings in this thesis.

REFERENCES

1. Komander, D., Clague, M. J. & Urbé, S. Breaking the chains: structure and function of the deubiquitinases. *Nat. Rev. Mol. Cell Biol.* **10**, 550–63 (2009).
2. Clague, M. J. *et al.* Deubiquitylases from genes to organism. *Physiol. Rev.* **93**, 1289–315 (2013).
3. Seki, T. *et al.* JsdD1, a membrane-targeted deubiquitinating enzyme, is activated by ubiquitination and regulates membrane dynamics, cell motility, and endocytosis. *J. Biol. Chem.* **288**, 17145–55 (2013).
4. Wang, B. *et al.* Abraxas and RAP80 form a BRCA1 protein complex required for the DNA damage response. *Science* **316**, 1194–1198 (2007).
5. Andersen, P. L., Xu, F. & Xiao, W. Eukaryotic DNA damage tolerance and translesion synthesis through covalent modifications of PCNA. *Cell Res.* **18**, 162–73 (2008).
6. Craney, A. & Rape, M. Dynamic regulation of ubiquitin-dependent cell cycle control. *Curr. Opin. Cell Biol.* **25**, 704–10 (2013).
7. Piper, R. C., Dikic, I. & Lukacs, G. L. Ubiquitin-dependent sorting in endocytosis. *Cold Spring Harb. Perspect. Biol.* **6**, (2014).
8. Zhang, Y. Transcriptional regulation by histone ubiquitination and deubiquitination. *Genes Dev.* **17**, 2733–40 (2003).

9. Streich, F. C. & Lima, C. D. Structural and functional insights to ubiquitin-like protein conjugation. *Annu. Rev. Biophys.* **43**, 357–79 (2014).
10. Plechanovová, A., Jaffray, E. G., Tatham, M. H., Naismith, J. H. & Hay, R. T. Structure of a RING E3 ligase and ubiquitin-loaded E2 primed for catalysis. *Nature* **489**, 115–120 (2012).
11. Metzger, M. B., Pruneda, J. N., Klevit, R. E. & Weissman, A. M. RING-type E3 ligases: master manipulators of E2 ubiquitin-conjugating enzymes and ubiquitination. *Biochim. Biophys. Acta* **1843**, 47–60 (2014).
12. Pruneda, J. N., Stoll, K. E., Bolton, L. J., Brzovic, P. S. & Klevit, R. E. Ubiquitin in motion: structural studies of the ubiquitin-conjugating enzyme~ubiquitin conjugate. *Biochemistry* **50**, 1624–33 (2011).
13. Pruneda, J. N. *et al.* Structure of an E3:E2~Ub complex reveals an allosteric mechanism shared among RING/U-box ligases. *Mol. Cell* **47**, 933–42 (2012).
14. Dou, H., Buetow, L., Sibbet, G. J., Cameron, K. & Huang, D. T. Essentiality of a non-RING element in priming donor ubiquitin for catalysis by a monomeric E3. *Nat. Struct. Mol. Biol.* **20**, 982–6 (2013).
15. Rotin, D. & Kumar, S. Physiological functions of the HECT family of ubiquitin ligases. *Nat. Rev. Mol. Cell Biol.* **10**, 398–409 (2009).
16. Smit, J. J. *et al.* The E3 ligase HOIP specifies linear ubiquitin chain assembly through its RING-IBR-RING domain and the unique LDD extension. *EMBO J.* **31**, 3833–44 (2012).
17. Spratt, D. E., Walden, H. & Shaw, G. S. RBR E3 ubiquitin ligases: new structures, new insights, new questions. *Biochem. J.* **458**, 421–37 (2014).
18. Wenzel, D. M., Lissounov, A., Brzovic, P. S. & Klevit, R. E. UBCH7 reactivity profile reveals parkin and HHARI to be RING/HECT hybrids. *Nature* **474**, 105–8 (2011).
19. Meyer, H.-J. & Rape, M. Enhanced protein degradation by branched ubiquitin chains. *Cell* **157**, 910–21 (2014).
20. Panier, S. & Durocher, D. Regulatory ubiquitylation in response to DNA double-strand breaks. *DNA Repair (Amst)*. **8**, 436–43 (2009).
21. Komander, D. & Rape, M. The ubiquitin code. *Annu. Rev. Biochem.* **81**, 203–29 (2012).
22. Rahighi, S. & Dikic, I. Selectivity of the ubiquitin-binding modules. *FEBS Lett.* **586**, 2705–10 (2012).
23. Clark, K., Nanda, S. & Cohen, P. Molecular control of the NEMO family of ubiquitin-binding proteins. *Nat. Rev. Mol. Cell Biol.* **14**, 673–85 (2013).
24. Hussain, S., Zhang, Y. & Galaray, P. J. DUBs and cancer: The role of deubiquitinating enzymes as oncogenes, non-oncogenes and tumor suppressors. *Cell Cycle* **8**, 1688–1697 (2009).
25. Ashida, H., Kim, M. & Sasakawa, C. Exploitation of the host ubiquitin system by human bacterial pathogens. *Nat. Rev. Microbiol.* **12**, 399–413 (2014).
26. Iyer, L. M., Burroughs, A. M. & Aravind, L. The prokaryotic antecedents of the ubiquitin-signaling system and the early evolution of ubiquitin-like beta-grasp domains. *Genome Biol.* **7**, R60 (2006).
27. Clerici, M., Luna-Vargas, M. P. a, Faesen, A. C. & Sixma, T. K. The DUSP-Ubl domain of USP4 enhances its catalytic efficiency by promoting ubiquitin exchange. *Nat. Commun.* **5**, 5399 (2014).
28. Faesen, A. C. *et al.* Mechanism of USP7/HAUSP activation by its C-terminal ubiquitin-like domain and allosteric regulation by GMP-synthetase. *Mol. Cell* **44**, 147–59 (2011).
29. Bozza, W. P. & Zhuang, Z. Enzyme Ubp15 and the Regulatory Role of Its Terminal Domains. *Biochemistry* **50**, 6423–6432 (2011).

30. Avvakumov, G. V *et al.* Two ZnF-UBP domains in isopeptidase T (USP5). *Biochemistry* **51**, 1188–98 (2012).
31. Reyes-Turcu, F. E. *et al.* The ubiquitin binding domain ZnF UBPs recognizes the C-terminal diglycine motif of unanchored ubiquitin. *Cell* **124**, 1197–208 (2006).
32. Burgie, S. E., Bingman, C. a, Soni, A. B. & Phillips, G. N. Structural characterization of human Uch37. *Proteins* **649–654** (2011). doi:10.1002/prot.23147
33. Chen, Y. *et al.* MINI-REVIEW Power and Promise of Ubiquitin Carboxyl-terminal Hydrolase 37 as a Target of Cancer Therapy. **14**, 2173–2179 (2013).
34. Fang, Y. *et al.* The interaction between ubiquitin C-terminal hydrolase 37 and glucose-regulated protein 78 in hepatocellular carcinoma. *Mol. Cell. Biochem.* **359**, 59–66 (2012).
35. Fang, Y. *et al.* Ubiquitin C-terminal Hydrolase 37, a novel predictor for hepatocellular carcinoma recurrence, promotes cell migration and invasion via interacting and deubiquitinating PRP19. *Biochim. Biophys. Acta* **1833**, 559–72 (2013).
36. Chen, Y. *et al.* Expression and clinical significance of UCH37 in human esophageal squamous cell carcinoma. *Dig. Dis. Sci.* **57**, 2310–7 (2012).
37. Wicks, S. J. *et al.* The deubiquitinating enzyme UCH37 interacts with Smads and regulates TGF-beta signalling. *Oncogene* **24**, 8080–4 (2005).
38. Yao, T. *et al.* Distinct modes of regulation of the Uch37 deubiquitinating enzyme in the proteasome and in the Ino80 chromatin-remodeling complex. *Mol. Cell* **31**, 909–17 (2008).
39. Hamazaki, J. *et al.* A novel proteasome interacting protein recruits the deubiquitinating enzyme UCH37 to 26S proteasomes. *EMBO J.* **25**, 4524–36 (2006).
40. Yao, T. *et al.* Proteasome recruitment and activation of the Uch37 deubiquitinating enzyme by Adrm1. *Nat. Cell Biol.* **8**, 994–1002 (2006).
41. Qiu, X.-B. *et al.* hRpn13/ADRM1/GP110 is a novel proteasome subunit that binds the deubiquitinating enzyme, UCH37. *EMBO J.* **25**, 5742–53 (2006).
42. Sahtoe, D. D. *et al.* Mechanism of UCH-L5 Activation and Inhibition by DEUBAD Domains in RPN13 and INO80G. *Mol. Cell* **57**, 887–900 (2015).
43. VanderLinden, R. T. *et al.* Structural Basis for the Activation and Inhibition of the UCH37 Deubiquitylase. *Mol. Cell* **57**, 901–11 (2015).
44. Lee, M. J., Lee, B.-H., Hanna, J., King, R. W. & Finley, D. Trimming of ubiquitin chains by proteasome-associated deubiquitinating enzymes. *Mol. Cell. Proteomics* **10**, R110.003871 (2011).
45. Husnjak, K. *et al.* Proteasome subunit Rpn13 is a novel ubiquitin receptor. *Nature* **453**, 481–488 (2008).
46. Chen, X., Lee, B.-H., Finley, D. & Walters, K. J. Structure of proteasome ubiquitin receptor hRpn13 and its activation by the scaffolding protein hRpn2. *Mol. Cell* **38**, 404–15 (2010).
47. Nishi, R. *et al.* Systematic characterization of deubiquitylating enzymes for roles in maintaining genome integrity. *Nat. Cell Biol.* (2014). doi:10.1038/ncb3028
48. Wang, L. *et al.* INO80 Facilitates Pluripotency Gene Activation in Embryonic Stem Cell Self-Renewal, Reprogramming, and Blastocyst Development. *Cell Stem Cell* **14**, 575–91 (2014).
49. Chia, N.-Y. *et al.* A genome-wide RNAi screen reveals determinants of human embryonic stem cell identity. *Nature* **468**, 316–20 (2010).
50. Jensen, D. E. *et al.* BAP1: a novel ubiquitin hydrolase which binds to the BRCA1 RING finger and enhances BRCA1-mediated cell growth suppression. *Oncogene* **16**, 1097–112 (1998).

51. Goldstein, A. M. Germline BAP1 mutations and tumor susceptibility. *Nat. Genet.* **43**, 925–6 (2011).
52. Bott, M. *et al.* The nuclear deubiquitinase BAP1 is commonly inactivated by somatic mutations and 3p21.1 losses in malignant pleural mesothelioma. *Nat. Genet.* **43**, 668–72 (2011).
53. White, A. E. & Harper, J. W. Cancer: Emerging anatomy of the BAP1 tumor suppressor system. *Science* **337**, 1463–4 (2012).
54. Dey, A. *et al.* Loss of the tumor suppressor BAP1 causes myeloid transformation. *Science* **337**, 1541–6 (2012).
55. Harbour, J. W. *et al.* Frequent mutation of BAP1 in metastasizing uveal melanomas. *Science* **330**, 1410–3 (2010).
56. Testa, J. R. *et al.* Germline BAP1 mutations predispose to malignant mesothelioma. *Nat. Genet.* **43**, 1022–5 (2011).
57. Kandoth, C. *et al.* Mutational landscape and significance across 12 major cancer types. *Nature* **502**, 333–9 (2013).
58. Carbone, M. *et al.* BAP1 and cancer. *Nat. Rev. Cancer* **13**, 153–9 (2013).
59. Misaghi, S. *et al.* Association of C-terminal ubiquitin hydrolase BRCA1-associated protein 1 with cell cycle regulator host cell factor 1. *Mol. Cell. Biol.* **29**, 2181–92 (2009).
60. Ji, Z. *et al.* The forkhead transcription factor FOXK2 acts as a chromatin targeting factor for the BAP1-containing histone deubiquitinase complex. *Nucleic Acids Res.* **42**, 6232–42 (2014).
61. Baymaz, H. I. *et al.* MBD5 and MBD6 interact with the human PR-DUB complex through their methyl-CpG-binding domain. *Proteomics* **14**, 2179–89 (2014).
62. Yu, H. *et al.* The ubiquitin carboxyl hydrolase BAP1 forms a ternary complex with YY1 and HCF-1 and is a critical regulator of gene expression. *Mol. Cell. Biol.* **30**, 5071–85 (2010).
63. Scheuermann, J. C. *et al.* Histone H2A deubiquitinase activity of the Polycomb repressive complex PR-DUB. *Nature* **465**, 243–7 (2010).
64. Yu, H. *et al.* Tumor suppressor and deubiquitinase BAP1 promotes DNA double-strand break repair. *Proc. Natl. Acad. Sci. U. S. A.* **111**, 285–90 (2014).
65. Lee, H.-S., Lee, S.-A., Hur, S.-K., Seo, J.-W. & Kwon, J. Stabilization and targeting of INO80 to replication forks by BAP1 during normal DNA synthesis. *Nat. Commun.* **5**, 5128 (2014).
66. Eletr, Z. M. & Wilkinson, K. D. An emerging model for BAP1's role in regulating cell cycle progression. *Cell Biochem. Biophys.* **60**, 3–11 (2011).
67. Sanchez-Pulido, L., Kong, L. & Ponting, C. P. A common ancestry for BAP1 and Uch37 regulators. *Bioinformatics* **28**, 1953–6 (2012).

chapter | TWO

Layers of DUB regulation

Danny D. Sahtoe and *Titia K. Sixma.

Division of Biochemistry and Cancer genomics center

Netherlands Cancer Institute, Plesmanlaan 121, 1066CX, Amsterdam, the Netherlands

**correnspondence: t.sixma@nki.nl*

Adapted from Sahtoe et al. Trends in Biochemical Sciences (2015), 40(8):456-467

ABSTRACT

Proteolytic enzymes such as (iso-)peptidases are potentially hazardous for cells. To neutralize their potential danger tight control of activities has evolved. Deubiquitylating enzymes (DUBs) are isopeptidases involved in eukaryotic ubiquitylation. They reverse ubiquitin signals by hydrolyzing ubiquitin adducts, giving them control over all aspects of ubiquitin biology. The importance of DUB function is underscored by their frequent deregulation in human disease, making these enzymes potential drug targets. Here we review the different layers of DUB enzyme regulation. We discuss how post-translational modification, regulatory domains within DUBs and incorporation of DUBs into macromolecular complexes contribute to activity. We conclude that most DUBs are likely to use a combination of these basic regulatory mechanisms.

DUB regulation: Background and overview

Conjugation of ubiquitin and ubiquitin-like molecules (Ubl) (Box I) to lysines of target proteins represents a major type of post-translational modification (PTMs) that regulates countless processes in eukaryotes¹. These modifications are catalyzed by an enzymatic cascade involving E1 activating enzymes, E2 conjugating enzymes and E3 ligases. Many different types of Ub/Ubl modification exist, since targets can be mono-ubiquitylated or modified with a variety of polyubiquitin chains that can each have different signaling outcomes.

Since the ubiquitin signals have profound cellular effects, conjugation events are kept in check by ubiquitin deconjugation. This function is performed by a specialized class of isopeptidases called deubiquitylating enzymes (DUBs) that hydrolyze the isopeptide bond between ubiquitin and target proteins^{2,3}. Five different DUB families have been identified: ubiquitin C-terminal hydrolase (UCH), ubiquitin specific protease (USP), ovarian tumor (OTU), Machado-Joseph disease (MJD) and Jab1/Mpn/Mov34 (JAMM) families. All of these are cysteine isopeptidases except the JAMM family members which have metallo-isopeptidase activity³.

Due to their critical role in cellular functions, deregulation of enzymes of the ubiquitin-system is important in cancer, infectious diseases and neurological diseases⁴⁻⁶. Hence there is an increasing interest in targeting these molecules pharmaceutically. Since E2 conjugating enzymes and most E3 ligases lack distinct catalytic clefts, approaches to therapeutic intervention are currently focused on DUBs⁷.

In the cell, the activity of degrading enzymes is carefully controlled. This was long known for peptidases, the distant cousins of DUBs, which are tightly regulated through production as inactive enzymes (zymogens), but also through proteinaceous inhibitors and elaborate activation cascades to prevent aberrant proteolysis⁸. This tight control is essential, as unscheduled activation can be disastrous for the cell. It is gradually becoming clear that this is also true for the DUB isopeptidases. The need for regulation of DUB activity can be explained by the large number of ubiquitin conjugates in cells. Without proper regulation, DUBs could unspecifically hydrolyze any ubiquitin conjugate they encounter, potentially deregulating cellular physiology.

To cope with this, cells have adopted several strategies to ensure DUB activity is channeled to the right locations at the right time. Some of this regulation takes place at the transcriptional level, but the proteins themselves are regulated in many different ways. A clear understanding of these processes is important for our knowledge of ubiquitin biology and will assist in the development of therapeutic agents targeting specific DUBs. In recent years the insight in DUBs whose catalytic activity is regulated has steadily expanded;

Box 1: Ubiquitin and ubiquitin-like molecules

Eukaryotes have a diverse repertoire of post translational modifications to fine-tune or alter molecular processes. Among these is ubiquitination, where the small 76 amino acid protein ubiquitin is attached to target proteins¹. Ubiquitin is characterized by a globular beta-grasp fold followed by an extended tail harboring a Gly-Gly motif required for conjugation to target proteins. Over the past decades other small proteins that share these characteristics with ubiquitin have been identified. Among these are NEDD8, SUMO-1, SUMO-2, SUMO-3, ATG8, ISG15 and FAT10 but more have been identified, that can be conjugated to proteins to alter their fate or function. The enzymes responsible for their conjugation and deconjugation are, moreover, also homologous to the enzymes from the ubiquitin-system and follow similar mechanisms. Because of these commonalities with ubiquitin, these proteins are collectively called ubiquitin-like molecules (Ubl).

through advances in the cellular physiology, biophysics and structural biology of DUBs, we are starting to elucidate the intricate mechanisms that underlie DUB regulation.

The general roles of DUBs and their target and chain specificity have been discussed elsewhere^{3,9,10}. Here we discuss the emerging themes in regulation of DUBs at the protein level. We distinguish different “layers” of DUB regulation and describe how they affect activity (Figure 1). After examination of the individual layers we analyze how these different mechanisms can cooperate. Although our list of examples is not exhaustive (Table 1), it provides a good basis for discussing the different layers of DUB regulation.

Cellular and target recruitment

In figure 1 we present a simplified classification of the different layers of DUB regulation. The first layer we discuss is that of DUB recruitment factors. Guiding the almost hundred DUBs encoded in the human genome to their relevant substrates and pathways is crucial for cellular physiology since it insulates DUBs from unwanted interactions and the cell from spurious activity. It can be mediated by distinct regions within the enzyme or by external factors: For instance, the Ubl domain of USP14 recruits it to the proteasome where its activity is increased 500-fold¹¹. The endosomal adaptor protein STAM recruits the DUBs AMSH and USP8 to the endosome pathway by interacting with an SH3 binding motif or MIT domain respectively^{12,13}.

Another pathway that requires proper DUB recruitment is the DNA damage response (DDR). After UV-induced DNA damage mono-ubiquitylated PCNA mediates signaling that leads to repair. The DUB complex USP1/UAF1 deubiquitylates PCNA after the complex is recruited to the substrate by recruitment factor ELG1¹⁴. BRCC36 is another DUB in DDR where it deubiquitylates several proteins as catalytic subunit of the BRCA1-A complex. In this complex specialized ubiquitin and SUMO binding domains recruit BRCC36 to sites of damage^{15–19}. Finally, also in the nucleus, transcription factor FOXK2 targets the UCH class DUB BAP1 to chromatin to facilitate histone H2A deubiquitylation²⁰.

In NF- κ B signaling, ubiquitin conjugation has multiple roles. Different components of the

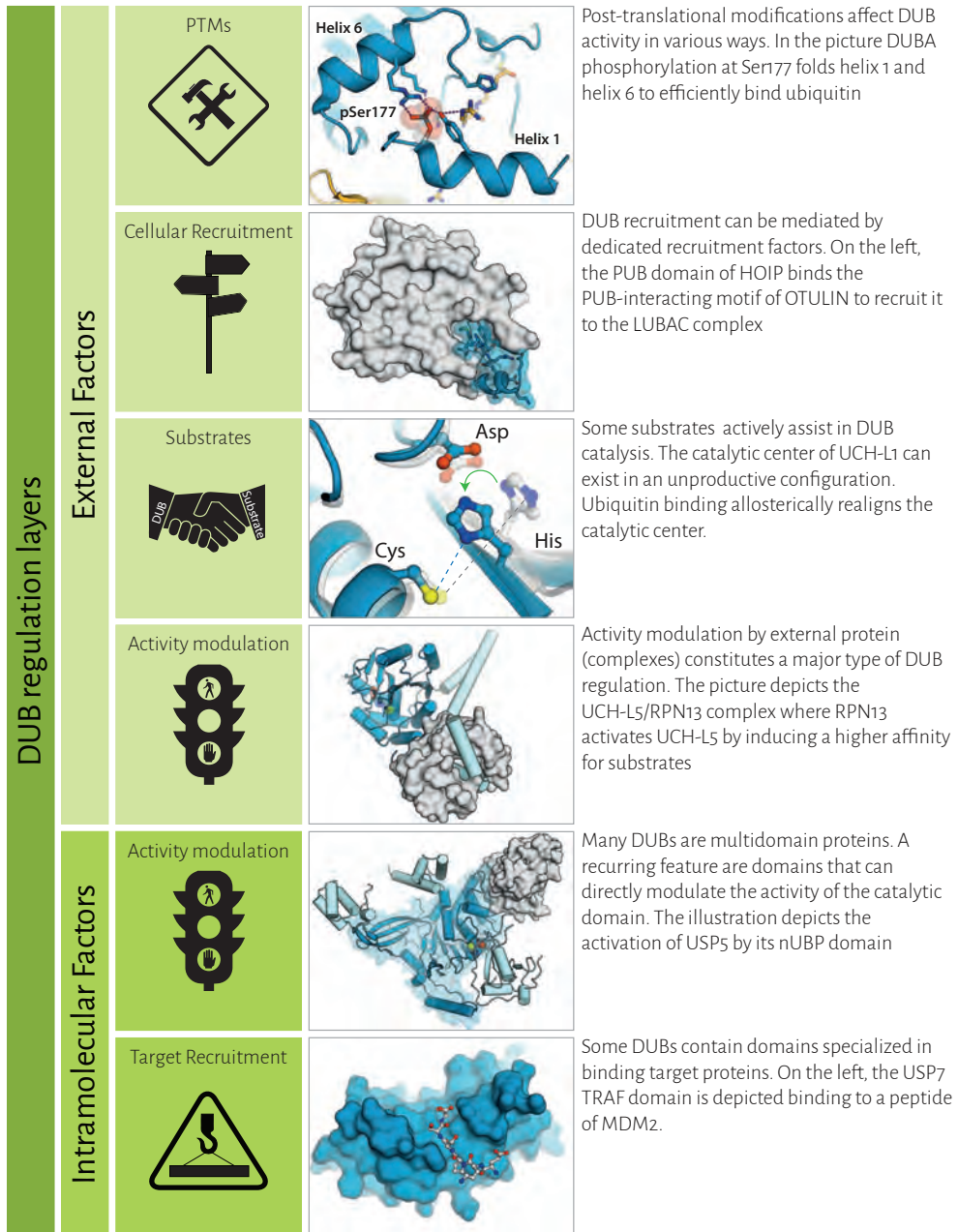


Figure 1. Classification of regulatory layers for Deubiquitylating enzymes (DUBs). Two major divisions are intramolecular factors, focused on domains within DUBs, and external factors focused on protein partners or modifications. Each of these two divisions contains additional layers of DUB regulation. DUBs are colored blue or cyan. Regulatory elements are colored in light grey.

pathway recruit the DUBs USP10 and CYLD. MCPIP-1 recruits USP10 whereas CYLD is recruited by the E3 ligase HOIP (Figure 1). CYLD moreover contains a B-box domain that

Table 1 | Summary of known DUB regulatory mechanisms

Family	DUB	Intramolecular Factors			External Factors			Refs	
		Activity modulation	Target recruitment	Activity modulation	PTMs	Cellular recruitment	Substrate assistance		
UCH	UCH-L1				Ubiquitylation of K157 decreases activity. Inhibited by ROS.		Ubiquitin binding to an exosite aligns catalytic site to active configuration	29,81	
	UCH-L5			RPN13 increases while INO80G decreases ub binding		Recruited to proteasome by RPN13 and to INO80 complexes by INO80C		62–66	
	BAP1			ASX11 promotes activity	Ubiquitylation of the NLS mislocalizes BAP1	Targeted to genomic loci by several protein partners		20,61	
USP	USP1	UV induced auto-cleavage impairs activity		UAF1 increases k_{cat}	Phosphorylation of Ser313 promotes UAF1 binding. Inhibited by ROS	ELC1 recruits the USP1/UAF1 complex to PCNA while Spartan prevents it.		14,48,50,51,71,72,75,89	
	USP3					USP3, ZnF domain recruits target H2A		26	
	USP4	DUSP-Ubl domain promotes ubiquitin release			Phosphorylation by AKT alters localization			45,85	
	USP5	nUBP allosterically activates while other UBDs assist in substrate binding					Ubiquitin moiety can bind to ZnF UBP domain and allosterically activate USPs	43,44	
	USP7	HUBL domain activates CD		GMPS increases k_{cat}			Ubiquitin binding realigns active site	23,24,27,28,47	
	USP8					STAM binds USP8		12	
	USP12			Activated by UAF1 and		MIT domain to recruit it to endosomes		52,54	

	OTULIN				ubiquitin binding Tyr56 phosphorylation decreases LUBAC association	The HOIP PUB domain recruits OTULIN to LUBAC	Substrate aided catalysis by linear polyubiquitin	33,76,77
	OTUB1			UbcH5B promotes K48 polyubiquitin binding				59
MJD	ATXN3				Ubiquitylation activates chain hydrolysis activity			82
	JosD1				Ubiquitylation activates chain hydrolysis activity			83
JAMM	AMSH			STAM activates chain hydrolysis		SH3 binding motif in AMSH recruits to ESCRT complexes		13,55
	CSN5	Autoinhibited by Inst1-loop		Only active in COP9 signalosome			Neddylated CRLs activate COP9 catalysis	34,35
	BRCC36			Activated in BRCA1-A and BRISC complexes		Recruited to DNA damage foci by by repair protein through UJMs and SIMs in BRCA1-A complex		15,16,38
	RPN11			Activated in proteasomal 19S particle				36,37
SENP	SENP1-2 and SENP5-8						Globular SUMO domain activates catalysis	30-32

promotes its cytoplasmic localization^{21,22}.

The previous examples illustrated how external proteins can recruit DUBs to relevant pathways or substrates. While DUBs in general can recognize the ubiquitin part of a substrate via their catalytic domains, sometimes extra specificity is achieved by specialized domains that are present in DUBs themselves. One of the best studied examples is the DUB USP7. Here, the N-terminal TRAF domain of USP7 binds small peptide motifs in its targets EBNA-1, p53 and Mdm2 to facilitate their deubiquitylation (Figure 1)^{23,24}. USP15 employs its DUSP-Ubl domain to recruit and deubiquitylate the E3 ligase BRAP²⁵ while the H2A deubiquitinase USP3 requires its intact Zinc finger domain to bind H2A²⁶.

Thus, specialized domains within DUBs and external proteins can guide DUB activity to the correct pathways and substrates by functioning as recruitment factors.

Substrate mediated regulation

Besides recruitment, some DUBs require further activation. Surprisingly the cognate ubiquitin-like molecule can affect the activity of the DUB or ubiquitin-like protease by rearranging the catalytic triad. Early structural studies on the catalytic domain (CD) of USP7 revealed that its catalytic triad can exist in an inactive configuration²⁷. Binding of a ubiquitin derivative “realigned” the catalytic triad towards an active configuration and also changed the conformation of the “switching loop”, a surface loop close to the active site that is important for activation^{27,28}. These effects suggest that USP7 CD can only be active when ubiquitin is correctly bound. In UCH-L1 (Figure 1), ubiquitin binding at an ‘exosite’ (i.e. distant from the active site), also induces a cascade of conformational changes that rearranges the catalytic triad²⁹. This type of allosteric activation also occurs in the SENP class of SUMO proteases, where it has been elegantly quantified. When SENPs are incubated with the tail-less SUMO β -grasp domain, this increases the catalytic turnover against a model peptide substrate³⁰⁻³². However, this type of ubiquitin/Ubl induced rearrangement is not generically present, since other inactive DUBs do contain correctly aligned active sites, even in the absence of ubiquitin. When present, this regulation by a Ubl itself cannot give much specificity. Thus, it is not surprising that regulation of for example USP7 has further layers of complexity, as discussed later.

Substrates can give rise to more complex types of activation, generating high specificity. In OTULIN, a member of the OTU class DUBs, the substrate actively assists in catalysis. OTULIN regulates NF- κ B signaling by its exclusive ability to disassemble linear ubiquitin chains³³. In these chains, ubiquitin moieties are linked via the amino terminus at Met1 instead of via one of its lysines. They are made by the HOIP E3 ligase in the linear chain assembly (LUBAC) complex. Interestingly, OTULIN uses this unique linkage to sense its substrate. Normally OTULIN Asp336 functions as an auto-inhibitory element that favors

an unproductive catalytic triad conformation, but Glu16 of the proximal ubiquitin (the target-ubiquitin) in linear chains reorganizes the catalytic triad towards an active state. Mutation of this substrate Glu16 reduces the k_{cat} 240-fold but hardly affects the binding indicating that actively it promotes catalysis. Of all ubiquitin chain types, only a linear chain can bind such that the Glu16 in the proximal ubiquitin is correctly positioned to assist in catalysis, explaining how OTULIN activity is specifically restricted to cellular pathways that feature linear polyubiquitin signaling.

A different example of substrate-dependent activation is seen in the CSN5, a JAMM-type DUB found in the eight subunit COP9 signalosome (CSN)³⁴. The CSN deconjugates NEDD8 from Cullin Ring ubiquitin E3 ligases (CRLs). Through this activity CSN decreases the ubiquitin E3 ligase activity of CRLs. A recent structural analysis of CSN rationalized how interaction between DUB and its neddylated CRL substrate leads to activation³⁵. The catalytic subunit CSN5 forms a sub-complex with CSN6 and CNS4. In absence of substrate a loop in CSN5, Ins1, occludes the active site, leading to auto-inhibition. In the presence of neddylated CRLs, the CSN4 subunit undergoes a large conformational change to bind the substrate, at the expense of its interaction with the so-called 'Ins-2' loop of CSN6. These substrate-induced conformational changes alleviate the auto-inhibition and prime CSN for deconjugation. Point mutations in the Ins1 and Ins2 loops can activate CSN even in the absence of neddylated CRLs confirming that they act as auto-inhibitory elements³⁵. The ability of CSN4 to sense neddylated CRLs assures that activation only occurs in the presence of the substrate.

The examples above illustrate an important safeguard mechanism for unwanted proteolytic activity by only allowing enzymatic activity to take place in the presence of the correct substrates.

DUB regulation by intramolecular and external factors

The next layer of regulation is the direct regulation of DUB catalytic activity. In this mode of activation, the catalytic domains (CD) of DUBs can be viewed as core units whose catalytic activity is modulated by interaction with other protein modules, either external, or within the DUB itself².

A common form of regulation of this type is that given by a large molecular machine. There are several examples of DUBs that only attain optimal activity and localization within the structural integrity of such multi-subunit molecular machines like the COP9 signalosome. Other notable examples of this type include USP14 and RPN11 in the proteasome^{11,36,37}, BRCC36 within the BRCA1-A and BRISC complexes^{15,16,38} and Ubp8 in the yeast SAGA DUB module³⁹⁻⁴¹. In these cases the DUBs display low activity in isolation, but are robustly activated within the complex. For Ubp8, complex formation likely stabilizes the active site and

the ubiquitin binding surface^{40,42}. In general, the exact molecular mechanism of activation in these large complexes remains poorly understood, but may depend on a combination of regulatory influences.

Apart from these examples where DUBs are activated as part of large macromolecular assemblies, many well studied examples exist where simple domains, within the DUB or from outside, specifically modulate the activity of catalytic domains. USP5 contains several ubiquitin binding domains (UBDs) that assist in the disassembly of polyubiquitin chains of a variety of linkages⁴³. The crystal structure of full length USP5 revealed a previously unpredicted domain, named nUBP, that packs tightly against the CD and allosterically activates it 1000-fold (Figure 1)⁴⁴. Moreover addition of free ubiquitin to USP5 can further stimulate USP5 activity through binding to the ZnF-UBP domain via an as yet unknown mechanism⁴³.

A second example where additional domains are important is USP4, a DUB with roles in TGF- β signaling and splicing. The isolated USP4 CD was found to have an unusually high affinity for ubiquitin (low nanomolar range) suggesting that it could be constitutively product-inhibited in cells, since the ubiquitin concentration is in the range of 4-20 μM ⁴⁵. The N-terminal DUSP-Ubl domain present in full length USP4 can however allosterically promote product release, thereby increasing k_{cat} of USP4. This effect involves the “switching loop”, a loop close to the catalytic triad.

This “switching loop” also plays a role in USP7 or its yeast homolog Ubp15 activity. The C-terminal HUBL domain of USP7 can dynamically fold back onto the CD to allow contact of a C-terminal peptide at the end of the HUBL domain with the “switching loop”, a region close to the catalytic triad. This intramolecular interaction increases both k_{cat} and K_M of the CD²⁸. Unlike USP7, the N-terminal TRAF domain of Ubp15 also affects intrinsic activity⁴⁶. Apparently the ‘switching loop’ plays a conserved regulatory function in multiple USPs, although the details of the activation differ.

External factors such as protein partners can also activate DUBs by either reinforcing the stimulatory effects of intramolecular factors or by other means. The intramolecular activation of the USP7 CD by its HUBL domain is allosterically potentiated by external factor GMP synthase (GMPS) that consolidates the active state leading to an additional increase in k_{cat} ^{28,47}.

One of the best-studied examples of DUB activation by external factors is USP1. This DUB controls DNA repair signaling by deubiquitylating FANCD2 and PCNA^{48,49}. USP1 is regulated by auto-cleavage⁴⁸ and its k_{cat} is strongly stimulated by the WD40 repeat protein USP1 associated factor 1 (UAF-1)⁵⁰. UAF-1 achieves this by increasing the basicity of the

Box II : Outstanding questions

- How is DUB regulation achieved temporally?
- Do DUBs dynamically cycle between different complexes to meet functional requirements or are they stably associated in separate complexes?
- Are DUBs merely catalytic modules or do they also perform scaffolding or adaptor functions in large molecular assemblies?
- How many different targets do DUBs generally have and how specific are they for these targets?
- Is target specificity intrinsic to a certain DUB or is it achieved through formation of multi protein complexes?

histidine general base in the USP1 catalytic triad⁵¹. Two closely related DUBs, USP12 and USP46, are similarly activated by UAF-1, but unlike USP1, these can be hyper-activated by another WD40 repeat protein named WDR20⁵²⁻⁵⁴.

DUB activation also occurs in endocytosis and autophagy pathways. The JAMM class enzyme AMSH is recruited to endosomes by the adaptor protein STAM⁵⁵. Besides recruitment, STAM can also directly activate AMSH hydrolysis of polyubiquitin chains on endosome-targeted proteins. The exact mechanism of this activation is unclear but both k_{cat} and K_M effects were suggested^{13,55}. In autophagy, the activity of USP10 and USP13 is modulated by Beclin-1. Beclin-1 is a subunit of the essential Vps34 complexes that play a role in phagosome nucleation. These complexes can be rapidly degraded by ubiquitylation of Beclin-1. Beclin-1 prevents this however, by binding USP10 and USP13, and stimulating these DUBs to remove ubiquitin from itself both in cells and in vitro⁵⁶.

A particularly interesting example of DUB regulation by external proteins involves stimulation of OTUB1 activity by ubiquitin E2 enzymes. OTUB1 can non-catalytically interfere with polyubiquitin synthesis by specifically inhibiting E2 enzyme Ubc13 linked to ubiquitin at its active site (charged E2)^{57,58}. Conversely, a subset of charged and uncharged E2s, including UbcH5B, stimulate Lys48-linked polyubiquitin hydrolysis by OTUB1 by increasing substrate affinity⁵⁹. Crystal structures indicate UbcH5B achieves this increased affinity by stabilizing a ubiquitin binding site on OTUB1. Whether charged E2s stimulate OTUB1 activity, or whether OTUB1 inhibits polyubiquitin synthesis of the E2 depends on the relative concentrations of charged E2 and free ubiquitin. Therefore the authors suggested an elegant model wherein OTUB1-E2 complexes can dynamically regulate the level of polyubiquitin chains in cells by either activating chain hydrolysis or inhibiting E2-mediated chain synthesis.

The activities of the UCH family DUBs UCH-L5 and BAP1 are regulated by related DEUBAD domains⁶⁰. BAP1 is a tumor suppressor that is activated by ASX to deubiquitylate H2A in

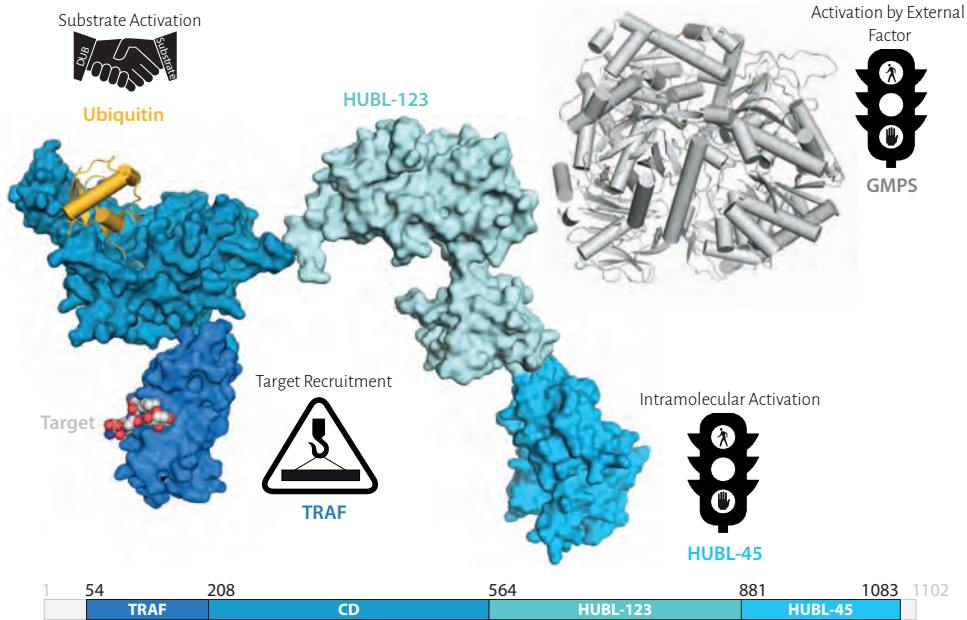


Figure 2. Combining the layers of DUB regulation. The different layers of DUB regulation can co-exist in a single DUB. In the picture a model of USP7 (blue surfaces) is presented based on existing structures (1nbf, 2ylm, 1yy6) where ubiquitin (part of the substrate) in yellow itself can activate the catalytic domain of USP7. This activation is reinforced intramolecularly by the HUBL-45 subdomain of USP7 and from outside by GMPS (gray cartoon). The USP7 N-terminal TRAF domain can furthermore recruit targets such as EBNA-1 (sphere representation) to the DUB. This multi-layered regulation likely exist for many more DUBs.

Polycomb gene repression⁶¹. In the proteasome, the DEUBAD domain of RPN13 activates UCH-L5 by increasing the affinity for substrates⁶²⁻⁶⁶. This occurs through a combination of mild effects including the allosteric stabilization of the so-called ‘active site crossover loop’ and the restriction of the inhibitory mobility of the C-terminal ULD domain of UCH-L5^{65,66}.

These examples illustrate how domains within DUBs or external proteins can activate the catalytic domains of DUBs through a variety of different mechanisms.

Negative regulation of DUBs

While all DUBs discussed so far are activated by intramolecular domains or external proteins, in a limited number of rare cases DUBs are directly inhibited by other proteins. The first example of this type is UCH-L5 inhibition by INO80G. INO80G is a metazoan-specific subunit of INO80 chromatin remodeling complexes and is associated with UCH-L5 during DNA repair^{67,68}. This interaction strongly inhibits UCH-L5⁶⁷. Similar to UCH-L5 activator RPN13 (discussed earlier), INO80G contains a DEUBAD domain⁶⁰ and recent structural analyses have revealed that it inhibits UCH-L5 by occupying the ubiquitin docking site on the enzyme through an unique hairpin-structure that is absent in the DEUBAD domain of

activator RPN13^{65,66}. While the DEUBAD domain of RPN13 activates UCH-L5 by increasing its affinity for substrates, in INO80G it does the opposite and dramatically decreases the affinity for substrates. Thus the regulation of UCH-L5 is achieved at the level of substrate affinity, leading to a change in K_M rather than k_{cat} as observed in for instance USP1 regulation⁵⁰. The dual mode of regulation of UCH-L5 suggests that strict spatial and temporal control should exist to ensure the right activity at the right place. For example, the inhibition of UCH-L5 by INO80G must be alleviated during DNA repair since the catalytic activity of UCH-L5 is required in this pathway⁶⁸.

Another example of negative regulation is the inhibition of the yeast endosome associated DUB Doa4 by Rfu1. In a yeast genetics screen, deletion of Rfu1 was serendipitously found to alter global ubiquitin levels⁶⁹. DUBs can regulate these levels by liberating conjugated ubiquitin from targets. Changes in global ubiquitin levels are often associated with cellular stress responses⁶⁹. Rfu1 was shown to directly inhibit Doa4 activity through a mechanism that is unknown on the molecular level, suggesting that Doa4/Rfu1 system may contribute to the regulation of global ubiquitin levels⁶⁹. Interestingly Doa4 can also be activated by the endosome associated protein Bro1 indicating that, like UCH-L5, Doa4 is subject to both positive and negative regulation⁷⁰.

A final example of negative regulation is the deubiquitylation of mono-ubiquitylated PCNA (PCNA-Ub) by the USP1/UAF1 complex. During replication stress the protein Spartan binds to mono-ubiquitylated PCNA^{71,72}. This binding event was suggested to protect PCNA-Ub from deubiquitylation by the USP1/UAF1 complex in order to drive the stress response that is dependent on the ubiquitin signal⁷¹. This is different from UCH-L5/INO80G, where INO80G directly prevents substrate docking onto the DUB; Instead, Spartan blocks the DUB-binding site on the substrate, protecting it from deubiquitylation.

Hence although less common than the stimulation of DUB activity, inhibition of DUBs by external proteins constitutes another type of DUB regulation. Activity can however also be regulated by direct covalent modification of DUBs through PTMs.

Post-translational modifications

PTMs such as sumoylation, ubiquitylation and phosphorylation are a convenient way for cells to further fine-tune DUB activity. An example is DUBA, an OTU class enzyme that plays an important role in the immune system. DUBA is only active when it is phosphorylated at Ser177 (pSer177)⁷³ and crystal structures demonstrated that phosphorylation refolds part of the protein that assists in ubiquitin binding, explaining the importance of the modification (Figure 1). This is highlighted in antigen-stimulated macrophages, in which pSer177 DUBA levels are increased to regulate the immune response. Activation by phosphorylation also takes place during the cell cycle where USP37 is modified by CDK-2

to directly stimulate DUB activity⁷⁴. In an analogous manner USP1 phosphorylation was suggested to be required for complex formation with activator UAF-1⁷⁵.

Phosphorylation can also negatively affect DUB activity. The DUB OTULIN is recruited to the NF- κ B pathway by binding the HOIP PUB domain with its PUB Interacting Motif (PIM)^{76,77}, thus connecting the E3 ligase (HOIP in the LUBAC complex) and the DUB for linear ubiquitin chains. Phosphorylation of Tyr56 within the PIM abrogates this interaction and the ability of OTULIN to antagonize NF- κ B signaling.

The activity of the NF- κ B associated DUB CYLD is negatively affected by both phosphorylation and sumoylation^{78,79}, while sumoylation also impedes USP25 activity. This multi-domain DUB contains ubiquitin binding domains (UBDs) that are required for efficient polyubiquitin hydrolysis. Sumoylation at one of these UBDs decreases USP25 chain hydrolysis activity⁸⁰.

In addition to sumoylation, ubiquitylation of DUBs has also been reported to regulate activity. UCH-L1 mono-ubiquitylation at Lys157 of the active site cross-over loop decreased its activity⁸¹. By contrast, ubiquitylation of the MJD class DUBs ATXN3 and Jsd1 stimulates their polyubiquitin chain hydrolysis activities^{82,83}.

In some cases PTMs can alter DUB subcellular localization. Ubiquitylation of BAP1 near its nuclear localization sequence negatively regulates its activity by excluding BAP1 from the nucleus where most of its targets reside⁸⁴. Similarly, phosphorylation of USP4 by AKT also leads to its redistribution from the nucleus to the cytoplasm where it ultimately reaches the cell membrane to deubiquitylate the TFG- β receptor I⁸⁵. Conversely, during DNA damage, the predominantly cytoplasmic DUB USP10 is translocated to the nucleus after phosphorylation to deubiquitylate p53⁸⁶.

More unusual modifications also regulate DUBs. Recent reports have illustrated how reactive oxygen species (ROS) can regulate DUB activity⁸⁷⁻⁹⁰. ROS can serve as potent signaling molecules by reacting with active site cysteines of tyrosine phosphatases and some cysteine peptidases to form reversible sulphenic acid adducts or irreversible sulphinic or sulphonic acid adducts⁹¹. Oxidation of active site cysteines to sulphenic acid appears to be widespread in the OTU, USP and UCH classes of DUBs where it reduces DUB activity. Functionally the modification may play important roles in cells as exemplified by the oxidative inactivation of the PCNA deubiquitinase USP1⁸⁹. This results in the accumulation of mono-ubiquitinated PCNA, a mark for cellular stress responses^{88,89}.

In summary, several types of PTMs of DUBs have been described that can have a variety of effects on DUBs and thereby further fine-tune activity.

Multiple layers of regulation

In the previous sections we discussed how certain types of regulation impinge on DUB activity separately for illustrative purposes. In practice however many regulatory mechanisms co-exist. This situation sometimes even occurs within a single domain. The RPN13 DEUBAD domain for example is responsible for both the activation of UCH-L5 and for recruiting the enzyme to the proteasome⁶²⁻⁶⁴. We expect that more factors exist that have multiple regulatory roles at the same time.

The concept of multiple regulatory layers can best be exemplified by considering USP7 (Figure 2 and Table 1). The USP7 CD can exist in a catalytically incompetent state that can be activated by ubiquitin binding and USP7 HUBL-45^{27,28}. This active state can be further reinforced allosterically by the external factor GMPS, which binds to HUBL-123^{28,47} and target recruitment is promoted by its N-terminal TRAF domain^{23,24}. Another example of multiple layers of regulation impinging on a single protein is the tumor suppressor BAP1. This enzyme is activated by ASXL1 to deubiquitylate H2A and can be targeted to certain genomic loci by its association with transcriptional regulators^{20,61,92}. BAP1 can furthermore be spatially separated from its targets by ubiquitylation of its C-terminal nuclear localization signal (NLS) by UBE2O, causing mislocalization to the cytoplasm⁸⁴. This type of multi-layered regulation is likely a feature of many DUBs and multi-protein DUB complexes and contributes to tight control of deubiquitylation.

Concluding remarks

Research on the mechanisms of DUB regulation has advanced significantly in the past years. The regulation takes place at different layers and a notable feature is the diversity of the known mechanisms. This variety is also present at the biochemical level: the activation mechanisms range from solely impinging on catalytic activity (k_{cat}) to primarily substrate interaction (K_M) to combinations of both. The accumulated regulatory effects of the layers determine DUB activity and ultimately the fate of ubiquitylated substrates.

Even though we understand some aspects of DUB mechanism, there are important outstanding questions (Box II), such as how DUB activity is regulated within the large macromolecular complexes. For example recently determined UCH-L5/RPN13 structures give insights into the basic activation mechanisms of UCH-L5^{65,66}, but these do not explain the polyubiquitin hydrolysis activity of UCH-L5 as part of the proteasome. Similar challenges exist for other DUBs and can only be addressed by studying large holo-enzyme complexes over different activation states.

As more details of DUB/regulator systems become available, an important task will be to identify possible common elements in DUB regulation that underlie the apparent diversi-

ty. This information may allow a more guided design of potential therapeutic compounds. That many DUBs are allosterically regulated raises the interesting prospect of developing therapeutic agents that target allosteric and exo sites rather than active sites. This type of targeting may allow for greater specificity towards certain functions of DUBs since they may have multiple substrates. A lack of information about DUB substrates poses a major hurdle for targeted therapy and that future studies will need to address.

Acknowledgements

We thank group members for discussion, Michael Uckelmann for critical reading of the manuscript. We acknowledge support from NWO-Gravity program CGC.nl, ERC advanced grant 249997, Ubiquitin Balance, and KWF 2012-5398

REFERENCES

1. Streich, F. C. & Lima, C. D. Structural and functional insights to ubiquitin-like protein conjugation. *Annu. Rev. Biophys.* **43**, 357–79 (2014).
2. Komander, D., Clague, M. J. & Urbé, S. Breaking the chains: structure and function of the deubiquitinases. *Nat. Rev. Mol. Cell Biol.* **10**, 550–63 (2009).
3. Clague, M. J. *et al.* Deubiquitylases from genes to organism. *Physiol. Rev.* **93**, 1289–315 (2013).
4. Hussain, S., Zhang, Y. & Galardy, P. J. DUBs and cancer: The role of deubiquitinating enzymes as oncogenes, non-oncogenes and tumor suppressors. *Cell Cycle* **8**, 1688–1697 (2009).
5. Nanduri, B., Suvarnapunya, A. E., Venkatesan, M. & Edelman, M. J. Deubiquitinating enzymes as promising drug targets for infectious diseases. *Curr. Pharm. Des.* **19**, 3234–47 (2013).
6. Ristic, G., Tsou, W.-L. & Todi, S. V. An optimal ubiquitin-proteasome pathway in the nervous system: the role of deubiquitinating enzymes. *Front. Mol. Neurosci.* **7**, 72 (2014).
7. Ndubaku, C. & Tsui, V. Inhibiting the deubiquitinating enzymes (DUBs). *J. Med. Chem.* **58**, 1581–95 (2015).
8. Drag, M. & Salvessen, G. S. Emerging principles in protease-based drug discovery. *Nat. Rev. Drug Discov.* **9**, 690–701 (2010).
9. Eletr, Z. M., Wilkinson, K. D., Sommer, T. & Wolf, D. H. Biochimica et Biophysica Acta Regulation of proteolysis by human deubiquitinating enzymes. *BBA - Mol. Cell Res.* **1843**, 114–128 (2014).
10. Komander, D. *et al.* Molecular discrimination of structurally equivalent Lys 63-linked and linear polyubiquitin chains. *EMBO Rep.* **10**, 466–473 (2009).
11. Hu, M. *et al.* Structure and mechanisms of the proteasome-associated deubiquitinating enzyme USP14. *EMBO J.* **24**, 3747–56 (2005).
12. Row, P. E. *et al.* The MIT domain of UBPY constitutes a CHMP binding and endosomal localization signal required for efficient epidermal growth factor receptor degradation. *J. Biol. Chem.* **282**, 30929–37 (2007).
13. Davies, C. W. & Paul, Lake N; Das, C. Mechanism of Recruitment and Activation of the Endosome-associated Deubiquitinase AMSH. *Biochemistry* **52**, 7818–7829 (2013).
14. Lee, K.-Y. *et al.* Human ELG1 regulates the level of ubiquitinated proliferating cell nuclear antigen (PCNA) through its interactions with PCNA and USP1. *J. Biol. Chem.* **285**, 10362–9 (2010).

15. Wang, B. *et al.* Abraxas and RAP80 form a BRCA1 protein complex required for the DNA damage response. *Science* **316**, 1194–1198 (2007).
16. Sobhian, B. *et al.* RAP80 targets BRCA1 to specific ubiquitin structures at DNA damage sites. *Science* **316**, 1198–1202 (2007).
17. Kim, H., Chen, J. & Yu, X. Ubiquitin-binding protein RAP80 mediates BRCA1-dependent DNA damage response. *Science* **316**, 1202–1205 (2007).
18. Guzzo, C. M. *et al.* RNF4-dependent hybrid SUMO-ubiquitin chains are signals for RAP80 and thereby mediate the recruitment of BRCA1 to sites of DNA damage. *Sci. Signal.* **5**, ra88 (2012).
19. Hu, X., Paul, A. & Wang, B. Rap80 protein recruitment to DNA double-strand breaks requires binding to both small ubiquitin-like modifier (SUMO) and ubiquitin conjugates. *J. Biol. Chem.* **287**, 25510–25519 (2012).
20. Ji, Z. *et al.* The forkhead transcription factor FOXK2 acts as a chromatin targeting factor for the BAP1-containing histone deubiquitinase complex. *Nucleic Acids Res.* **42**, 6232–42 (2014).
21. Komander, D. *et al.* The Structure of the CYLD USP Domain Explains Its Specificity for Lys63-Linked Polyubiquitin and Reveals a B Box Module. *Mol. Cell* **29**, 451–464 (2008).
22. Niu, J. *et al.* USP10 inhibits genotoxic NF- κ B activation by MCP1P1-facilitated deubiquitination of NEMO. *EMBO J.* **32**, 3206–3219 (2013).
23. Saridakis, V. *et al.* Structure of the p53 binding domain of HAUSP/USP7 bound to Epstein-Barr nuclear antigen 1 implications for EBV-mediated immortalization. *Mol. Cell* **18**, 25–36 (2005).
24. Sheng, Y. *et al.* Molecular recognition of p53 and MDM2 by USP7/HAUSP. *Nat. Struct. Mol. Biol.* **13**, 285–91 (2006).
25. Hayes, S. D. *et al.* Direct and indirect control of mitogen-activated protein kinase pathway-associated components, BRAP/IMP E3 ubiquitin ligase and CRAF/RAF1 kinase, by the deubiquitylating enzyme USP15. *J. Biol. Chem.* **287**, 43007–43018 (2012).
26. Nicassio, F. *et al.* Human USP3 Is a Chromatin Modifier Required for S Phase Progression and Genome Stability. *Curr. Biol.* **17**, 1972–1977 (2007).
27. Hu, M. *et al.* Crystal Structure of a UBP-Family Deubiquitinating Enzyme in Isolation and in Complex with Ubiquitin Aldehyde. *Cell* **111**, 1041–1054 (2002).
28. Faesen, A. C. *et al.* Mechanism of USP7/HAUSP activation by its C-terminal ubiquitin-like domain and allosteric regulation by GMP-synthetase. *Mol. Cell* **44**, 147–59 (2011).
29. Boudreaux, D. a, Maiti, T. K., Davies, C. W. & Das, C. Ubiquitin vinyl methyl ester binding orients the misaligned active site of the ubiquitin hydrolase UCHL1 into productive conformation. *Proc. Natl. Acad. Sci. U. S. A.* **107**, 9117–22 (2010).
30. Mikolajczyk, J. *et al.* Small ubiquitin-related modifier (SUMO)-specific proteases: profiling the specificities and activities of human SENPs. *J. Biol. Chem.* **282**, 26217–24 (2007).
31. Drag, M., Mikolajczyk, J., Krishnakumar, I. M., Huang, Z. & Salvesen, G. S. Activity profiling of human deSUMOylating enzymes (SENPs) with synthetic substrates suggests an unexpected specificity of two newly characterized members of the family. *Biochem. J.* **409**, 461–9 (2008).
32. Chen, C.-H., Namanja, A. T. & Chen, Y. Conformational flexibility and changes underlying activation of the SUMO-specific protease SENP1 by remote substrate binding. *Nat. Commun.* **5**, 4968 (2014).
33. Keusekotten, K. *et al.* OTULIN antagonizes LUBAC signaling by specifically hydrolyzing Met1-linked polyubiquitin. *Cell* **153**, 1312–26 (2013).

34. Cope, G. A. *et al.* Role of Predicted Metalloprotease Motif of Jab1 / Csn5 in Cleavage of Nedd8 from Cul1. *Science (80-.)*. **298**, 608–611 (2002).
35. Lingaraju, G., Bunker, R. & Cavadini, S. Crystal structure of the human COP9 signalosome. *Nature* (2014). doi:10.1038/nature13566
36. Worden, E. J., Padovani, C. & Martin, A. Structure of the Rpn11-Rpn8 dimer reveals mechanisms of substrate deubiquitination during proteasomal degradation. *Nat. Struct. Mol. Biol.* **21**, 220–7 (2014).
37. Pathare, G. R. *et al.* Crystal structure of the proteasomal deubiquitylation module Rpn8-Rpn11. *Proc. Natl. Acad. Sci. U. S. A.* **111**, 2984–9 (2014).
38. Cooper, E. M. *et al.* K63-specific deubiquitination by two JAMM/MPN+ complexes: BRISC-associated Brcc36 and proteasomal Poh1. *EMBO J.* **28**, 621–31 (2009).
39. Lee, K. K., Florens, L., Swanson, S. K., Washburn, M. P. & Workman, J. L. The deubiquitylation activity of Ubp8 is dependent upon Sgf11 and its association with the SAGA complex. *Mol. Cell. Biol.* **25**, 1173–82 (2005).
40. Samara, N. L. *et al.* Structural insights into the assembly and function of the SAGA deubiquitinating module. *Science* **328**, 1025–9 (2010).
41. Köhler, A., Zimmerman, E., Schneider, M., Hurt, E. & Zheng, N. Structural basis for assembly and activation of the heterotetrameric SAGA histone H2B deubiquitinase module. *Cell* **141**, 606–17 (2010).
42. Yan, M. & Wolberger, C. Uncovering the role of Sgf73 in maintaining SAGA Deubiquitinating Module Structure and Activity. *J. Mol. Biol.* **427**, 1765–1778 (2015).
43. Reyes-Turcu, F. E. *et al.* The ubiquitin binding domain ZnF UBP recognizes the C-terminal diglycine motif of unanchored ubiquitin. *Cell* **124**, 1197–208 (2006).
44. Avvakumov, G. V. *et al.* Two ZnF-UBP domains in isopeptidase T (USP5). *Biochemistry* **51**, 1188–98 (2012).
45. Clerici, M., Luna-Vargas, M. P. a, Faesen, A. C. & Sixma, T. K. The DUSP-Ubl domain of USP4 enhances its catalytic efficiency by promoting ubiquitin exchange. *Nat. Commun.* **5**, 5399 (2014).
46. Bozza, W. P. & Zhuang, Z. Enzyme Ubp15 and the Regulatory Role of Its Terminal Domains. *Biochemistry* **50**, 6423–6432 (2011).
47. Van der Knaap, J. A. *et al.* GMP synthetase stimulates histone H2B deubiquitylation by the epigenetic silencer USP7. *Mol. Cell* **17**, 695–707 (2005).
48. Huang, T. T. *et al.* Regulation of monoubiquitinated PCNA by DUB autocleavage. *Nat. Cell Biol.* **8**, 339–347 (2006).
49. Nijman, S. M. B. *et al.* The deubiquitinating enzyme USP1 regulates the fanconi anemia pathway. *Mol. Cell* **17**, 331–339 (2005).
50. Cohn, M. A. *et al.* A UAF1-containing multisubunit protein complex regulates the Fanconi anemia pathway. *Mol. Cell* **28**, 786–97 (2007).
51. Villamil, M. A., Chen, J., Liang, Q. & Zhuang, Z. A noncanonical cysteine protease USP1 is activated through active site modulation by USP1-associated factor 1. *Biochemistry* **51**, 2829–39 (2012).
52. Kee, Y. *et al.* WDR20 regulates activity of the USP12 x UAF1 deubiquitinating enzyme complex. *J. Biol. Chem.* **285**, 11252–7 (2010).
53. Cohn, M. A. *et al.* Article A UAF1-Containing Multisubunit Protein Complex Regulates the Fanconi Anemia Pathway. **1**, 786–797 (2007).
54. Cohn, M. A. *et al.* UAF1 is a subunit of multiple deubiquitinating enzyme complexes. *J. Biol. Chem.* **284**, 5343–51 (2009).

55. McCullough, J. *et al.* Activation of the endosome-associated ubiquitin isopeptidase AMSH by STAM, a component of the multivesicular body-sorting machinery. *Curr. Biol.* **16**, 160–5 (2006).
56. Liu, J. *et al.* Beclin1 controls the levels of p53 by regulating the deubiquitination activity of USP10 and USP13. *Cell* **147**, 223–34 (2011).
57. Juang, Y.-C. *et al.* OTUB1 co-opts Lys48-linked ubiquitin recognition to suppress E2 enzyme function. *Mol. Cell* **45**, 384–97 (2012).
58. Wiener, R., Zhang, X., Wang, T. & Wolberger, C. The mechanism of OTUB1-mediated inhibition of ubiquitination. *Nature* **483**, 618–22 (2012).
59. Wiener, R. *et al.* E2 ubiquitin-conjugating enzymes regulate the deubiquitinating activity of OTUB1. *Nat. Struct. Mol. Biol.* **20**, 1033–9 (2013).
60. Sanchez-Pulido, L., Kong, L. & Ponting, C. P. A common ancestry for BAP1 and Uch37 regulators. *Bioinformatics* **28**, 1953–6 (2012).
61. Scheuermann, J. C. *et al.* Histone H2A deubiquitinase activity of the Polycomb repressive complex PR-DUB. *Nature* **465**, 243–7 (2010).
62. Yao, T. *et al.* Proteasome recruitment and activation of the Uch37 deubiquitinating enzyme by Adrm1. *Nat. Cell Biol.* **8**, 994–1002 (2006).
63. Hamazaki, J. *et al.* A novel proteasome interacting protein recruits the deubiquitinating enzyme UCH37 to 26S proteasomes. *EMBO J.* **25**, 4524–36 (2006).
64. Qiu, X.-B. *et al.* hRpn13/ADRM1/GP110 is a novel proteasome subunit that binds the deubiquitinating enzyme, UCH37. *EMBO J.* **25**, 5742–53 (2006).
65. Sahtoe, D. D. *et al.* Mechanism of UCH-L5 Activation and Inhibition by DEUBAD Domains in RPN13 and INO80G. *Mol. Cell* **57**, 887–900 (2015).
66. VanderLinden, R. T. *et al.* Structural Basis for the Activation and Inhibition of the UCH37 Deubiquitylase. *Mol. Cell* **57**, 901–11 (2015).
67. Yao, T. *et al.* Distinct modes of regulation of the Uch37 deubiquitinating enzyme in the proteasome and in the Ino80 chromatin-remodeling complex. *Mol. Cell* **31**, 909–17 (2008).
68. Nishi, R. *et al.* Systematic characterization of deubiquitylating enzymes for roles in maintaining genome integrity. *Nat. Cell Biol.* (2014). doi:10.1038/ncb3028
69. Kimura, Y. *et al.* An inhibitor of a deubiquitinating enzyme regulates ubiquitin homeostasis. *Cell* **137**, 549–59 (2009).
70. Richter, C., West, M. & Odorizzi, G. Dual mechanisms specify Doa4-mediated deubiquitination at multivesicular bodies. *EMBO J.* **26**, 2454–64 (2007).
71. Juhasz, S. *et al.* Characterization of human Spartan/C1orf124, an ubiquitin-PCNA interacting regulator of DNA damage tolerance. *Nucleic Acids Res.* **40**, 10795–808 (2012).
72. Centore, R. C., Yazinski, S. a, Tse, A. & Zou, L. Spartan/C1orf124, a reader of PCNA ubiquitylation and a regulator of UV-induced DNA damage response. *Mol. Cell* **46**, 625–35 (2012).
73. Huang, O. W. *et al.* Phosphorylation-dependent activity of the deubiquitinase DUBA. *Nat. Struct. Mol. Biol.* **19**, 171–5 (2012).
74. Huang, X. *et al.* Deubiquitinase USP37 Is Activated by CDK2 to Antagonize APCCDH1 and Promote S Phase Entry. *Mol. Cell* **42**, 511–523 (2011).
75. Villamil, M. a *et al.* Serine phosphorylation is critical for the activation of ubiquitin-specific protease 1 and

- its interaction with WD40-repeat protein UAF1. *Biochemistry* **51**, 9112–23 (2012).
76. Elliott, P. R. *et al.* Article Molecular Basis and Regulation of OTULIN-LUBAC Interaction. *Mol. Cell* **54**, 335–348 (2014).
 77. Schaeffer, V. *et al.* Binding of OTULIN to the PUB Domain of HOIP Controls NF- κ B Signaling. *Mol. Cell* **54**, 349–361 (2014).
 78. Hutti, J. E. *et al.* Phosphorylation of the tumor suppressor CYLD by the breast cancer oncogene IKKepsilon promotes cell transformation. *Mol. Cell* **34**, 461–72 (2009).
 79. Kobayashi, T., Masoumi, K. C. & Massoumi, R. Deubiquitinating activity of CYLD is impaired by SUMOylation in neuroblastoma cells. *Oncogene* 1–10 (2014). doi:10.1038/onc.2014.159
 80. Meulmeester, E., Kunze, M., Hsiao, H. H., Urlaub, H. & Melchior, F. Mechanism and consequences for paralog-specific sumoylation of ubiquitin-specific protease 25. *Mol. Cell* **30**, 610–9 (2008).
 81. Meray, R. K. & Lansbury, P. T. Reversible monoubiquitination regulates the Parkinson disease-associated ubiquitin hydrolase UCH-L1. *J. Biol. Chem.* **282**, 10567–75 (2007).
 82. Todi, S. V. *et al.* Ubiquitination directly enhances activity of the deubiquitinating enzyme ataxin-3. *EMBO J.* **28**, 372–82 (2009).
 83. Seki, T. *et al.* Jsd1, a membrane-targeted deubiquitinating enzyme, is activated by ubiquitination and regulates membrane dynamics, cell motility, and endocytosis. *J. Biol. Chem.* **288**, 17145–55 (2013).
 84. Mashtalir, N. *et al.* Autodeubiquitination Protects the Tumor Suppressor BAP1 from Cytoplasmic Sequestration Mediated by the Atypical Ubiquitin Ligase UBE2O. *Mol. Cell* **54**, 392–406 (2014).
 85. Zhang, L. *et al.* USP4 is regulated by AKT phosphorylation and directly deubiquitylates TGF- β type I receptor. *Nat. Cell Biol.* **14**, 717–726 (2012).
 86. Yuan, J., Luo, K., Zhang, L., Cheville, J. C. & Lou, Z. USP10 Regulates p53 Localization and Stability by Deubiquitinating p53. *Cell* **140**, 384–396 (2010).
 87. Kulathu, Y. *et al.* Regulation of A20 and other OTU deubiquitinases by reversible oxidation. *Nat. Commun.* (2013). doi:10.1038/ncomms2567
 88. Lee, J.-G., Baek, K., Soetandyo, N. & Ye, Y. Reversible inactivation of deubiquitinases by reactive oxygen species in vitro and in cells. *Nat. Commun.* **4**, 1568 (2013).
 89. Cotto-Rios, X. M., Békés, M., Chapman, J., Ueberheide, B. & Huang, T. T. Deubiquitinases as a Signaling Target of Oxidative Stress. *Cell Rep.* **2**, 1475–1484 (2012).
 90. Silva, G. M., Finley, D. & Vogel, C. K63 polyubiquitination is a new modulator of the oxidative stress response. *Nat. Struct. Mol. Biol.* **22**, 116–23 (2015).
 91. Finkel, T. Signal transduction by reactive oxygen species. *J. Cell Biol.* **194**, 7–15 (2011).
 92. Baymaz, H. I. *et al.* MBD5 and MBD6 interact with the human PR-DUB complex through their methyl-CpG-binding domain. *Proteomics* **14**, 2179–89 (2014).
 93. Komander, D. & Rape, M. The ubiquitin code. *Annu. Rev. Biochem.* **81**, 203–29 (2012).
 94. Meyer, H.-J. & Rape, M. Enhanced protein degradation by branched ubiquitin chains. *Cell* **157**, 910–21 (2014).
 95. Reverter, D. *et al.* Structure of a complex between Nedd8 and the Ulp/Senp protease family member Den1. *J. Mol. Biol.* **345**, 141–51 (2005).

chapter | THREE

Mechanism of UCH-L5 activation and inhibition by DEUBAD domains in RPN13 and INO80C

¹Danny D. Sahtoe, ¹Willem J. Van Dijk, ^{2,3}Farid El Oualid,
²Reggy Ekkebus, ²Huib Ovaa and ^{1*}Titia K. Sixma.

¹*Division of Biochemistry and Cancer genomics center*

²*Division of Cell biology II*

Netherlands Cancer Institute, Plesmanlaan 121, 1066CX, Amsterdam, the Netherlands

³*UbiQ, Science Park 408, 1098XH Amsterdam, the Netherlands*

**correspondence: t.sixma@nki.nl*

Molecular Cell (2015), 57(5):887-900

ABSTRACT

Deubiquitinating enzymes (DUBs) control vital processes in eukaryotes by hydrolyzing ubiquitin adducts. Their activities are tightly regulated but the mechanisms remain elusive. In particular, the DUB UCH-L5 can be either activated or inhibited by conserved regulatory proteins RPN13 and INO80G respectively. Here we show how the DEUBAD domain in RPN13 activates UCH-L5 by positioning its C-terminal ULD domain and cross-over loop to promote substrate binding and catalysis. The related DEUBAD domain in INO80G inhibits UCH-L5, by exploiting similar structural elements in UCH-L5 to promote a radically different conformation and employs molecular mimicry to block ubiquitin docking. In this process large conformational changes create small but highly specific interfaces that mediate activity modulation of UCH-L5 by altering the affinity for substrates. Our results establish how related domains can exploit enzyme conformational plasticity to allosterically regulate DUB activity. These allosteric sites may present novel insights for pharmaceutical intervention in DUB activity.

INTRODUCTION

The ubiquitin conjugation machinery regulates almost every process in the eukaryotic cell. Deubiquitinating enzymes (DUBs) are a critical component of the machinery since they can remove ubiquitin adducts and thereby control the level of ubiquitin signals¹. In accordance with their important roles, DUBs are frequently deregulated in human pathologies including cancer and neurological disease², making DUBs potential prime targets for therapeutic intervention.

The level of the intrinsic DUB activity is important and requires precise control. For a subset of DUBs there is emerging evidence that the catalytic activity can be modulated by regulatory proteins or by internal domains³. Notable examples include USP7 activation by its HUBL domain and GMPS⁴, USP1 activation by UAF1⁵ and Ubp8 activation in the SAGA complex^{6,7}. The most striking example is UCH-L5, for which both activation and inhibition have been observed⁸⁻¹¹, by two different proteins, RPN13 (ADRM1) and INO80G (NFRKB) respectively.

Understanding the mechanisms of DUB activation is important for interpreting their roles in specific cellular contexts. Mechanistic insight into regulatory mechanisms can also provide vital information for development of inhibitors or activators. So far, the only available crystal structure of a DUB-activator complex is that of the SAGA DUB module^{12,13}, but no structure is available for its inactive state. Due to this lack of structural data, detailed mechanisms of DUB regulation are still poorly understood.

UCH-L5 (UCH37) is a cysteine protease of the ubiquitin C-terminal hydrolase (UCH) family of DUBs, which also includes UCH-L1, UCH-L3 and BAP1. UCH-L5 is overexpressed in several carcinomas¹⁴⁻¹⁶ and knock-out of the gene is embryonically lethal in mice¹⁷. Functionally, it has been linked to TGF- β signaling, Alzheimer's disease and longevity¹⁸⁻²¹. UCH-L5 constitutes a component of proteasomes and INO80 chromatin remodeling complexes where it is activated and inhibited respectively.

As a non-essential component of the proteasome 19S regulatory particle, UCH-L5 catalyzes K48-linked polyubiquitin hydrolysis. This activity requires the RPN13 subunit whose C-terminal domain binds UCH-L5⁹⁻¹¹. *In vitro*, RPN13 is able to directly promote UCH-L5 activity against a minimal substrate⁹⁻¹¹.

UCH-L5 has a less well defined role in metazoan INO80 chromatin remodeling complexes. INO80 is an essential determinant of embryonic stem cell identity^{22,23} and participates in the DNA damage response²⁴, but the function of the metazoan-specific subunits, such as

INO80G is poorly defined. A recent report has implicated UCH-L5 and INO80G as key factors of the DNA double strand break response²⁵. Interestingly, in the context of the INO80 complex the DUB activity of UCH-L5 is inhibited by the INO80G subunit⁸. Intriguingly an artificial shorter version of INO80G was found to activate UCH-L5 *in vitro*⁸.

The UCH enzymes have a small highly conserved papain-like catalytic domain characterized by a flexible active site cross-over loop (CL). The CL is thought to select substrates according to leaving group size^{26,27}. In UCH-L5 and UCH family member BAP1 the CL is relatively large, enabling them to process larger substrates²⁷.

Within the UCH family UCH-L5 and BAP1 are close relatives. BAP1 is a critical tumor suppressor whose regulation is important for proper gene regulation²⁸⁻³⁰. UCH-L5 and BAP1 share an unusual C-terminal helical extension, called ULD³¹. The ULD domain could mediate protein-protein interactions, including higher order homo-oligomerization^{32,33}, and was proposed to act as an auto-inhibitory module¹¹.

Like UCH-L5, BAP1 can be activated by a regulatory protein, in this case ASX, to promote H2A deubiquitination³⁴. Phylogenetic analyses have uncovered a conserved domain within the UCH regulatory proteins RPN13, INO80G and ASX, that was named the DEUBAD domain³⁵. As all three proteins affect UCH activity, it was proposed that the DEUBAD domain is responsible for this modulation. The conservation suggests a common mechanism of regulation, but where ASX and RPN13 activate their cognate DUB, INO80G inhibits it. Thus the DEUBAD domain has shifted from activator to inhibitor mode. The mechanistic details of this dual mode of action of the DEUBAD domains are unclear.

Here we present structural and functional analyses that explain how DEUBAD domains can switch UCH-L5 activity and thus provide either positive or negative regulation. We show how the DEUBAD domain in RPN13 activates UCH-L5 by tuning the conformation of structural elements in UCH-L5, and inhibits in INO80G, where it exploits molecular mimicry and UCH-L5 conformational plasticity to prevent ubiquitin docking and catalysis. We also show how the inhibitory domain in INO80G has retained the ability to activate, by its N-terminal INO80G_{short} region and identify the structural elements in the DEUBAD domains that confer the activating or inhibitory effects on UCH-L5 enzymatic activity. Our data show that this remarkable tuning of activity involves large conformational changes and is mediated by precise positioning of both the UCH-L5 C-terminal ULD and active site cross over loop (CL).

RESULTS

Crystal structures of activated and inhibited UCH-L5

To study the regulation of UCH-L5 by DEUBAD domains we purified human UCH-L5 in complex with the DEUBAD domains of RPN13 (aa 265-388, referred to as RPN13^{DEU}) and INO80G (aa 39-170, referred to as INO80G^{DEU}) (Figure 1A). We measured the catalytic activity of these complexes towards the minimal substrate ubiquitin-7-amido-4-methylcoumarin (Ub-AMC)^{36,37} in comparison to full-length UCH-L5 alone (U) and its isolated catalytic domain (CD). In line with previous data, we find that the DEUBAD domain of RPN13 activates UCH-L5 (UR) (Figure 1B)⁹⁻¹¹. Since the UCH-L5 CD is more active than the full-length alone, the ULD domain partially inhibits activity¹¹. However, in the presence of RPN13^{DEU} UCH-L5 is significantly more active than the UCH-L5 CD and therefore RPN13^{DEU} does more than simply removing autoinhibition (Figure 1B). Strikingly, INO80G^{DEU} severely inhibits activity under these conditions (UI) (Figure 1B).

We wondered how these related DEUBAD domains achieve such remarkably opposite effects on regulation. To assess this we performed structural studies on UCH-L5 in complex with DEUBAD domains and compared them with apo UCH-L5³² (Fig 1C). We determined a crystal structure of UCH-L5 in complex with the inhibitory domain INO80G^{DEU} at 3.7 Å (Figure 1D). Additionally, we determined crystal structures of UCH-L5 in complex with activating RPN13^{DEU}, with and without the suicide inhibitor ubiquitin-propargyl (Ub-Prg)^{38,39} at 2.3 Å and 2.8 Å respectively (Figures 1E and 1F). All structures were refined to acceptable statistics (Table 1).

The resulting structures display striking differences (Figures 1D-F). Both RPN13^{DEU} and INO80G^{DEU} primarily bind the C-terminal ULD domain of UCH-L5, but are positioned radically different relative to the UCH-L5 CD, which itself hardly changes conformation between all UCH-L5 structures. The differences arise from major changes in orientation of the ULDs relative to the catalytic domain (Figure 1G). The ULDs adopt a wide range of positions relative to the CD, even in previously known UCH-L5 structures^{32,40} suggesting that this element is flexible in solution. Activator and inhibitor may lock this domain in particular conformations.

To allow UCH-L5 binding, RPN13^{DEU} changes conformation compared to the previously determined RPN13^{DEU} apo-state⁴¹, by rearranging core helices $\alpha 1$ - $\alpha 4$ and the $\alpha 3$ - $\alpha 4$ loop (Figure 1H). In this new conformation, the core of INO80G^{DEU} and RPN13^{DEU} resemble each other, underscoring their common ancestry (Figures 1I and S1A). The C-termini of the DEUBAD domains, however, diverge dramatically. Where helices $\alpha 6$ - $\alpha 8$ (aa 350-384) form a platform in RPN13^{DEU}, the equivalent region in INO80G^{DEU} forms a single extended helix ($\alpha 6$). Another notable difference between the two DEUBAD domains is a short

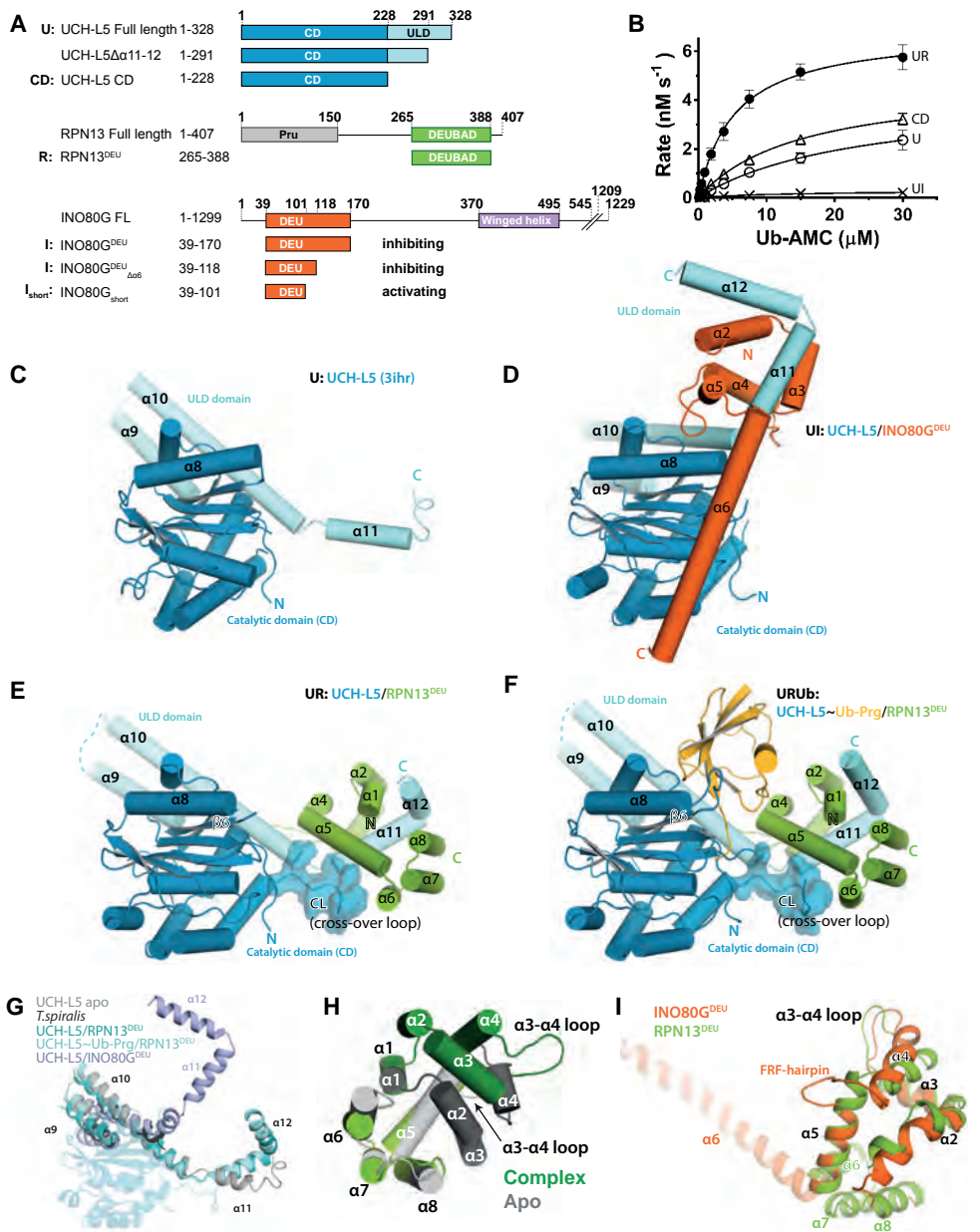


Figure 1 | Crystal structures UCH-L5/DEUBAD complexes. **A)** Constructs used in this study. **B)** RPN13^{DEU} activates UCH-L5 (UR) while INO80G^{DEU} inhibits UCH-L5 (UI) in Ub-AMC enzyme kinetics. The CD is slightly more active than FL UCH-L5 (U). See Fig. 1A for naming codes. Error bars represent standard deviation of mean. **C)** Structure of apo UCH-L5 (3ihr). The CD is colored in blue and the ULD domain in light blue. **D)** Structure of UCH-L5/INO80G^{DEU} (INO80G^{DEU} in orange). **E)** Structure of UCH-L5/RPN13^{DEU} (RPN13^{DEU} in green). **F)** Structure of UCH-L5~Ub-Prg/RPN13^{DEU} with Ub-Prg in yellow. **G)** The ULDs are found in different conformations across UCH-L5 structures. The catalytic domain is transparent for clarity. **H)** RPN13^{DEU} (green) changes towards an open state upon UCH-L5 complex formation compared to apo RPN13^{DEU} (grey). Helices α 1-4 and the α 3-4 loop that undergo the largest changes are colored in darker shades. **I)** Superposition of RPN13^{DEU} and INO80G^{DEU}. DEUBAD domains deviate most at FRF-hairpin and helix α 6.

Table 1 | Crystallography details

Data collection		UCH-L5/RPN13 ^{DEU}	UCH-L5~ UbPrg/ RPN13 ^{DEU}	UCH-L5/ INO80C ^{DEU}	UCH-L5~ Ub-Prg/ INO80C _{short}
Wavelength (Å)		0.98	0.87	0.91	0.87
Resolution (Å)		33.5(2.8)	45.3(2.3)	47.7(3.7)	47.7(3.7)
Space group		P2 ₁ 2 ₁ 2 ₁	P2 ₁ 2 ₁ 2 ₁	P4 ₁ 22	C2
Unit cell	a, b, c (Å)	56.6, 97.07, 100.6	59.34, 98.6, 100.2	94.88, 94.88, 132	152.1, 137.8, 98.9
	α, β, γ (°)	90, 90, 90	90, 90, 90	90, 90, 90	90, 102.5, 90
CC _{1/2} (%)		99.8(72.9)	99.9(67.6)	98.3(41.8)	98.4(72.6)
R _{merge} (%)		7.1(93.0)	12.6(83.2)	20.9(73.2)	19.9(66.4)
I/σI		15.3(2.2)	9.7(1.6)	7.4(2.4)	5.8(1.8)
Completeness (%)		98.5(97.3)	99.8(98.9)	99.5(100)	97.9(90.3)
Redundancy		3.9(3.7)	4.1(4.1)	6.7(6.8)	4.2(4.0)
Refinement					
Number of unique reflections		13635	26949	7004	21090
R _{work} /R _{free} (%)		23.2/28.4	19.5/23.5	30.4/35.4	23.8/26.6
R.m.s.d. Bond lengths (Å)		0.003	0.005	0.004	0.008
R.m.s.d. Bond angles (°)		0.7	1.0	0.7	1.2
*Ramachandran statistics (%) (preferred/allowed/not allowed)		99.2/0.8/0	98.5/1.5/0	97.7/2.03/0	95.02/4.98/0

High resolution shells in parentheses

*Molprobit

hairpin (aa 96-103) exclusively present in INO80G, that we named the FRF-hairpin. It is inserted between helix α4 and α5 of the DEUBAD domain and is conserved in INO80G orthologs (Figures 1I and S1B).

The structural conservation of the DEUBAD domains is also reflected in their similar binding modes to UCH-L5 (Figures 1D-F and S1C). In both complexes, the core DEUBAD domains bind primarily to the C-terminal ULD of UCH-L5 where amphipathic helix α11 is clasped by the DEUBAD domains and further stabilized by helix α12 in an extensive hydrophobic interface (Figure S1D and S1E). DEUBAD domain binding requires these helices, since a UCH-L5 variant that lacking these (UCH-L5_{Δα11-12}), does not interact with RPN13^{DEU}, whereas the wild type UCH-L5 binds tightly (K_D=6 nM) in isothermal titration calorimetry (ITC) (Figure S1F and Table S4).

In short, the conserved DEUBAD domains bind to UCH-L5 but show dramatically different arrangements. In the next sections we examine how these are achieved and how they can lead to differences in UCH-L5 activity. The structural consequences of ubiquitin binding are discussed in the light of the mechanism of activation and inhibition.

DEUBAD domains tune UCH-L5 substrate affinity

Analysis of UCH-L5 kinetic parameters (Figure 1B and Table S1) reveals that RPN13^{DEU} binding primarily changes the K_M of the enzyme but hardly affects k_{cat} . Therefore we wondered if changes in substrate affinity of UCH-L5 could explain regulation by DEUBAD domains

We assessed the ability of UCH-L5 to bind a model substrate in the presence and absence of the DEUBAD domains using ITC. The model substrate Ub-GlySerThr was titrated into active site cysteine (C88A) mutants of the different UCH-L5 complexes. We observed robust binding ($K_D=4.5 \mu\text{M}$) for UCH-L5/RPN13^{DEU}, whereas binding to UCH-L5 alone, UCH-L5 CD and UCH-L5/INO80G^{DEU} did not reach saturation, with the UCH-L5/INO80G^{DEU} complex giving the lowest signal (Figures 2A, S2A and Table S3). These results suggest that RPN13^{DEU} enhances UCH-L5 substrate binding, whereas INO80G^{DEU} diminishes it. We validated these results in fluorescence polarization (FP) binding assays, using Ub-LysGly-TAMRA as a model substrate⁴², demonstrating that DEUBAD domains tune UCH-L5 activity at the level of substrate binding (Figure 2B).

Ubiquitin binding by the UCH-L5/RPN13^{DEU} complex

UCH-L5 activation by the RPN13 DEUBAD domain results from enhanced ubiquitin-substrate binding, therefore we analyzed the details of ubiquitin interaction in the UCH-L5~UbPrg/RPN13^{DEU} crystal structure (Figures 2C). The presence of Ub-Prg hardly changes the global UCH-L5/RPN13^{DEU} conformation (Figure 1). Direct contact between ubiquitin and RPN13^{DEU} involves a small interface (286 Å²) with three hydrogen bonds (Figures 2C and 2D). Moreover, this interface does not affect the position and orientation of ubiquitin on UCH-L5, which resembles the previously solved *T.spiralis* UCH-L5 ubiquitin complex. In fact, it is identical to the canonical ubiquitin binding mode found in all UCH family members (Figure 2E).

In practice, ubiquitin binds via its C-terminal tail close to the active site and via its core relatively far from the active site, in a series of so-called ‘exosites’. In the UCH-L5 complex, the ubiquitin C-terminal tail adopts an extended conformation. It is buried and positioned by an extensive network of side chain and backbone interactions with the catalytic domain (Figures 2C and 2F).

The binding of the ubiquitin core creates three specific exosite interactions on the UCH-L5 CD. The first involves UCH-L5 Trp36, which rearranges, compared to apo UCH-L5/RPN13^{DEU}, to avoid clashes and to promote a direct contact with ubiquitin Ile44 (Figures 2C and 2G), the primary hydrophobic binding site on ubiquitin.

A second exosite interaction involves UCH-L5 Ile216 at the C-terminus of helix $\alpha 8$ (Figure

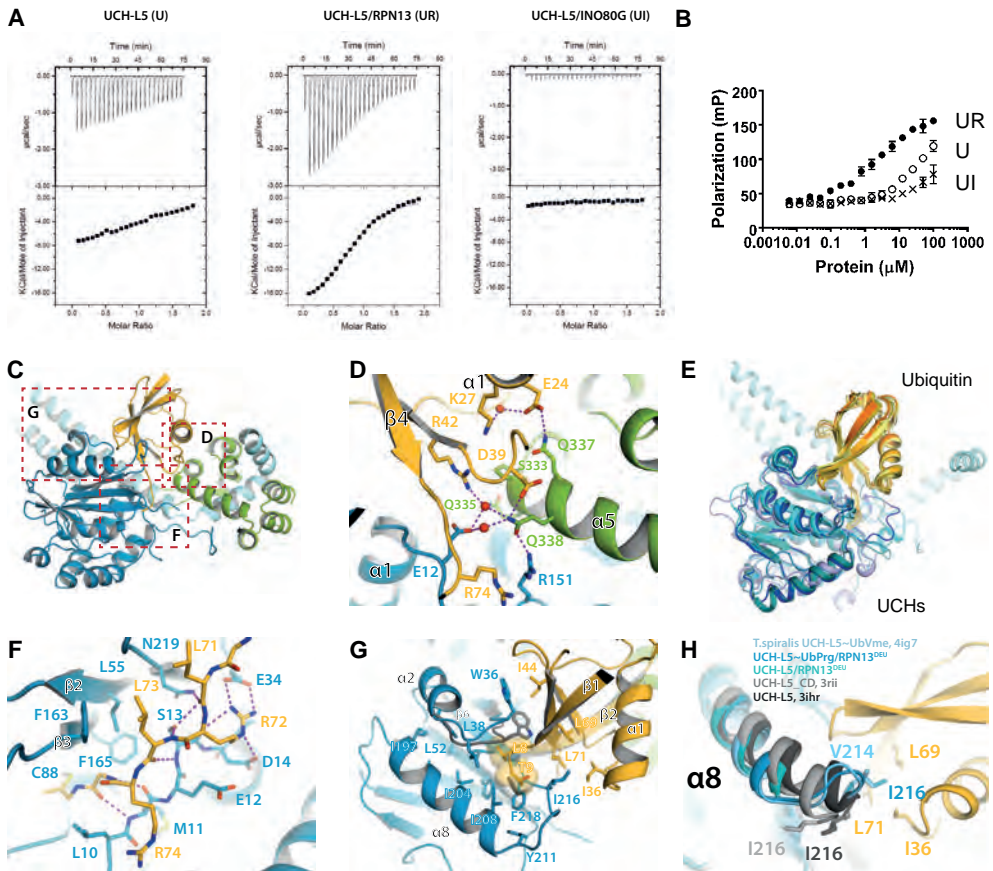


Figure 2 | Ubiquitin binding of UCH-L5 complexes. **A**) RPN13^{DEU} increases UCH-L5's affinity for model substrate Ub-GlySerThr whereas INO80G^{DEU} decreases the signal in ITC. **B**) Validation of binding results using model substrate Ub-LysGlyTAMRA in FP binding assays. **C**) Overview of the ubiquitin binding interface of the UCH-L5- Ub-Prg/RPN13^{DEU} complex. **D**) Contacts between ubiquitin and RPN13^{DEU} are limited. **E**) Ubiquitin binding in the UCH family is structurally conserved (UCH-L5/RPN13^{DEU}, *T.spiralis* UCH-L5: 4i6n, UCH-L1: 3ifw, UCH-L3: 1xd3, *P.faliciparum* UCH-L3: 2wdt). **F**) The ubiquitin tail is extensively coordinated. **G**) The ubiquitin core is stabilized by three specific exosite contacts. UCH-L5/RPN13^{DEU} (without Ub-Prg) displayed in grey sticks. **H**) Partial melting of UCH-L5 helix $\alpha 8$ relocates Ile216 to contact the ubiquitin Ile36 patch. This interaction is conserved in *T.spiralis* UCH-L5.

2G). This helix melts out in UCH-ubiquitin complexes but is extended in the absence of ubiquitin (Figure S2B). Partial melting of $\alpha 8$ is crucial since it rearranges Ile216 from a buried position to a position in the $\alpha 8$ - $\beta 6$ connecting loop that is compatible with ubiquitin binding, similar to *T.spiralis* UCH-L5 where Val214 (equivalent to human Ile216) contacts the ubiquitin Ile36 patch⁴⁰ (Figure 2H). Interestingly, in the UCH-L5/RPN13^{DEU} structure, the C-terminus of helix $\alpha 8$ is already disordered in the absence of ubiquitin, indicating that RPN13^{DEU} may affect this region allosterically to facilitate ubiquitin binding.

Finally, the melting of helix $\alpha 8$ and ordering of the $\alpha 8$ - $\beta 6$ connecting loop promotes po-

sitioning of Phe218 and formation of a highly conserved pocket that includes UCH-L5 Leu38. This hydrophobic pocket on UCH-L5 allows a snug interaction with the ubiquitin β 1- β 2 hairpin containing Leu8 and Thr9 (Figure 2G). Formation of this pocket was described for UCH-L1, upon ubiquitin interaction⁴³. In UCH-L1 the Phe214 positioning promotes rearrangement of Phe53 (equivalent to UCH-L5 residues: Phe218 and Phe56) which is necessary to organize the catalytic site conformation. In UCH-L5 this relay is not required, since Phe56 is already positioned such that the catalytic triad is active in the apo-structure. Nevertheless, the conformational change of UCH-L5 Phe218 in this pocket is conserved upon ubiquitin binding, as is the interaction with the ubiquitin β 1- β 2 hairpin. All three exosite interactions are well conserved in the UCH family, explaining the remarkably similar ubiquitin positioning on the UCH catalytic domains (Figure 2E).

The DEUBAD domain of RPN13 activates UCH-L5 by ULD and CL positioning

To investigate how RPN13^{DEU} promotes enhanced substrate binding by UCH-L5 we tested the effect of mutations on activity. We first focused on the effect on activation of the ubiquitin binding residues in UCH-L5. Mutations in these residues lowered the activity substantially, irrespective of the presence of RPN13^{DEU} indicating that they are primarily important for basic DUB function (Figure 3A). We then tested mutations of RPN13^{DEU} located in the interface with ubiquitin and found that these provided only a limited contribution to UCH-L5 activation (Figures 2D and S2C).

To further explore the molecular origins of the activation we analyzed the evolutionary conservation of surface residues on UCH-L5 with ConSurf⁴⁴. A UCH-L5 sequence alignment from species across all major eukaryotic lineages that possess both RPN13 and UCH-L5 was projected onto the UCH-L5 structure. This was compared to an analogous conservation analysis for UCH-L3, a prototype UCH member that lacks the C-terminal ULD domain. We noted several conserved regions. Both UCHs have a conserved surface patch where ubiquitin binds (Figure 3B). Adjacent to this patch, we found a second highly conserved site in UCH-L5 orthologs that is absent in UCH-L3 orthologs. This site centers on Glu283, and anchors the ULD to the catalytic domain through a polar interaction network (Figure 3C). The strong conservation of this ULD anchor is intriguing as the area is not directly involved in ubiquitin or RPN13^{DEU} binding.

We assessed the functional importance of the ULD anchor by testing UCH-L5 mutants in Ub-AMC assays. UCH-L5_{E283A} had similar activity to WT but this mutant could not be activated to the same extent as WT by RPN13^{DEU}, mainly due to weaker K_M (Figure 3D and Tables S1-2). The fact that this E283A mutation does not affect intrinsic UCH-L5 activity, but only the activity of the RPN13^{DEU} complex strongly suggests that an intact ULD anchor is required for RPN13^{DEU} dependent activation of UCH-L5. Next we tested the effect of

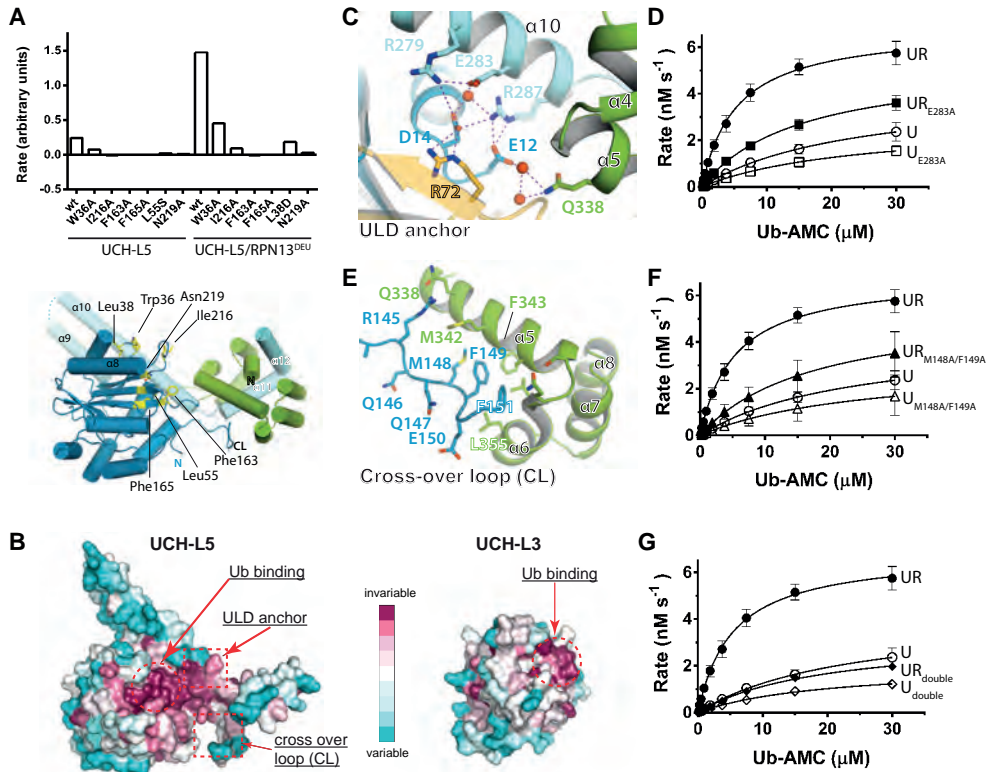


Figure 3 | Activation mechanism RPN13^{DEU}. **A**) Mutations in the ubiquitin interface severely compromise DUB activity irrespective of RPN13^{DEU} (top). Location mutants (yellow sticks) on UCH-L5 (bottom). **B**) Surface representation of UCH-L3 and UCH-L5 color coded by conservation. **C**) UCH-L5 helix $\alpha 10$ is anchored to the CD via an extensive polar network. **D and F**) In comparison with WT (UR and U from Figure 1B) UCH-L5 mutants E283A and M148A/F149A cannot be activated by RPN13^{DEU} to same extent on Ub-AMC. **E**) The CL is positioned by RPN13^{DEU}. **G**) Activation of the combined CL and ubiquitin anchor mutants E283A/M148A/F149A is almost completely abrogated in comparison to WT (UR and U from Figure 1B).

E283A mutation on substrate binding. Using ITC and stopped-flow binding analysis we found that UCH-L5_{E283A}/RPN13^{DEU} shows decreased affinity for Ub-substrates compared to WT complex (Figures S2A, S2D and Table S3). This indicates that RPN13^{DEU} induces a higher affinity for substrates by utilizing the intact ULD anchor.

Next, we focused our attention on the UCH-L5 cross-over loop (CL) that is disordered in most UCH-L5 crystal structures. In our complexes the CL makes contacts with RPN13^{DEU} (Figure 3E) via the highly conserved Met148 and Phe149, partially ordering the loop. Given the importance of the CL for the ability of UCHs to process larger substrates^{26,27} we made mutants to test whether the interface of the CL with RPN13^{DEU} could affect activity by positioning the loop. In a Ub-AMC assay, UCH-L5_{M148A/F149A} hydrolyzed Ub-AMC comparable to WT indicating that the mutant was still functional. However, this mutant

was only marginally activated by addition of RPN13^{DEU} (2.7 fold instead of 7-fold in WT) indicating that UCH-L5 activation by RPN13^{DEU} requires an intact CL (Figure 3F and Tables S1-2). Interestingly, unlike the ULD anchor mutant, the CL mutant and WT complexes bind model substrates with similar affinities (Figures S2A and S2D and Table S3).

Combining the CL and ULD anchor mutants into UCH-L5_{double} resulted in an almost complete abrogation of RPN13^{DEU} mediated activation illustrating that the CL and ULD anchor are the principal regulatory sites used by RPN13^{DEU} (Figure 3G). As none of the UCH-L5 mutants were compromised in RPN13^{DEU} binding as shown by ITC (Figure S2E and Table S4) we conclude that RPN13^{DEU} exerts its stimulatory effect on UCH-L5 through positioning of the CL and ULD anchor.

Mechanism of UCH-L5 inhibition by INO80G^{DEU}

Our binding assays show that INO80G^{DEU} decreases the affinity of UCH-L5 for substrates (Figures 2A and 2B). To understand this effect we analyzed how INO80G^{DEU} affects UCH-L5 conformation (Figure 1) in more detail. INO80G^{DEU} alters the ULD domain's relative position and conformation in two specific ways. First, helix $\alpha 9$ and $\alpha 10$ are tilted by ~ 30 degrees compared to the active ULD conformation and second, the C-terminal end of helix $\alpha 10$ is bent towards the catalytic domain (Figure 4A). As a result, sections of the ULD and INO80G^{DEU} occupy the canonical ubiquitin binding exosites on UCH-L5 and thus prevent substrate docking (Figure 4A). The blockage of the exosites by the INO80G^{DEU} complex present a structural rationale for the decreased substrate binding that we observe, and provides a simple yet unexpectedly striking explanation of the INO80G^{DEU} inhibition mechanism.

Analysis of the UCH-L5/INO80G^{DEU} interface shows how the large conformational changes in UCH-L5 organize novel interfaces where key elements for ubiquitin binding and RPN13^{DEU} mediated activation are exploited by INO80G^{DEU} to inhibit UCH-L5 activity. First, ULD conformational changes allow INO80G^{DEU} helix $\alpha 6$ to contact the UCH-L5 CD possibly stabilizing the inhibitory conformation of the ULD (Figures 1D and S1D). Second, in a neat example of molecular mimicry, the INO80G FRF-hairpin binds to the UCH-L5 Leu38 pocket in a fashion that resembles the binding of the structurally analogous ubiquitin $\beta 1$ - $\beta 2$ hairpin to this pocket (Figures 4B and 4C). Next, the C-terminus of UCH-L5 helix $\alpha 8$ refolds to make the extra helical turn seen in the apo-structure. As a result, UCH-L5 Ile216 rearranges towards the hydrophobic core, preventing the possibility of the important interaction with the ubiquitin Ile36 patch (Figure 4D). Finally, helix $\alpha 10$ bending in the INO80G^{DEU} complex relocates the ULD anchor residues towards UCH-L5 Trp36 creating a novel intramolecular interface consisting of a cation- π stacking interaction between the indole ring of the Trp36 and Arg287 in UCH-L5 helix $\alpha 10$ (Figure 4E). This relocation

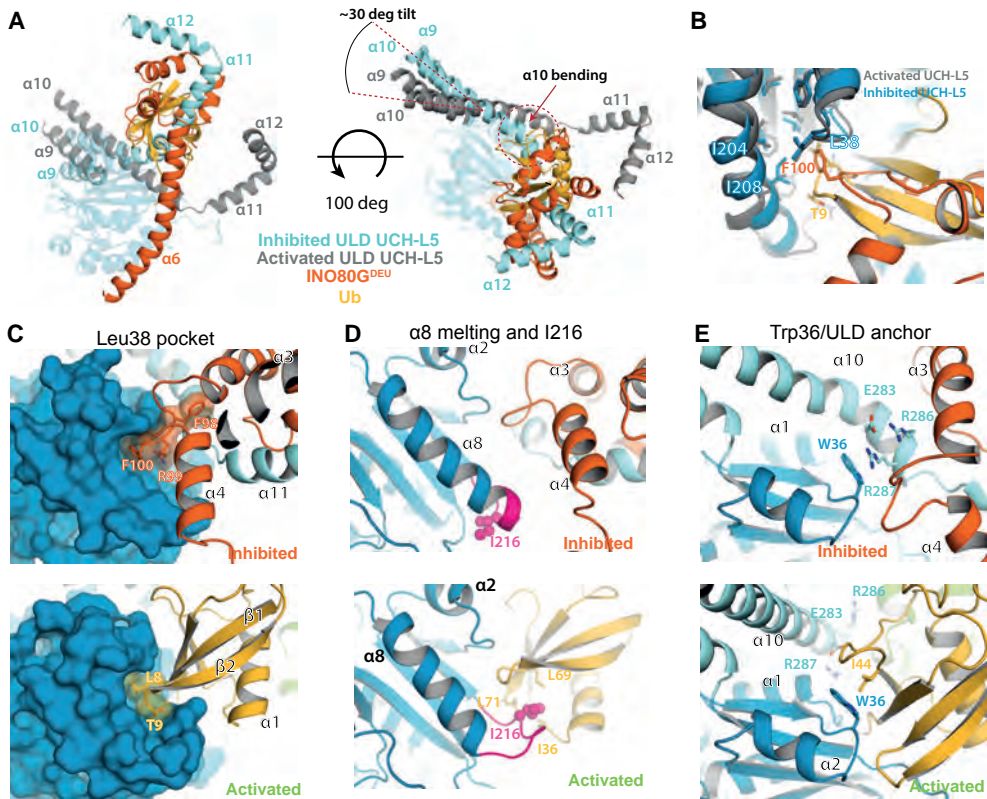


Figure 4 | Inhibition mechanism INO80G^{DEU}. **A)** The ubiquitin docking site on UCH-L5 is blocked as a result of INO80G^{DEU} induced conformational changes of the ULD. RPN13^{DEU} is removed for clarity. **B and C)** The FRF-hairpin mimics the ubiquitin $\beta 1$ - $\beta 2$ hairpin to bind the Leu38 pocket. **D)** In contrast to the activated state, helix $\alpha 8$ in UCH-L5 adopts an extended state in the INO80G^{DEU} complex to bury Ile216. **E)** The ULD anchor interaction is disrupted in the INO80G^{DEU} complex due to ULD tilting and helix $\alpha 10$ bending in favor of a new intramolecular interaction between Trp36 and Arg287.

simultaneously precludes Trp36 availability for ubiquitin binding and impedes the formation of the intricate polar interaction network in the ULD anchor that is required for UCH-L5 activation by RPN13^{DEU} (Figure 3C). Thus all elements for ubiquitin binding in UCH-L5 are effectively obscured by INO80G^{DEU} binding.

The FRF hairpin creates the activity switch in DEUBAD domains

To study what features in INO80G^{DEU} are required to achieve UCH-L5 inhibition we analyzed its differences with the activating DEUBAD domain of RPN13. The most striking difference between the DEUBAD domains of RPN13 and INO80G is the C-terminal part where three helices $\alpha 6$ - $\alpha 8$ in RPN13^{DEU} change to the extended $\alpha 6$ in INO80G^{DEU} that packs against the CD (Figures 5A and S1D). Therefore we created a shorter version of INO80G^{DEU}, where helix $\alpha 6$ is removed (Figure 1A, residues 39-118, INO80G^{DEU} _{$\Delta\alpha 6$}). Surprisingly, the

truncated protein, INO80G^{DEU}_{Δα6} still inhibited UCH-L5 (Figure 5B), demonstrating that helix α6 is not required for inhibition under these conditions.

We next assessed the importance of the INO80G FRF-hairpin which is the other major structural difference between the RPN13^{DEU} and INO80G^{DEU} (Figures 5A and 1I). In the hairpin, the side chain of the highly conserved Phe100 (Figure S1B) is accommodated by the UCH-L5 Leu38 pocket (Figure 4C), suggesting that this interaction is important for INO80G function. To address the relevance of this interaction we made a single point mutant F100A in INO80G^{DEU}.

This point mutant, INO80G^{DEU}_{F100A}, has lost the ability to inhibit UCH-L5 in Ub-AMC assays. In fact, it restores activity to the level of UCH-L5 alone, highlighting the importance of the FRF-hairpin interaction for UCH-L5 inhibition (Figure 5C and Tables S1-2). Moreover, the F100A complex gained a significant substrate binding ability in contrast to the WT INO80G^{DEU} complex (Figure 5D). Loss of the phenylalanine interaction will make the Leu38 pocket available again for binding of the β1-β2 hairpin of ubiquitin (Figure 2G), but most likely also allows helix α10 to revert to its extended state, affecting the ULD position.

The structural changes in the DEUBAD domains may have been a crucial evolutionary event facilitating novel regulatory modes of the DEUBAD domain. To test this we created a chimeric RPN13^{DEU} variant (RPN13^{DEU}_{chimera}) by inserting the INO80G FRF-hairpin into the

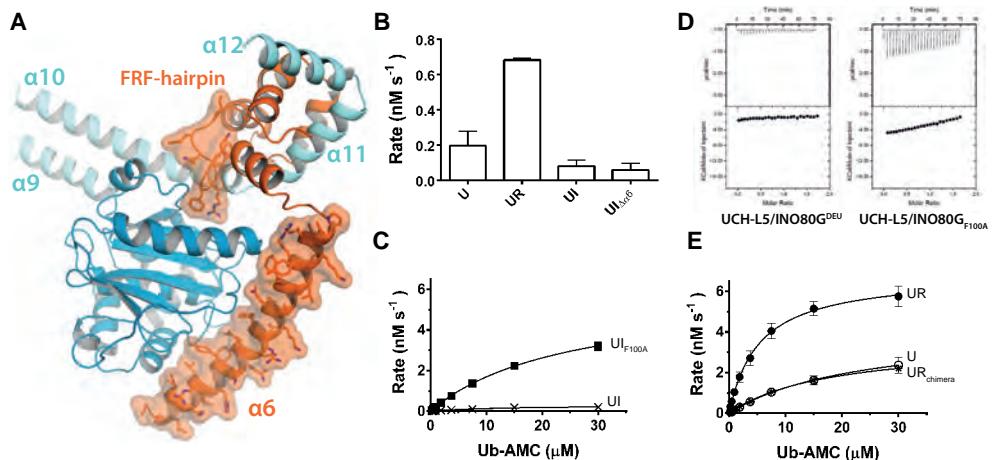


Figure 5 | The FRF-hairpin drives UCH-L5 inhibition. **A)** INO80G^{DEU} differs from RPN13^{DEU} mainly in the FRF-hairpin and helix α6 (orange surfaces). **B)** Helix α6 of INO80G^{DEU} dispensable for inhibition in Ub-AMC assays. **C)** Inhibition is completely lost in the INO80G^{DEU} F100A mutant (UI_{F100A}) on Ub-AMC. **D)** Mutant complex F100A gains Ub-GlySerThr binding ability compared to WT INO80G^{DEU} complex (from Figure 3A) in ITC. **E)** Insertion of the FRF-hairpin in RPN13^{DEU}_{chimera} abolishes the activation effect of WT RPN13^{DEU} on UCH-L5 (UR and U from Figure 1B).

structurally equivalent position in RPN13^{DEU} (Figure S3A). The chimera formed a stable complex with UCH-L5 (Figure S3B), but completely abolished the activation effect. The inserted FRF-hairpin was not sufficient to inhibit UCH-L5 to the same extent as INO80G^{DEU} however (Figure 5E and Table S1). In RPN13^{DEU} chimera the presence of the FRF-hairpin likely diminishes ubiquitin binding as it would be overlapping with the ubiquitin binding site explaining the loss of activation potential. These results demonstrate that the FRF-hairpin and its location within the DEUBAD domain have a crucial effect on UCH-L5 activity.

The INO80G_{short} activation mechanism also relies on ULD positioning

We wondered how lack of the FRF hairpin would affect the structure of UCH-L5 and INO80G. To this end we determined the 3.7 Å structure of UCH-L5 in complex with Ub-Prg and INO80G_{short} (aa 39-101), a shorter fragment of INO80G^{DEU} (Figure 1A). The artificial INO80G_{short} construct has the remarkable capability to activate UCH-L5 *in vitro*⁸. INO80G_{short} starts at the same residue as INO80G^{DEU} but terminates in the middle of the FRF-hairpin and is hence predicted not to contain a folded FRF-hairpin. Indeed, in the crystal structure, the C-terminal end of INO80G_{short} could not be unambiguously modeled, indicating that the FRF hairpin is not formed in this complex.

Strikingly, the UCH-L5~UbPrg/INO80G_{short} crystal structure resembles the activated RPN13^{DEU} complex rather than the inhibited state (Figure 6A and S4A-B). In this complex, the ULD has largely reverted to the conformation seen in the activated RPN13^{DEU} complexes with an extended helix α 10 (Figure S4C). All conformational changes in UCH-L5 required to create the canonical ubiquitin binding mode are now also in place (Figure S4D-E). The structure of INO80G_{short} itself and its binding mode to UCH-L5 are moreover identical to INO80G^{DEU} (apart from FRF-hairpin and α 5-6) and RPN13^{DEU} (Figure S4F).

Enzyme kinetics analysis confirmed that INO80G_{short} activates UCH-L5 on Ub-AMC (Figure 6B). The activation effect correlates with increased affinity for substrates since UCH-L5 binds substrates better in the presence of INO80G_{short} in ITC binding assays (Figure 6C). These results stress that DEUBAD domains mainly modulate activity by tuning substrate affinity.

The similarity in structure to the RPN13^{DEU} complex, suggests that INO80G_{short} makes use of the same activation mechanism. To test this hypothesis we used the UCH-L5_{E283A} ULD anchor mutant, asking whether loss of the ULD anchor would also affect the activation in this case. We found that the UCH-L5_{E283A}/INO80G_{short} mutant complex was compromised in Ub-AMC hydrolysis (Figure 6C and Table S1-2), reverting to the activity observed for UCH-L5 alone. This indicates the importance of the ULD anchor (Figure 6D) for INO80G_{short} activation and suggests that ULD positioning in general is a major feature of the activation.

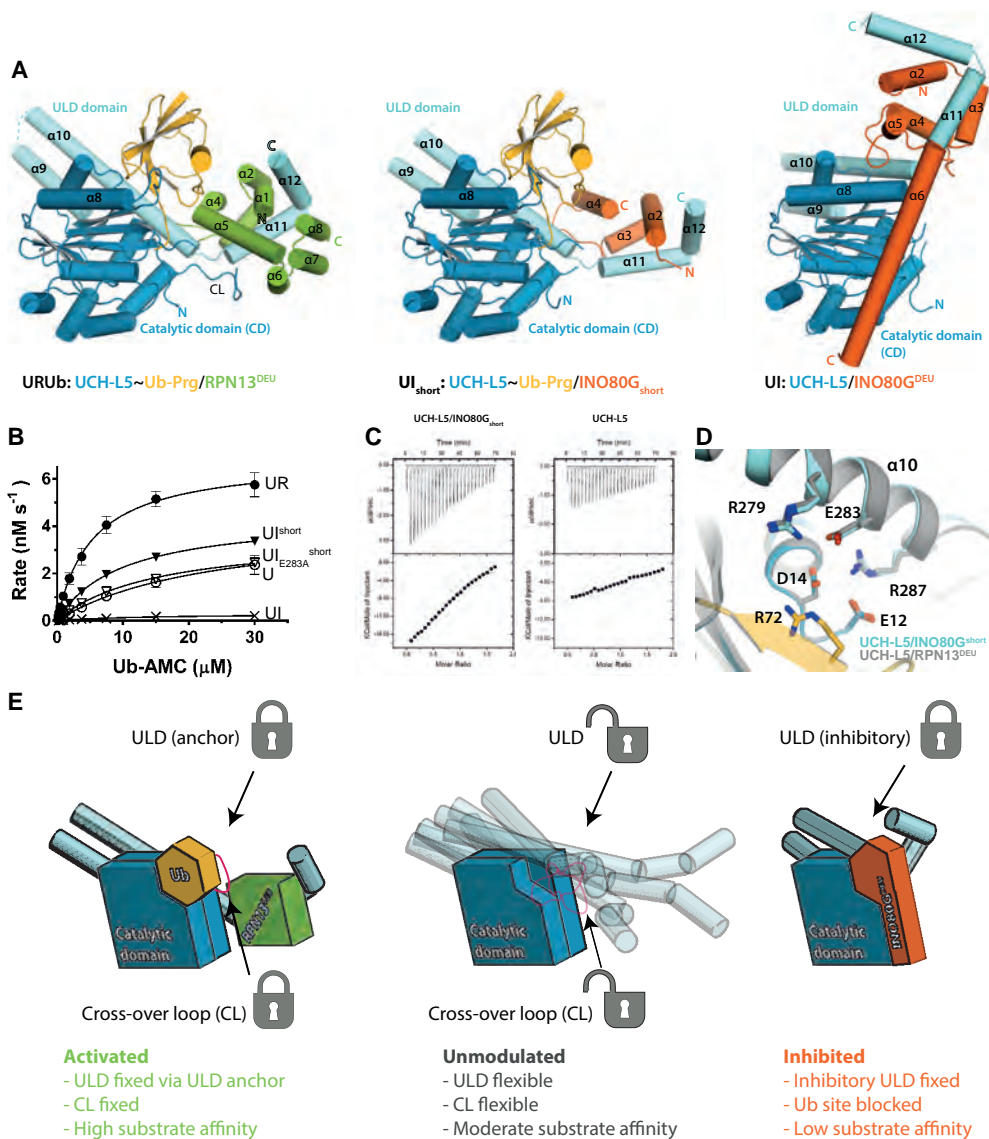


Figure 6 | Reactivation of the inhibitor and model for UCH-L5 regulation. A) The crystal structure of UCH-L5Ub-Prg/INO80G_{short} (middle) largely resembles the UCH-L5/RPN13^{DEU} structures (left from Figure 1F), but not the UCH-L5/INO80G^{DEU} structure (right, from Figure 1D). **B)** INO80G_{short} (UI_{short}) can activate UCH-L5 albeit not to RPN13^{DEU} levels (UR, UI and U from Figure 1B) and depends on the ULD anchor for activation on Ub-AMC. **C)** Activation by INO80G_{short} correlates with enhanced Ub-GlySerThr binding in ITC compared to WT UCH-L5 (from Figure 3A). **D)** The ULD anchors in the INO80G_{short} (lightblue) and RPN13^{DEU} (grey) superimpose very well and stabilize the same intramolecular interaction. **E)** Unmodulated UCH-L5 (middle) is characterized by CL and ULD flexibility that limits substrate binding and catalysis. Activation by RPN13^{DEU} (left) limits flexibility by locking the ULD and CL in favorable conformations. INO80G^{DEU} (right) locks the ULD in a conformation incompatible with substrate docking

INO80G_{short} containing only the helices $\alpha 2$ - $\alpha 4$ of the DEUBAD domain, can activate UCH-L5 demonstrating that the core DEUBAD fold is already sufficient to bind and provide modest activation. The INO80G_{short} complex does not attain UCH-L5/RPN13^{DEU} activity levels however. Most likely this is because it lacks helix $\alpha 5$, which RPN13^{DEU} uses to position the CL (Figure S4G).

Collectively the UCH-L5/INO80G_{short} structure analysis reconciles all our previous findings. First, it confirms that the FRF-hairpin is the crucial factor for inhibition since absence of this element results in loss of inhibition. Second, loss of the FRF-hairpin destabilizes the inhibitory ULD conformation causing it to snap back to a substrate binding competent conformation. Third, the core DEUBAD fold is sufficient to provide the basic UCH-L5 activation function. Like RPN13 it executes activation by stabilizing the substrate binding competent conformation of the ULD through ULD anchor.

DISCUSSION

Our data show how UCH-L5 activity can be modulated by DEUBAD domains present in RPN13 and INO80G through remarkably large conformational changes. Functionally, the activity of UCH-L5 is tuned at the level of substrate affinities where RPN13^{DEU} increases the affinity for substrates and INO80G^{DEU} dramatically decreases substrate affinity. Our structural and biochemical analyses indicate that RPN13^{DEU} achieves this effect by precise positioning of the ULD anchor and CL. The direct contact between RPN13^{DEU} and ubiquitin furthermore confers a mild activation effect on UCH-L5 by stabilizing ubiquitin. Conversely INO80G^{DEU} exploits molecular mimicry and ULD conformational plasticity to prevent ubiquitin docking and catalysis. We show which structural changes in DEUBAD domains may have been instrumental for the evolution of different modes of UCH-L5 regulation.

The proposed evolutionary conservation of the DEUBAD domains³⁵ is confirmed by structural analyses in this study. The DEUBAD domains appear to be modular. The core DEUBAD fold ($\alpha 1$ - $\alpha 4$) is shared among INO80G^{DEU}, RPN13^{DEU} and INO80G_{short} and is responsible for binding to UCH-L5 and modest activation. Accessory structural modules in RPN13^{DEU} (helix $\alpha 5$ that positions the CL) and INO80G^{DEU} (FRF-hairpin) lead to full activation or inhibition of UCH-L5. The modular nature of the DEUBAD domains explains their versatility as regulatory domains.

A key feature of UCH-L5 activity modulation is the conformational plasticity of the ULD that is found in a variety of conformations in the available UCH-L5 crystal structures (Figure 1G). This plasticity and the current data are consistent with a model where the UCH-L5 ULD can adopt a multitude of possible conformations in a dynamic fashion when free in

solution (Figure 6E). As a consequence of the ULD's proximity to the ubiquitin docking site, some of these conformations will be sterically incompatible with ubiquitin binding while others will allow efficient ubiquitin binding. The DEUBAD domain in RPN13^{DEU} and INO80G^{DEU} restricts ULD conformational plasticity by preferentially stabilizing specific conformations. RPN13^{DEU} activates and increases the affinity for substrates by fixing the ULD into a substrate binding competent conformation, using the ULD anchor. Additionally, full activation is achieved by the stabilization of the ubiquitin orientation by RPN13^{DEU} and correct positioning of the CL. On the other hand, INO80G^{DEU} binds to UCH-L5 and uses ULD conformational flexibility to dock its unique inhibitory FRF-hairpin into the Leu38 pocket. This interaction fixes the ULD in such a way that the ubiquitin binding site is blocked by INO80G^{DEU} and the ULD. In the process key molecular elements for ubiquitin binding and RPN13 dependent activation are masked or disrupted, effectively inhibiting activity.

This regulatory model may co-exist with possible roles of the UCH-L5 oligomeric state for regulation of its activity^{11,32,33}. As the enzyme concentrations under our assay conditions are low it is unlikely that we capture these phenomena. However, we cannot exclude that additional layers of regulatory complexity may exist in cells that involve UCH-L5 oligomeric states.

Our structures of UCH-L5/RPN13^{DEU} explain the basic mechanisms of activation by the RPN13 DEUBAD module. It will be interesting to investigate the additional activation that is required to hydrolyze K48-polyubiquitin in the proteasomal 19S regulatory particle. It is conceivable that efficient K48 polyubiquitin hydrolysis will only take place after steps that are possibly related to proper positioning and unfolding of the compact K48 polyubiquitin chains. A key step here will be the identification of the minimal proteasomal complex required to perform chain hydrolysis.

The UCH-L5/INO80G^{DEU} structure may provide novel approaches in unraveling the enigmatic role of UCH-L5 and INO80G in INO80 chromatin remodeling complexes. INO80G is a key factor in embryonic stem cells and knock out leads to loss of pluripotency²³. Of specific interest is why UCH-L5 is kept in an inhibited state in the INO80 complex⁸. A possibility is that INO80 controls UCH-L5 in a temporal manner where in some circumstances UCH-L5 is inhibited while under other circumstances post-translational modifications and/or conformational changes release the inhibition and activate UCH-L5, allowing for additional layers of regulation. We have already seen in INO80G_{short} that the core DEUBAD fold has the intrinsic ability to activate UCH-L5 and all that is required for INO80G^{DEU} to relieve inhibition is disruption of the FRF-hairpin. Such relief of inhibition would be important for the recently reported UCH-L5/INO80G role in DNA double strand break response, since UCH-L5 catalytic activity is required for proper DNA end resection²⁵.

A unique element of the INO80G^{DEU} domain is the extended helix $\alpha 6$. This helix packs against the CD close to the active site and was therefore initially thought by us to confer INO80G^{DEU} inhibitory function. In our in vitro assays this element is dispensable for inhibition, but this may be different in a cellular context, where the additional contacts between this helix and the catalytic domain may further stabilize the inactivated state. An interesting feature of helix $\alpha 6$ is the presence of a large solvent exposed positively charged patch. We speculate that this patch may be important in cells as a binding platform for INO80 chromatin remodeling factors. As the equivalent region in RPN13^{DEU} folds into a helical platform it may also be possible that under some conditions, driven by e.g. post translational modifications (PTMs), $\alpha 6$ could refold into a conformation seen in RPN13 to meet functional requirements. DUB activity regulation by PTMs such as phosphorylation have been shown previously to be important for DUBA⁴⁵.

The ULD is conserved in UCH family member BAP1 that is activated by the ASXL1 DEUBAD-domain to deubiquitinate H2A³⁴. Because of the strong conservation of key elements between UCH-L5/RPN13^{DEU} and BAP1/ASXL1 we anticipate that the ASXL1 DEUBAD domain employs similar strategies to activate BAP1. Both BAP1 and ASXL1 are important cancer drivers. BAP1 is a key tumor suppressor that is mutated in a number of cancers where loss of BAP1 is associated with poor prognosis and tumor aggressiveness^{28,30}. Our crystal structures have valuable implications for BAP1 function in its cellular roles and pathogenesis.

The mechanisms of DUB regulation that we describe are different from those in previously studied DUB regulators. UAF1 increases the basicity of the USP1 catalytic histidine, increasing its potency as a general base⁴⁶. Likewise, incorporation of Ubp8 in the SAGA complex stabilizes the catalytic center, also facilitating catalysis^{12,13}. Activation of USP7 by GMPS against a minimal substrate changes only k_{cat} ⁴. All of these differ from UCH-L5 where a major part of the activity modulation involves tuning substrate affinities, rather than actual catalytic steps.

Whereas inhibition of DUBs by proteins is still a rare phenomenon, inhibition of general proteases by proteins has been well described^{47,48}. Serpins inhibit serine proteases by irreversibly trapping the acyl-enzyme intermediate. Additionally general cysteine proteases can be inhibited by cystatins and related proteins by occupying active site clefts. Instead INO80G functions as an exosite inhibitor where not the active site cleft but an exosite, in this case the ubiquitin-core docking site, is blocked. Enzyme exosite targeting by a naturally evolved inhibitor could provide powerful clues about the most efficient way for DUB inhibition and may thus be promising from a pharmaceutical perspective.

EXPERIMENTAL PROCEDURES

Plasmids and cloning

Human UCH-L5, RPN13 and INO80G cDNA were subcloned from the HAP1 cell line. RPN13^{DEU}_{chimera} was purchased as a synthetic construct. All constructs were cloned into the pGEX or pET bacterial expression vectors of the NKI LIC suite⁴⁹.

Protein expression and purification

All protein variants and protein complexes were (co-) expressed in *E.coli*. UCH-L5 and variants were purified using GST affinity purification (GSH 4B sepharose, GE Healthcare) followed by a desalting (HiPrep 26/10, GE Healthcare) and final size exclusion chromatography step (Superdex S200, GE Healthcare). UCH-L5 complexes were purified similarly except for an additional first nickel purification step. RPN13^{DEU} alone was expressed in *E.coli* and purified using nickel affinity chromatography, desalting and size exclusion chromatography (Superdex S75, GE Healthcare).

Ub-AMC enzymatic assays

Enzyme activity was followed as release of fluorescent AMC from the quenched Ub-AMC substrate, providing a direct read-out of DUB activity. Michealis-Menten parameters were determined using 1 nM of enzyme while varying the substrate concentration. Initial rates were plotted against substrate concentration and fitted to the Michealis-Menten model using non-linear regression in Prism 6. In single concentration experiments, 1 nM of enzyme was allowed to react with 1 μM of substrate. Activity was quantified by calculating the initial rates.

FP binding assays

Binding assays between UCH-L5 complexes and model substrate Ub-LysGly^{TAMRA} were performed by measuring fluorescence polarization. Model substrate (5 nM) was incubated at 25°C with varying amounts of different UCH-L5 complexes to obtain binding curves. To prevent substrate hydrolysis inactive C88A mutants of UCH-L5 were used.

Stopped-flow fluorescent polarization binding assay

Pre-steady state binding events between UCH-L5 (C88A) complexes and Ub-LysGly^{TAMRA} were monitored in stopped-flow fluorescent polarization experiments. Varying concentrations of UCH-L5 variants were injected together with 20 nM (final concentration) Ub-KG^{TAMRA} after which fluorescent polarization was followed during 10 s. Association binding traces were fitted to a one-phase exponential model in Prism6 to obtain k_{obs} . The k_{obs} values were plotted against protein concentration to estimate k_{on} , k_{off} and K_D .

Isothermal Titration Calorimetry

ITC experiments were performed in a VP-ITC Microcal calorimeter at 25°C. In 10 μ l injections, 450 μ M UbGlySerThr was titrated into 45 μ M of UCH-L5 (C88A), or 110 μ M UCH-L5 into 12.5 μ M RPN13^{DEU}. Data were fitted to a one-site binding model with the manufacturer' Origin software.

Structure determination

Data collection was done at the ESRF and SLS at 100K. Images were integrated with XDS⁵⁰ and merged/scaled with Aimless⁵¹, followed by molecular replacement with Phaser⁵². Model refinement was carried out by Phenix⁵³, autoBUSTER⁵⁴ and Refmac⁵⁵ and models were build using COOT⁵⁶. All structure figures were generated using PyMOL.

Supplemental information

Detailed experimental procedures, supplemental figures and tables can be found in the supplemental data.

CONFLICT OF INTEREST STATEMENT

Huib Ovaa and Farid El Oualid are co-founders and share-holders of UbiQ.

ACKNOWLEDGEMENTS

We thank B8 members and Haico van Attikum for discussion and critical reading of the manuscript. We thank Marcello Clerici and Flora Groothuizen for advice in structure determination, Tatjana Heidebrecht for assistance in crystal harvesting, Vincent Blomen and Thijn Brummelkamp for the HAP1 cDNA library, Paul Geurink for Ub-LysGly^{TAMRA} and beamline scientists at SLS and ESRF for data collection assistance. This work was supported by ERC advanced grant 249997 and NWO ECHO 700.59.009.

D.D.S. designed, performed and analyzed all experiments and wrote the manuscript. W.J.D. and D.D.S. expressed and purified proteins. F.E. and R.E. performed ubiquitin-conjugate synthesis. H.O. supervised ubiquitin-conjugate research. T.K.S. supervised and designed research and wrote manuscript. All authors critically read the manuscript.

REFERENCES

1. Komander, D., Clague, M. J. & Urbé, S. Breaking the chains: structure and function of the deubiquitinases. *Nat. Rev. Mol. Cell Biol.* **10**, 550–63 (2009).
2. Clague, M. J. *et al.* Deubiquitylases from genes to organism. *Physiol. Rev.* **93**, 1289–315 (2013).
3. Sowa, M. E., Bennett, E. J., Gygi, S. P. & Harper, J. W. Defining the human deubiquitinating enzyme interaction landscape. *Cell* **138**, 389–403 (2009).
4. Faesen, A. C. *et al.* Mechanism of USP7/HAUSP activation by its C-terminal ubiquitin-like domain and allosteric regulation by GMP-synthetase. *Mol. Cell* **44**, 147–59 (2011).

5. Cohn, M. A. *et al.* A UAF1-containing multisubunit protein complex regulates the Fanconi anemia pathway. *Mol. Cell* **28**, 786–97 (2007).
6. Lee, K. K., Florens, L., Swanson, S. K., Washburn, M. P. & Workman, J. L. The deubiquitylation activity of Ubp8 is dependent upon Sgf11 and its association with the SAGA complex. *Mol. Cell Biol.* **25**, 1173–82 (2005).
7. Köhler, A., Schneider, M., Cabal, G. G., Nehrbass, U. & Hurt, E. Yeast Ataxin-7 links histone deubiquitination with gene gating and mRNA export. *Nat. Cell Biol.* **10**, 707–15 (2008).
8. Yao, T. *et al.* Distinct modes of regulation of the Uch37 deubiquitinating enzyme in the proteasome and in the Ino80 chromatin-remodeling complex. *Mol. Cell* **31**, 909–17 (2008).
9. Qiu, X.-B. *et al.* hRpn13/ADRM1/GP110 is a novel proteasome subunit that binds the deubiquitinating enzyme, UCH37. *EMBO J.* **25**, 5742–53 (2006).
10. Hamazaki, J. *et al.* A novel proteasome interacting protein recruits the deubiquitinating enzyme UCH37 to 26S proteasomes. *EMBO J.* **25**, 4524–36 (2006).
11. Yao, T. *et al.* Proteasome recruitment and activation of the Uch37 deubiquitinating enzyme by Adrm1. *Nat. Cell Biol.* **8**, 994–1002 (2006).
12. Köhler, A., Zimmerman, E., Schneider, M., Hurt, E. & Zheng, N. Structural basis for assembly and activation of the heterotetrameric SAGA histone H2B deubiquitinase module. *Cell* **141**, 606–17 (2010).
13. Samara, N. L. *et al.* Structural insights into the assembly and function of the SAGA deubiquitinating module. *Science* **328**, 1025–9 (2010).
14. Chen, Y. *et al.* Expression and clinical significance of UCH37 in human esophageal squamous cell carcinoma. *Dig. Dis. Sci.* **57**, 2310–7 (2012).
15. Fang, Y. *et al.* Ubiquitin C-terminal Hydrolase 37, a novel predictor for hepatocellular carcinoma recurrence, promotes cell migration and invasion via interacting and deubiquitinating PRP19. *Biochim. Biophys. Acta* **1833**, 559–72 (2013).
16. Fang, Y. *et al.* The interaction between ubiquitin C-terminal hydrolase 37 and glucose-regulated protein 78 in hepatocellular carcinoma. *Mol. Cell. Biochem.* **359**, 59–66 (2012).
17. Al-Shami, A. *et al.* Regulators of the proteasome pathway, Uch37 and Rpn13, play distinct roles in mouse development. *PLoS One* **5**, e13654 (2010).
18. Wicks, S. J. *et al.* The deubiquitinating enzyme UCH37 interacts with Smads and regulates TGF-beta signalling. *Oncogene* **24**, 8080–4 (2005).
19. Wicks, S. J. *et al.* Reversible ubiquitination regulates the Smad/TGF-beta signalling pathway. *Biochem. Soc. Trans.* **34**, 761–3 (2006).
20. Kikuchi, M. *et al.* Identification of unstable network modules reveals disease modules associated with the progression of Alzheimer's disease. *PLoS One* **8**, e76162 (2013).
21. Matilainen, O., Arpalahhti, L., Rantanen, V., Hautaniemi, S. & Holmberg, C. I. Insulin/IGF-1 signaling regulates proteasome activity through the deubiquitinating enzyme UBH-4. *Cell Rep.* **3**, 1980–95 (2013).
22. Chia, N.-Y. *et al.* A genome-wide RNAi screen reveals determinants of human embryonic stem cell identity. *Nature* **468**, 316–20 (2010).
23. Wang, L. *et al.* INO80 Facilitates Pluripotency Gene Activation in Embryonic Stem Cell Self-Renewal, Reprogramming, and Blastocyst Development. *Cell Stem Cell* **14**, 575–91 (2014).
24. Smeenk, G. & van Attikum, H. The chromatin response to DNA breaks: leaving a mark on genome integrity. *Annu. Rev. Biochem.* **82**, 55–80 (2013).

25. Nishi, R. *et al.* Systematic characterization of deubiquitylating enzymes for roles in maintaining genome integrity. *Nat. Cell Biol.* (2014). doi:10.1038/ncb3028
26. Popp, M. W., Artavanis-Tsakonas, K. & Ploegh, H. L. Substrate filtering by the active site crossover loop in UCHL3 revealed by sortagging and gain-of-function mutations. *J. Biol. Chem.* **284**, 3593–602 (2009).
27. Zhou, Z., Zhang, Y., Liu, S., Song, A. & Hu, H. Length of the active-site crossover loop defines the substrate specificity of ubiquitin C-terminal hydrolases for ubiquitin chains. *Biochem. J.* **441**, 143–149 (2011).
28. White, A. E. & Harper, J. W. Cancer. Emerging anatomy of the BAP1 tumor suppressor system. *Science* **337**, 1463–4 (2012).
29. Goldstein, A. M. Germline BAP1 mutations and tumor susceptibility. *Nat. Genet.* **43**, 925–6 (2011).
30. Carbone, M. *et al.* BAP1 and cancer. *Nat. Rev. Cancer* **13**, 153–9 (2013).
31. Misaghi, S. *et al.* Association of C-terminal ubiquitin hydrolase BRCA1-associated protein 1 with cell cycle regulator host cell factor 1. *Mol. Cell Biol.* **29**, 2181–92 (2009).
32. Burgie, S. E., Bingman, C. a, Soni, A. B. & Phillips, G. N. Structural characterization of human Uch37. *Proteins* 649–654 (2011). doi:10.1002/prot.23147
33. Jiao, L. *et al.* Mechanism of the Rpn13-induced activation of Uch37. *Protein Cell* **5**, 616–30 (2014).
34. Scheuermann, J. C. *et al.* Histone H2A deubiquitinase activity of the Polycomb repressive complex PR-DUB. *Nature* **465**, 243–7 (2010).
35. Sanchez-Pulido, L., Kong, L. & Ponting, C. P. A common ancestry for BAP1 and Uch37 regulators. *Bioinformatics* **28**, 1953–6 (2012).
36. El Oualid, F. *et al.* Chemical synthesis of ubiquitin, ubiquitin-based probes, and diubiquitin. *Angew. Chem. Int. Ed. Engl.* **49**, 10149–53 (2010).
37. Dang, L. C., Melandri, F. D. & Stein, R. L. Kinetic and mechanistic studies on the hydrolysis of ubiquitin C-terminal 7-amido-4-methylcoumarin by deubiquitinating enzymes. *Biochemistry* **37**, 1868–79 (1998).
38. Ekkebus, R. *et al.* On terminal alkynes that can react with active-site cysteine nucleophiles in proteases. *J. Am. Chem. Soc.* **135**, 2867–70 (2013).
39. Sommer, S., Weikart, N. D., Linne, U. & Mootz, H. D. Covalent inhibition of SUMO and ubiquitin-specific cysteine proteases by an in situ thiol-alkyne addition. *Bioorg. Med. Chem.* **21**, 2511–7 (2013).
40. Morrow, M. E. *et al.* Stabilization of an Unusual Salt Bridge in Ubiquitin by the Extra. (2013).
41. Chen, X., Lee, B.-H., Finley, D. & Walters, K. J. Structure of proteasome ubiquitin receptor hRpn13 and its activation by the scaffolding protein hRpn2. *Mol. Cell* **38**, 404–15 (2010).
42. Geurink, P. P., El Oualid, F., Jonker, A., Hameed, D. S. & Ovaa, H. A general chemical ligation approach towards isopeptide-linked ubiquitin and ubiquitin-like assay reagents. *Chembiochem* **13**, 293–7 (2012).
43. Boudreaux, D. a, Maiti, T. K., Davies, C. W. & Das, C. Ubiquitin vinyl methyl ester binding orients the misaligned active site of the ubiquitin hydrolase UCHL1 into productive conformation. *Proc. Natl. Acad. Sci. U. S. A.* **107**, 9117–22 (2010).
44. Glaser, F. *et al.* ConSurf: identification of functional regions in proteins by surface-mapping of phylogenetic information. *Bioinformatics* **19**, 163–4 (2003).
45. Huang, O. W. *et al.* Phosphorylation-dependent activity of the deubiquitinase DUBA. *Nat. Struct. Mol. Biol.* **19**, 171–5 (2012).
46. Villamil, M. A., Chen, J., Liang, Q. & Zhuang, Z. A noncanonical cysteine protease USP1 is activated through

- active site modulation by USP1-associated factor 1. *Biochemistry* **51**, 2829–39 (2012).
47. Rzychon, M., Chmiel, D. & Stec-Niemczyk, J. Modes of inhibition of cysteine proteases. *Acta Biochim. Pol.* **51**, 861–73 (2004).
48. Dubin, G. Proteinaceous cysteine protease inhibitors. *Cell. Mol. Life Sci.* **62**, 653–69 (2005).
49. Luna-Vargas, M. P. A. *et al.* Enabling high-throughput ligation-independent cloning and protein expression for the family of ubiquitin specific proteases. *J. Struct. Biol.* **175**, 113–119 (2011).
50. Kabsch, W. XDS. *Acta Crystallogr. D. Biol. Crystallogr.* **66**, 125–32 (2010).
51. Evans, P. R. & Murshudov, G. N. How good are my data and what is the resolution? *Acta Crystallogr. D. Biol. Crystallogr.* **69**, 1204–14 (2013).
52. McCoy, A. J. *et al.* Phaser crystallographic software. *J. Appl. Crystallogr.* **40**, 658–674 (2007).
53. Adams, P. D. *et al.* PHENIX: a comprehensive Python-based system for macromolecular structure solution. *Acta Crystallogr. D. Biol. Crystallogr.* **66**, 213–21 (2010).
54. Smart, O. S. *et al.* Exploiting structure similarity in refinement: automated NCS and target-structure restraints in BUSTER. *Acta Crystallogr. D. Biol. Crystallogr.* **68**, 368–80 (2012).
55. Murshudov, G. N., Vagin, A. A. & Dodson, E. J. Refinement of macromolecular structures by the maximum-likelihood method. *Acta Crystallogr. D. Biol. Crystallogr.* **53**, 240–55 (1997).
56. Emsley, P., Lohkamp, B., Scott, W. G. & Cowtan, K. Features and development of Coot. *Acta Crystallogr. D. Biol. Crystallogr.* **66**, 486–501 (2010).

Supplemental Information table of contents

Figure S1	68
Figure S2	69
Figure S3	70
Figure S4	70
Supplemental tables	71
Supplemental experimental procedures	72

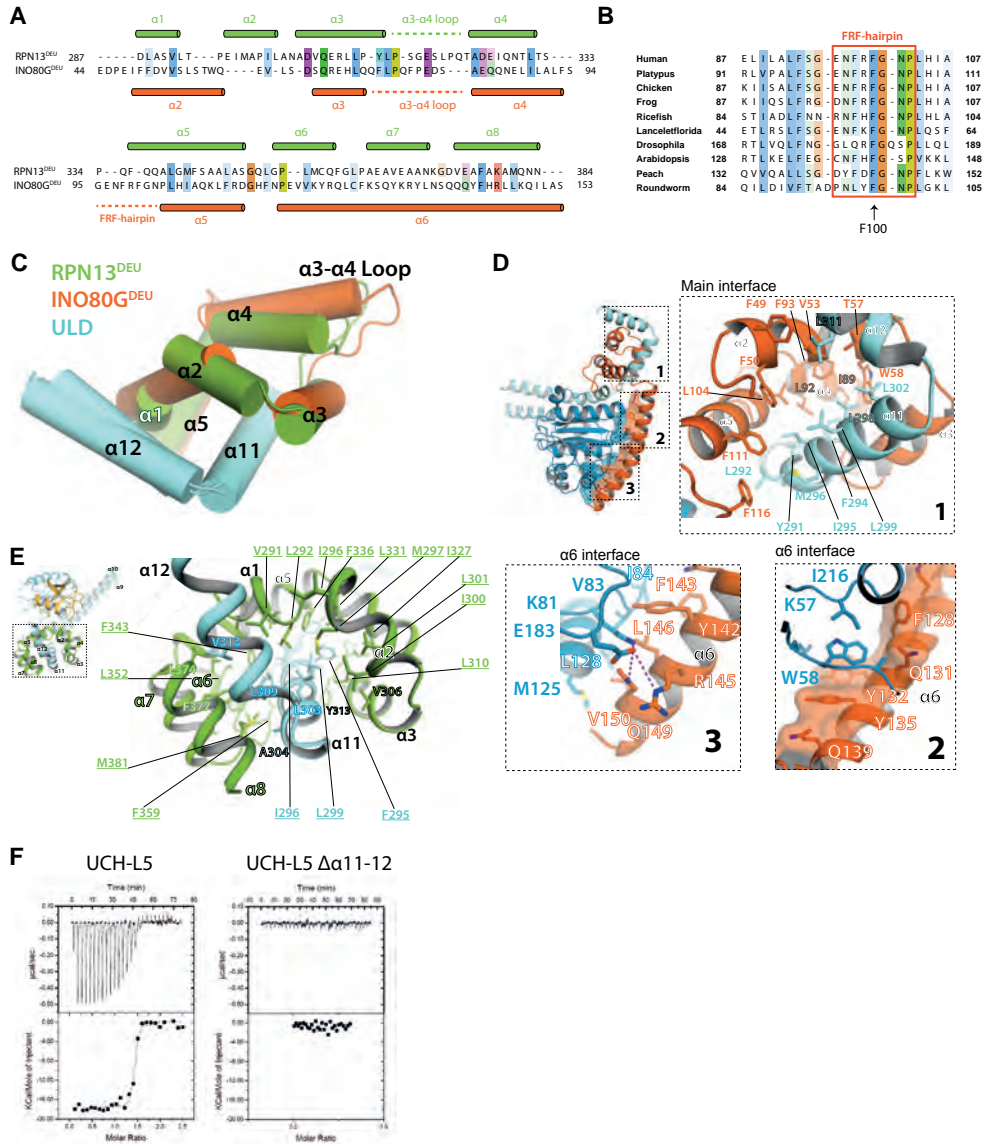


Figure S1 | Binding of DEUBAD domains to UCH-L5. A) Structure based sequence alignment DEUBAD domains RPN13 and INO80G. **B)** The INO80G FRF-hairpin is highly conserved. **C)** DEUBAD domains of both RPN13 and INO80G bind UCH-L5 helices $\alpha 11$ - $\alpha 12$ in a highly similar fashion. **D)** Binding interfaces of the UCH-L5/INO80G^{DEU} complex. The ULD is clasped by the INO80G DEUBAD domain in an hydrophobic interface (1). Helix $\alpha 6$ packs against the UCH-L5 catalytic domain (2 and 3). **E)** Close up of the main interface between RPN13^{DEU} and UCH-L5. **F)** UCH-L5 helices $\alpha 11$ - $\alpha 12$ are required to bind RPN13^{DEU} in ITC binding assays.

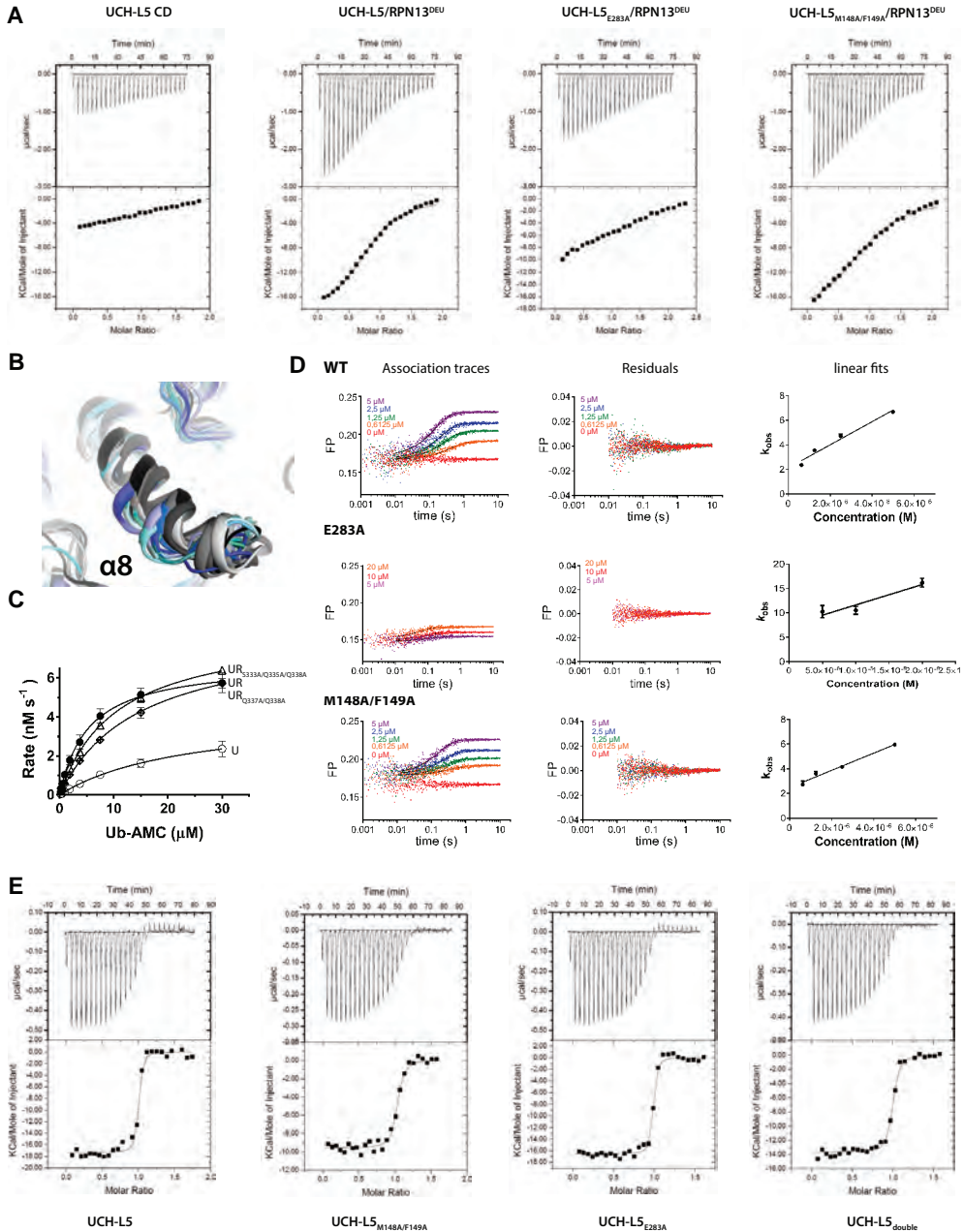


Figure S2 | UCH-L5 activation. **A**) UCH-L5 variants binding to model substrate Ub-GlySerThr in ITC assays. UCH-L5/RPN13^{DEU} from Figure 2. **B**) In UCHs in complex with ubiquitin (pdb codes: 1ucha, 1xd3, 2etl, 2wdt, 2we6, 3irt, 3kvf, 3kw5, 4dm9, 4i6n, 4ig7, 4jkj, UR, URUB shown in blue/green tints.) helix 8 is partially melted at the C-terminus. This is in contrast with apo UCH structures (pdb codes: 1cmx, 2len, 3a7s, 3ihr, 3rii, 3ris, 3tb3 shown in gray tints.) were helix 8 makes an extra turn **C**) RPN13^{DEU} mutants in the ubiquitin interface have a small effect on UCH-L5 activation. “U” from Figure 1B **D**) Stopped flow fluorescence polarization binding assays between UCH-L5 complexes and model substrate Ub-LysClyTAMRA. **E**) All UCH-L5 variants bind RPN13^{DEU} with similar affinity in ITC.

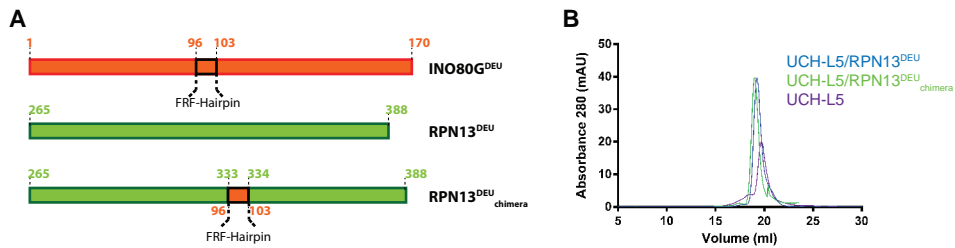


Figure S3 | The RPN13 FRF-hairpin chimera forms a complex with UCH-L5 **A)** Schematic depiction to illustrate that in RPN13^{DEU} chimera the INO80G FRF-hairpin is inserted between RPN13 helices α4 and α5. **B)** UCH-L5 forms a complex with RPN13^{DEU} chimera as demonstrated in Superdex S200 size exclusion chromatography.

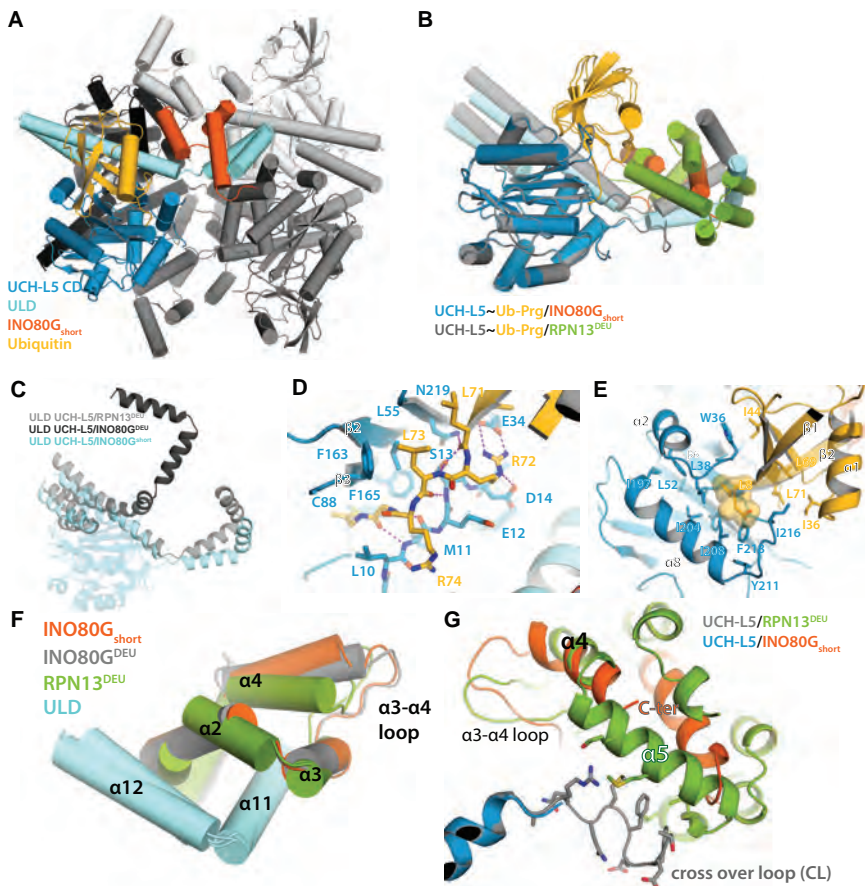


Figure S4 | The UCH-L5~Ub-Prg/INO80G_{short} complex. **A)** Asymmetric unit of UCH-L5~Ub-Prg/INO80G_{short} shows 4-fold non-crystallographic symmetry. **B)** Superposition of the UCH-L5~Ub-Prg/INO80G_{short} (UCH-L5 in blue) and UCH-L5~Ub-Prg/RPN13^{DEU} (UCH-L5 in gray) shows that the complexes look similar. **C)** The ULD of the INO80G_{short} complex (lightblue) has reverted from the inhibited orientation (darkgrey) to an orientation similar to the RPN13^{DEU} complex (lightgray). **D and E)** Ubiquitin binding occurs in a canonical fashion in the INO80G_{short} complex. **F)** The DEUBAD domain of INO80G_{short} and its binding mode to UCH-L5 are highly similar to the RPN13^{DEU} and INO80G^{DEU} complexes. **G)** INO80G_{short} lacks helix α5 that RPN13^{DEU} employs to bind and position the UCH-L5 CL.

SUPPLEMENTAL TABLES

Table S1 | Ub-AMC Enzyme kinetics parameters, related to figures 1, 3, 5 and 6.

	k_{cat} (s ⁻¹)	K_M (μM)	k_{cat}/K_M (M ⁻¹ s ⁻¹) *10 ⁻⁵
UCH-L5	4,2 ± 0,3	23,5 ± 3,2	1,8
UCH-L5 CD	4,8 ± 0,2	14,9 ± 1,2	3,2
UCH-L5/RPN13 ^{DEU}	6,4 ± 0,2	4,4 ± 0,4	14,5
UCH-L5 _{E283A}	2,8 ± 0,2	24,2 ± 2,2	1,2
UCH-L5 _{E283A} /RPN13 ^{DEU}	5,4 ± 0,3	15,2 ± 1,3	3,6
UCH-L5 _{M148A/F149A}	3,1 ± 1,0	25,5 ± 14,3	1,2
UCH-L5 _{M148A/F149A} /RPN13 ^{DEU}	5,6 ± 0,7	17,5 ± 4,3	3,2
UCH-L5 _{double}	2,1 ± 0,2	20,1 ± 3,2	1,0
UCH-L5 _{double} /RPN13 ^{DEU}	3,3 ± 0,2	19,4 ± 2,0	1,7
UCH-L5/INO80C ^{DEU}	0,3 ± 0,05	13,5 ± 4,5	0,2
UCH-L5/INO80C ^{DEU} _{F100A}	6,5 ± 0,2	28,1 ± 1,0	2,3
UCH-L5/INO80C ^{short}	4,5 ± 0,04	9,2 ± 0,2	4,9
UCH-L5 _{E283A} /INO80C ^{short}	3,7 ± 0,04	14,3 ± 0,3	2,6
UCH-L5/RPN13 ^{DEU} _{chimera}	3,6 ± 0,3	17,8 ± 1,2	2,0

Table S2 | Fold activation effect on kcat/Km per UCH-L5 variant, related to figures 1, 3, 5 and 6.

Enzyme variant	Modulator	Fold Activation effect by modulator (kcat/Km _{modulated})/(kcat/Km _{unmodulated})
UCH-L5	RPN13 ^{DEU}	8
UCH-L5 _{E283A}	RPN13 ^{DEU}	3
UCH-L5 _{M148A/F149A}	RPN13 ^{DEU}	2,7
UCH-L5 _{double}	RPN13 ^{DEU}	1,7
UCH-L5	INO80C ^{DEU}	0,1
UCH-L5	INO80C ^{DEU} _{F100A}	1,3
UCH-L5	INO80C ^{short}	2,7
UCH-L5 _{E283A}	INO80C ^{short}	2
UCH-L5	RPN13 ^{DEU} _{chimera}	1,1

Table S3 | Substrate binding parameters, related to figures 2, 5, 6, and S2.

	ITC Ub-GlySerThr binding				Stopped-flow Ub-LysGly ^{TAMRA} binding		
	N	ΔH (kcal/mol)	TΔS (kcal/mol)	K _D (μM)	K _D (μM)	k _{off} (s ⁻¹)	k _{on} (μM ⁻¹ s ⁻¹)
UCH-L5	nf	nf	nf	nf			
UCH-L5/RPN13 ^{DEU}	0,83 ± 0,01	-18,27	-10,96	4,5	2,3	2,1 ± 0,3	0,9 ± 0,1
UCH-L5 _{E283A} /RPN13 ^{DEU}	nf	nf	nf	nf	18	7,4 ± 1,7	0,42 ± 0,13
UCH-L5 _{M148A/F149A} /RPN13 ^{DEU}	0,93 ± 0,02	-19,15	-12,07	6,5	3,6	2,5 ± 0,2	0,7 ± 0,07
UCH-L5/INO80C ^{short}	0,81 ± 0,01	-22,25	-15,67	9,8	11	11,6 ± 1,3	1,1 ± 0,1
UCH-L5 CD	nf	nf	nf	nf			

Nf: Model not fitted. The UCH-L5/INO80C^{DEU} complex results are omitted since it did not show binding signal in binding experiments. Gray boxes represent experiments that were not done.

Table S4 | ITC parameters RPN13^{DEU} binding, related to figures S1 and S2.

	K _D (nM)	ΔH (kcal/mol)	TΔS (kcal/mol)
UCH-L5	6,4	-17,0	-6,2
UCH-L5 _{Δam1-12}	nf	nf	nf
UCH-L5 _{E283A}	5,1	-9,35	-5,2
UCH-L5 _{M148A/F149A}	25	-16,5	0,8
UCH-L5 _{double}	17	-13,7	-3,1

Nf: Model not fitted. Stoichiometry in these ITC experiment was fixed at 1 (see supplemental experimental procedures).

SUPPLEMENTAL EXPERIMENTAL PROCEDURES

Plasmids and cloning

Human UCH-L5 (uniprot Q9Y5K5, isoform3) RPN13 (uniprot Q16186), INO80G (uniprot Q6P4R8) were produced from a cDNA library originating from HAP1 cells¹ by PCR and were subsequently cloned into bacterial expression vectors from the NKI Ligation Independent Cloning (LIC) Suite². Specifically full length UCH-L5 was cloned into pGEXNKI-GST3C-LIC (carbenicilin), RPN13^{DEU} (aa 265-388) into pCDFNKI-his3C-LIC (streptomycin), INO80G^{DEU} (aa 39-170), INO80G^{DEU}_{Δα6} and INO80G_{short} (aa 39-101) into pETNKI-his3C-LIC (kanamycin), Point mutations were generated using site directed mutagenesis procedure by Quikchange (Agilent). Ub-GlySerThr was produced from WT ubiquitin (pET 3A) via Quikchange insertional mutagenesis. DNA for RPN13^{DEU}_{chimera} was purchased commercially as a codon optimized gene (Figure S3A) and cloned into pETNKI-his3C-LIC (kanamycin). All clones were verified using DNA sequencing.

Protein expression and purification

All proteins were expressed in BL21 Rosetta2 T1-resistant competent cells (Novagen). Cells were grown at 37°C to an OD₆₀₀ of ~0.6 before inducing protein expression by the addition of 0.25 mM IPTG. Expression took place for 4-6 hours at 25°C after which cells were harvested. UCH-L5 complexes, UCH-L5 complexes UCH-L5/RPN13^{DEU}, UCH-L5/INO80G^{DEU}, UCH-L5/INO80G_{short} and their mutants were co-expressed.

All purification steps were performed in the cold room or on ice. Cells were lysed by sonication in lysis buffer (50 mM Tris-HCl pH 8.0, 200 mM NaCl, 50 mM Imidazole and 0.5 mM TCEP) in the presence of complete EDTA-free protease inhibitor cocktail (Roche). GST-tagged UCH-L5 variants were purified by GST affinity chromatography using GSH 4B sepharose beads (GE Healthcare) and eluted with 25 mM Tris-HCl pH 8.0, 150 mM NaCl, 50 mM GSH_{reduced} pH 8.0, 10% glycerol, 0.5 mM TCEP after first washing beads with >10 column volumes (CV) lysis buffer. Excess of DNA was removed by ResourceQ anion exchange chromatography (GE Healthcare) using a linear gradient from 0-75% buffer B (25 mM Tris-HCl pH 8.0, 1000 mM NaCl, 0.5 mM TCEP). The column was equilibrated with Buffer A (25 mM Tris-HCl pH 8.0, 50 mM NaCl, 0.5 mM TCEP).

In case of the UCH-L5 complexes, first nickel affinity chromatography was performed using chelating sepharose (GE Healthcare) pre-loaded with Ni²⁺ to pull down either His-RPN13^{DEU}, His-INO80G^{DEU} or His-INO80G_{short}. Protein was eluted using 25 mM Tris-HCl pH 8.0, 200 mM NaCl, 250 mM Imidazole pH 8.0, 10%gly and 0.5 mM TCEP before applying the resulting eluate to GST affinity chromatography (see above). His tagged RPN13^{DEU} alone was purified by nickel affinity chromatography as described above. INO80G^{DEU} or its variants were unstable/insoluble and were therefore not purified as single proteins.

After the initial affinity or anion exchange chromatography steps samples all single variants proteins and complexes were desalted against desalting buffer (25 mM Tris-HCl pH 8.0, 150 mM NaCl, 10% glycerol, 0.5 mM TCEP) using a 26/10 desalting column (GE Healthcare). For GST-fusion proteins, this was followed by o/n cleavage with GST-3C-protease in the cold room. A GlyProGly tripeptide remained at the protein N-terminus after 3C cleavage. GST and GST-3C-protease were removed by reverse purification using GSH beads (GE Healthcare). Samples were next concentrated with Amicon Ultra 15 concentrating columns (Millipore) and injected onto a Superdex S200 or S75 size exclusion chromatography column (GE Healthcare) in gel filtration buffer (10 mM HEPES pH 7.5, 100 mM NaCl, 0.5 mM TCEP). Positive fractions were concentrated to 3-15 mg/ml, aliquotted and flash frozen in liquid nitrogen to be stored at -80°C.

Preparation of Ub-Propargyl complexes

Ubiquitin-propargyl (UbPrg) is a suicide inhibitor^{3,4} that reacts selectively with the DUB active site cysteine creating an irreversible quarternary vinyl thioether bond, that serves as transition states mimic. UbPrg was synthesized and purified as described³. Typically 10-40 μ M of either UCH-L5/RPN13^{DEU} or UCH-L5/INO80G_{short} was reacted with a 2-fold molar excess of UbPrg. The reaction took place in desalting buffer supplemented with 5 mM DTT and was allowed to proceed for 3h on ice or o/n. The reaction mixture was subsequently fractionated on a Superdex S200 size exclusion chromatography column (GE Healthcare) in gel filtration buffer after which the positive fractions were concentrated to ~10 mg/ml and used in crystallization trials.

Ub-AMC enzymatic assays

Enzyme activity was followed as release of fluorescent AMC from the quenched Ub-AMC substrate, providing a direct read-out of DUB activity⁵. Ub-AMC was synthesized as described previously⁶. The purified Ub-AMC was dissolved in pure DMSO. The residual amount of DMSO left in the enzymatic reaction was never higher than 6%. Kinetic parameters were determined using 1 nM of enzyme while varying the substrate concentration in 30 μ l reactions using reaction buffer (25 mM HEPES pH 7.5, 150 mM NaCl, 5 mM DTT and 0.05% Tween-20) at 25°C. Reactions took place in black 384-well non-binding surface low flange plates (Corning). In the single concentration experiments, 1 nM of enzyme was allowed to react with 1 μ M of substrate and activity was quantified by calculating the initial rates. Experiments were performed in a Pherastar (BMG Labtechnologies) plate reader using 350 nm and 450 nm excitation and emission wavelengths respectively. Measurements were taken every 10 s for 10 minutes. Fluorescence and velocities were related using an AMC standard curve. The initial rates were plotted against substrate concentration and fitted to the Michealis-Menten model using non-linear regression in Prism 6. Error bars represent the standard deviation. At least 2 different preparations were measured in

duplicate per enzyme/complex variant.

Equilibrium FP binding assays

Binding assays between UCH-L5 complexes and model substrate Ub-LysGly^{TAMRA} 7 were performed by measuring fluorescence polarization at room temperature. In this substrate a TAMRA-labeled Lys-Gly dipeptide is conjugated to ubiquitin via an isopeptide bond. To prevent hydrolysis of the substrate in these assays, the active site cysteine of UCH-L5 was mutated to alanine (C88A). Assays were carried out using 10 nM model substrate Ub-LysGly^{TAMRA} with varying concentrations of UCH-L5 variants at 25°C in FP binding buffer (25 mM HEPES pH 7.5, 150 mM NaCl, 0.05% Tween-20, 1mg/ml BSA, 0.5 mM TCEP). Reactions were 10-20 ul volumes and were allowed to equilibrate before measuring FP in a Pherastar (BMG Labtechnologies) with an excitation filter of 531 nm, and P and S emission filters of 579 nm. Error bars represent the standard deviation.

Stopped-flow fluorescent polarization binding assays

Pre-steady state binding events between UCH-L5 (C88A) complexes and Ub-LysGly^{TAMRA} were monitored in stopped-flow fluorescent polarization experiments. The experiments were performed on a TgK Scientific stopped-flow system (model SF-61DX2) equipped with a photomultiplier tube R10699 (Hamamatsu). Monochromatic light at 544 nm and a 570 nm cutoff filter were used for excitation and readout, respectively. The light was polarized using a calcite prism for the incident beam and dichroic sheet polarizers in front of each of two photo-multiplier detectors arranged in a T-configuration.

The experiments were performed in stopped-flow binding buffer (25 mM HEPES pH 7.5, 150 mM NaCl, 0.05% Tween-20 and 0.5 mM TCEP) at 20°C. For the association 20 nM of Ub-LysGly^{TAMRA} (final concentration) and various concentrations of UCH-L5 variant complexes (C88A mutant) were injected in equal volumes and rapidly mixed after which FP signal was followed during 10 s. For each concentration 10 injections were averaged to improve signal. Association binding traces were fitted to a one-phase exponential model in Prism6 to obtain k_{obs} . The k_{obs} values were plotted against protein concentration to estimate k_{on} , k_{off} and $-K_D$.

Isothermal titration calorimetry

To determine the affinities between UCH-L5 variants and RPN13^{DEU} and UCH-L5 complexes to model substrate UbGlySerThr ITC experiments were performed. In UbGlySerThr, ubiquitin Gly76 is fused via a peptide bond to the tri peptide GlySerThr. Measurements were done in a VP-ITC Microcal calorimeter at 25°C in binding buffer (25 mM HEPES pH7.5, 150 mM NaCl, 10% Glycerol and 0.5 mM TCEP). Prior to the experiment both binding partners were dialyzed separately in the same container to equilibrate buffers. The syringe

contained 450 μM UbGlySerThr while 45 μM of UCH-L5 variant was present in the cell. For the UCH-L5/RPN13 binding, 110 μM UCH-L5 was present in the syringe. Ten μl of sample was added to the cell per injection. Data were fitted to a one-site binding model with the manufacturer's Origin software. Experiments not showing saturation were not fitted. Due to lack of absorbance at 280 nm and weak Coomassie staining, RPN13^{DEU} concentrations were difficult to estimate. Therefore a 1:1 stoichiometry of UCH-L5 and RPN13^{DEU} was assumed during curve fitting, in line with the crystal structures. In this way, the concentration of RPN13^{DEU} in the cell was calculated to be 12.5 μM .

Structure determination

The complexes were crystallized using the vapor diffusion method in sitting drops. X-Ray data collection was done at the European Synchrotron Radiation Facility (ESRF) and Swiss Light Source (SLS) at 100K. The images were integrated with XDS⁸ or iMosflm⁹ and merging/scaling was performed in Aimless¹⁰.

In all cases starting phases were obtained by molecular replacement (MR) in Phaser (McCoy et al., 2007). Model refinement was carried out in Phenix¹², autoBUSTER¹³ and Refmac¹⁴ with TLS. Models were build using COOT¹⁵. Data collection and refinement results are presented in table 1.

UCH-L5/RPN13^{DEU} was crystallized at 4°C in 100 mM Bis-Tris-Propane pH 6.4, 230 mM NaBr, 21%PEG 3350. Data was collected at ESRF ID14-4. UCH-L5 (3ihr) was used as a MR search model. Initial MR with apo RPN13 failed due to the large conformational changes in complexed RPN13^{DEU}. Initial electron density maps showed density for RPN13^{DEU} helix $\alpha 5$. After iterative cycles of manual building of RPN13^{DEU} refinement in refmac and autoBUSTER, most of the RPN13^{DEU} backbone and side chains could be discerned. To confidently build RPN13^{DEU} helices 1 and 2, the UCH-L5~UbPrg/RPN13^{DEU} structure that was obtained later at higher resolution was used. Of the 328 residues in full length UCH-L5, 7-150, 163-244 and 254-315 were build into density. Of the RPN13^{DEU} construct (aa 265-388), residues 287-384 were modeled.

To determine the structure of the UCH-L5~UbPrg/RPN13^{DEU} complex, we crystallized the complex at 4°C in 100 mM Bis-Tris-Propane pH 5.8, 300 mM NaBr, 21%PEG 3350 and measured diffraction at ESRF ID23-2. MR was performed using the partially build UCH-L5/RPN13^{DEU} structure. After obtaining a solution, ubiquitin could be unambiguously docked into the difference density. Cycles of building and refinement with Refmac allowed completion RPN13^{DEU} model, where residues 287-384 could be modeled (of 265-388). UCH-L5 residues, 6-153, 160-245 and 253-320 were build into density. All residues of ubiquitin were build.

The inhibitory UCH-L5/INO80G^{DEU} was crystallized at room temperature in 100 mM Tris pH 9.0, 200 mM LiCl, 17% PEG 8000. Two isomorphous datasets were collected on ID23-2 at the ESRF, and PXIII at the SLS, that were merged. Initial phases of the UCH-L5/INO80G^{DEU} structure were obtained by MR using UCH-L5 (3ihr) as a search model. Electron density maps clearly indicated the altered ULD conformation. After refinement with Refmac and docking the ULD into the density, more features of INO80G^{DEU} became visible. Multiple rounds of manual building and refinement using autoBUSTER, phenix.den_refinement¹⁶ led to complete tracing of the INO80G^{DEU} main chain. The quality of the maps around INO80G^{DEU} helix $\alpha 6$ allowed modeling of side chains from halfway helix $\alpha 5$ up to residue 153. Extensive refinement with phenix.refine and autoBUSTER allowed modeling of the FRF-hairpin and modeling of side chains in parts of $\alpha 2-4$. Additionally, using phenix feature enhanced maps INO80G^{DEU} Phe49 and Phe50 could be modeled. The structure was completed using models that were obtained later of the UCH-L5~UbPrg/INO80G_{short} complex. In the end residues, 6-147, 160-243 and 254-320 of UCH-L5 were built into density. Of the crystallized INO80G^{DEU} construct (aa 39-170), residues 44-153 were modeled.

The UCH-L5~UbPrg/INO80G_{short} complex was crystallized at 4°C in 100 mM MIB pH 5.0, 250 mM ammonium acetate, 25% PEG 3350. Data were collected at ESRF beamline ID23-2. The structure was determined 3.7 Å resolution by using the UCH-L5~UbPrg structure from UCH-L5~UbPrg/RPN13^{DEU} complex and residues 44-101 of the INO80G^{DEU} (discussed above) as MR search models. Four-fold non-crystallographic symmetry (NCS) was present and this was exploited using NCS map averaging in COOT to obtain higher quality maps. After this procedure several residues in INO80G^{DEU} including anchor residue Trp58 could be modeled with confidence. By iteratively model building/refinement and switching between the UCH-L5~UbPrg/INO80G_{short} and UCH-L5/INO80G^{DEU} structures, all remaining unmodelled side chain could be built in both INO80G structures. NCS restraints were employed during refinement as well as high-resolution target restraints. UCH-L5 and ubiquitin from the 2.3 Å UCH-L5~UbPrg/RPN13^{DEU} structure were used a target in autoBUSTER and phenix.refine.

Structure improvement and validation were performed by PBD_redo and Molprobity^{17,18}.

Structure and sequence alignments

Visual analysis of our UCH-L5 structures indicated that the ULD is the main conformationally flexible region. Pairwise structural superpositions of our complexes with RAPIDO¹⁹ confirmed this and identified the UCH-L5 catalytic domain (aa 1-226) as common invariant region. All subsequent structural alignments of UCH-L5 complexes were subsequently performed using aa 1-226 in SSM to allow for multiple structural alignments. Structural superpositioning of the DEUBAD domains was performed by SSM,

using the pdbeFold webserver²⁰.

Other multiple sequence alignment were generated using the MAFFT algorithm²¹. Sequence alignment figures were generated with Jalview²².

SUPPLEMENTAL REFERENCES

1. Carette, J. E. *et al.* Ebola virus entry requires the cholesterol transporter Niemann-Pick C1. *Nature* **477**, 340–3 (2011).
2. Luna-Vargas, M. P. A. *et al.* Enabling high-throughput ligation-independent cloning and protein expression for the family of ubiquitin specific proteases. *J. Struct. Biol.* **175**, 113–119 (2011).
3. Ekkebus, R. *et al.* On terminal alkynes that can react with active-site cysteine nucleophiles in proteases. *J. Am. Chem. Soc.* **135**, 2867–70 (2013).
4. Sommer, S., Weikart, N. D., Linne, U. & Mootz, H. D. Covalent inhibition of SUMO and ubiquitin-specific cysteine proteases by an in situ thiol-alkyne addition. *Bioorg. Med. Chem.* **21**, 2511–7 (2013).
5. Dang, L. C., Melandri, F. D. & Stein, R. L. Kinetic and mechanistic studies on the hydrolysis of ubiquitin C-terminal 7-amido-4-methylcoumarin by deubiquitinating enzymes. *Biochemistry* **37**, 1868–79 (1998).
6. El Oualid, F. *et al.* Chemical synthesis of ubiquitin, ubiquitin-based probes, and diubiquitin. *Angew. Chem. Int. Ed. Engl.* **49**, 10149–53 (2010).
7. Geurink, P. P., El Oualid, F., Jonker, A., Hameed, D. S. & Ovaa, H. A general chemical ligation approach towards isopeptide-linked ubiquitin and ubiquitin-like assay reagents. *ChemBiochem* **13**, 293–7 (2012).
8. Kabsch, W. XDS. *Acta Crystallogr. D. Biol. Crystallogr.* **66**, 125–32 (2010).
9. Batty, T. G. G., Kontogiannis, L., Johnson, O., Powell, H. R. & Leslie, A. G. W. iMOSFLM: a new graphical interface for diffraction-image processing with MOSFLM. *Acta Crystallogr. D. Biol. Crystallogr.* **67**, 271–81 (2011).
10. Evans, P. R. & Murshudov, G. N. How good are my data and what is the resolution? *Acta Crystallogr. D. Biol. Crystallogr.* **69**, 1204–14 (2013).
11. McCoy, A. J. *et al.* Phaser crystallographic software. *J. Appl. Crystallogr.* **40**, 658–674 (2007).
12. Adams, P. D. *et al.* PHENIX: a comprehensive Python-based system for macromolecular structure solution. *Acta Crystallogr. D. Biol. Crystallogr.* **66**, 213–21 (2010).
13. Smart, O. S. *et al.* Exploiting structure similarity in refinement: automated NCS and target-structure restraints in BUSTER. *Acta Crystallogr. D. Biol. Crystallogr.* **68**, 368–80 (2012).
14. Murshudov, G. N., Vagin, A. A. & Dodson, E. J. Refinement of macromolecular structures by the maximum-likelihood method. *Acta Crystallogr. D. Biol. Crystallogr.* **53**, 240–55 (1997).
15. Emsley, P., Lohkamp, B., Scott, W. G. & Cowtan, K. Features and development of Coot. *Acta Crystallogr. D. Biol. Crystallogr.* **66**, 486–501 (2010).
16. DiMaio, F. *et al.* Improved low-resolution crystallographic refinement with Phenix and Rosetta. *Nat. Methods* **10**, 1102–4 (2013).
17. Chen, V. B. *et al.* MolProbity: all-atom structure validation for macromolecular crystallography. *Acta Crystallogr. D. Biol. Crystallogr.* **66**, 12–21 (2010).
18. Joosten, R. P., Long, F., Murshudov, G. N. & Perrakis, A. The PDB_REDO server for macromolecular structure

model optimization. *IUCrj* **1**, 213–20 (2014).

19. Mosca, R., Brannetti, B. & Schneider, T. R. Alignment of protein structures in the presence of domain motions. *BMC Bioinformatics* **9**, 352 (2008).
20. Krissinel, E. & Henrick, K. Secondary-structure matching (SSM), a new tool for fast protein structure alignment in three dimensions. *Acta Crystallogr. D. Biol. Crystallogr.* **60**, 2256–68 (2004).
21. Katoh, K. & Toh, H. Recent developments in the MAFFT multiple sequence alignment program. *Brief. Bioinform.* **9**, 286–98 (2008).
22. Waterhouse, A. M., Procter, J. B., Martin, D. M. A., Clamp, M. & Barton, G. J. Jalview Version 2--a multiple sequence alignment editor and analysis workbench. *Bioinformatics* **25**, 1189–91 (2009).

chapter | FOUR

BAP1/ASXL1 recruitment and activation for H2A deubiquitination

¹Danny D. Sahtoe, ¹Willem J. Van Dijk, ²Reggy Ekkebus,
²Huib Ovaa and ^{1*}Titia K. Sixma.

¹*Division of Biochemistry and Cancer genomics center*

²*Division of Cell biology II*

Netherlands Cancer Institute, Plesmanlaan 121, 1066CX, Amsterdam, the Netherlands

**correspondence: t.sixma@nki.nl*

Submitted

ABSTRACT

The deubiquitinating enzyme BAP1 is an important tumor suppressor that has drawn attention in the clinic since its loss leads to a variety of cancers. BAP1 is activated by ASXL1 to deubiquitinate mono-ubiquitinated H2A at K119 in Polycomb gene repression, but the mechanism of this reaction remains poorly defined. Here we show that the BAP1 C-terminal extension is important for H2A deubiquitinating activity by auto-recruiting BAP1 to nucleosomes in a process that does not require the nucleosome acidic patch. This initial encounter-like complex is unproductive and needs to be activated by the DEUBAD domains of ASXL1, ASXL2 or ASXL3 to increase BAP1's affinity for mono-ubiquitinated H2A, and drive the deubiquitination reaction. The reaction is specific for Polycomb modifications of H2A as the complex cannot deubiquitinate the DNA damage-dependent ubiquitination at H2A K13/15. Our results contribute to the molecular understanding of this important tumor suppressor.

INTRODUCTION

The deubiquitinating enzyme (DUB) **B**RCA-1 **A**ssociated **P**rotein **1** (BAP1) is a critical tumor suppressor that has attracted medical interest in the past years since its loss leads to a variety of cancers¹ including metastatic cutaneous and uveal melanoma, pleural mesothelioma, renal cell carcinoma and bladder tumors²⁻⁸. Germ-line loss of BAP1 leads to a predisposition for cancer and BAP1 tumors are associated with high tumor aggressiveness and poor prognosis⁹. The molecular pathogenesis of disorders associated with BAP1 dysfunction is poorly understood which reflects our incomplete understanding of BAP1 biology.

BAP1 has several targets and functions of which many take place in the nucleus. It participates in the DNA damage response (DDR), DNA synthesis and cell cycle progression¹⁰⁻¹². For many of these functions the catalytic activity of the enzyme is required. An emerging, but poorly understood role for BAP1 is in transcriptional regulation. Several studies indicate that BAP1 associates with transcription related proteins such as FOXK2, HCF-1, OGT, LSD2, MBD-6, MBD-5, ASXL1 and ASXL2 to regulate the expression of target genes^{8,13-15}.

One function of BAP1 in transcriptional regulation is its role in Polycomb gene repression. A hallmark of Polycomb repression is the monoubiquitination of histone 2A (H2A) at K119 by the Polycomb Repressive complex-1 (PRC-1). Paradoxically both the generation and removal of this modification are required for gene repression. In *Drosophila* the removal is catalyzed by the Polycomb Repressive DUB complex that consists of BAP1 and the Polycomb protein ASX, a protein necessary for the long-term repression of HOX genes^{16 17}. In this complex BAP1 is activated by ASX to deubiquitinate H2A¹⁶. The complex is highly conserved and also deubiquitinates H2A in mammals^{7,11,14}.

Humans possess three homologs of *Drosophila* ASX, named **A**dditional **s**excombs **l**ike **1** (ASXL1), ASXL2 and ASXL3 which are all linked to gene regulation and are often disrupted in human cancers¹⁸. ASXL1 disruption is especially detrimental, as it is strongly associated with acute and chronic myeloid leukemia, chronic myelomonocytic leukemia and other cancers¹⁸. ASXL1 deregulation is also linked to myelodysplastic syndrome, a disorder that conditional BAP1 knock-out mice also develop, and can lead to leukemia⁸. Additionally, ASXL1 is together with ASXL3 implicated in the Böhrling-Opitz syndrome, a disorder characterized by malformation of the body and intellectual disability¹⁹.

BAP1 is a member of the ubiquitin C-terminal hydrolase family of DUBs, together with UCH-L1, UCH-L3 and UCH-L5. These are all cysteine proteases with a conserved catalytic UCH domain (CD). Only BAP1 and UCH-L5 share a conserved ULD domain at their C-ter-

mini. In UCH-L5 the orientation of the ULD domain is important for enzymatic activity^{20,21}. The ULD domain in BAP1 is likely structurally related to the UCH-L5 ULD, but BAP1 contains a ~350 aa insert between CD and ULD. This insert does not resemble any known conserved domains but is nevertheless important for certain functions such as binding to the HCF-1 protein^{7,13}.

While regulation of DUB activity by protein partners is widespread^{22,23}, in the UCH family, BAP1 and UCH-L5 are known to be regulated by protein partners. Phylogenetical analysis of these protein partners, ASXL1 for BAP1, and RPN13 and INO80G for UCH-L5, indicates that they all share a conserved DEUbi-ubiquitinase ADaptor (DEUBAD) domain²⁴. While for UCH-L5 regulators RPN13 and INO80G the regulatory mechanisms have been described^{20,21}, it is still unknown whether the putative ASXL1 DEUBAD domain is sufficient to regulate BAP1 and if this mechanism is related to the UCH-L5 regulatory mechanism.

Here we analyze the mechanism of H2A deubiquitination by the BAP1/ASXL1 complex. We demonstrate that the enzymatic activity is mechanistically similar to the related UCH-L5/RPN13 complex. The DEUBAD domains of ASXL1, ASXL2 and ASXL3 can activate BAP1 by increasing its affinity for ubiquitin. This by itself not sufficient for deubiquitination of BAP1's physiological substrate mono-ubiquitinated H2A K119, but also requires the BAP1 C-terminal extension that auto-recruits BAP1 to nucleosomes.

RESULTS

ASX family DEUBAD domains activates BAP1 deubiquitination of H2A K119

The N-terminus of ASXL1 is responsible for BAP1 activation¹⁶. This region contains a predicted HARE-HTH DNA binding domain and DEUBAD domain (Fig. 1a)^{24,25}. We expressed and purified constructs of these domains and tested what their contribution was to BAP1 activation in vitro using the minimal DUB substrate ubiquitin-7-amido-4-methylcoumarin (Ub-AMC)²⁶. We found that ASXL1₁₋₃₉₀ could activate the reaction (Fig. 1b). Within this region most of the activity is present in the ASXL1 DEUBAD domain (ASXL1^{DEU}), since a construct (238-390), lacking the HARE-HTH domain (ASXL1^{HH}), could activate BAP1 to the same extent (Fig. 1b). Enzyme kinetics analysis indicated that the activation effect of ASXL1^{DEU} is modest on this artificial substrate, lowering the K_M 4-fold while it has a minor effect on k_{cat} (Fig. 1c and Supplementary Table 1).

To investigate BAP1 activity on a relevant substrate, we purified oligonucleosomes and mono-ubiquitinated H2A at K119 with the E3 ligase RING1B/BMI1, one of the possible catalytic modules for PRC-1 complexes (Supplementary Fig. 1a). Like on Ub-AMC, ASXL1₁₋₃₉₀ could activate BAP1 to the same extent as ASXL1^{DEU} (Fig. 1d). The activation effect was however more dramatic on H2A compared to Ub-AMC. The ASXL1^{HH} domain hardly

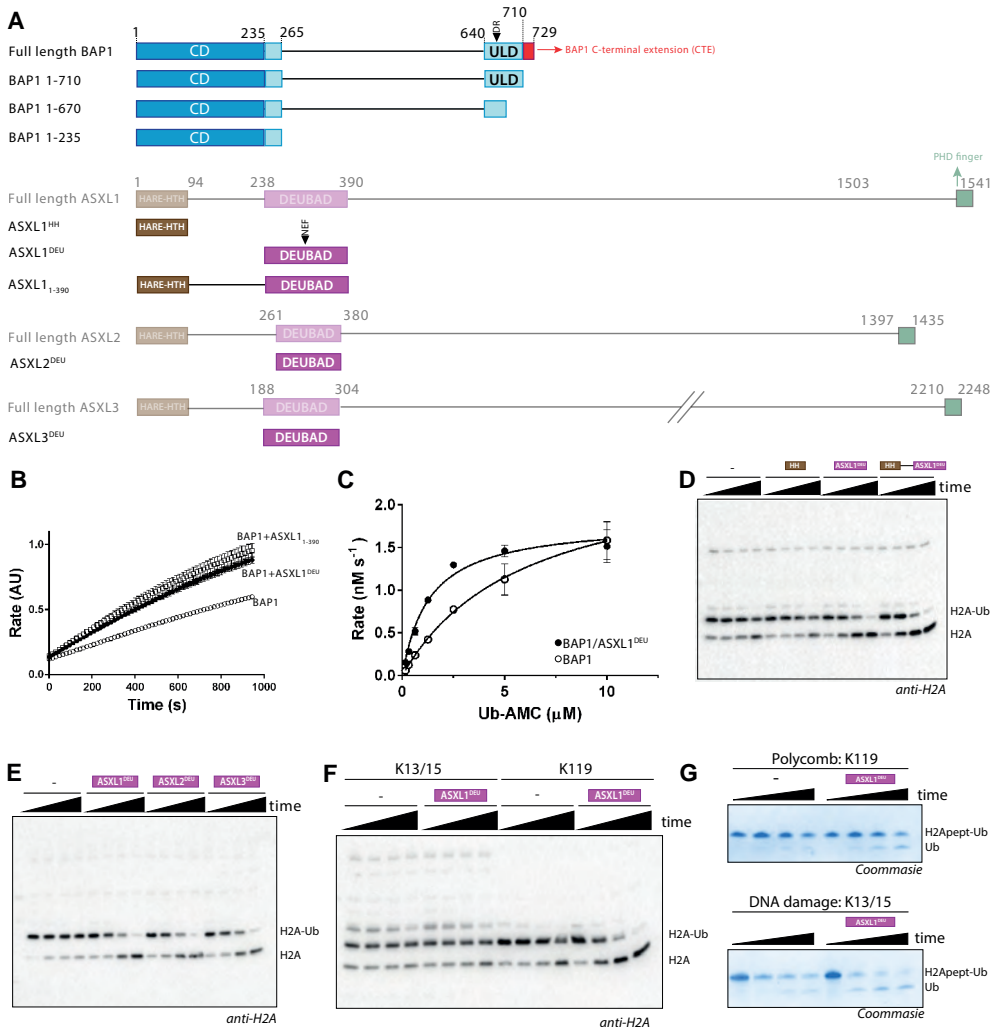


Figure 1 | The DEUBAD domain in ASXL proteins activates BAP1 to specifically deubiquitinate K119 on H2A. A) Overview of constructs. Locations of point mutant indicated with filled triangles. **B)** The DEUBAD domain but not the HARE-HTH domain can stimulate BAP1 activity against Ub-AMC. Error bars, SD (n=3 independent experiments). **D)** The BAP1/ASXL1^{DEU} complex (closed circles) has a lower K_M than BAP1 alone (open circles) in Ub-AMC kinetics. Error bars, SD (n=3 independent experiments). **D)** The DEUBAD domain but not the HARE-HTH domain can stimulate BAP1 activity against mono-ubiquitinated H2A in oligonucleosomes (time points: 0, 1, 5, 25 min). BAP1 alone reactions indicated with "-". **E)** The DEUBAD domains of ASXL2 and ASXL3 can also activate BAP1 on oligonucleosomes. **F)** The BAP1/ASXL1^{DEU} complex is inactive against H2A mono-ubiquitinated at Lys13/15 in oligonucleosomes (time points: 0, 1, 5, 25 min). **G)** The BAP1/ASXL1^{DEU} can deubiquitinate mono-ubiquitinated H2A at Lys13/15 in a minimal H2A substrate.

affected BAP1 activity on Ub-AMC, but since this construct contains a putative DNA binding domain, we tested if it was active on nucleosomal H2A. This was not the case; the ASXL1^{HH} construct had no effect on H2A deubiquitination, confirming that the ASXL1-dependent activation effect is fully contained in the DEUBAD domain (Fig. 1d).

ASXL2 and ASXL3 also contain predicted DEUBAD domains (Supplementary Fig. 1b), with more than 60% sequence identity to ASXL1. Proteomics analyses have observed interaction of BAP1 with ASXL2^{DEU}, but not yet with ASXL3^{DEU}. We tested whether the ASXL2 and ASXL3 DEUBAD domains could also stimulate H2A deubiquitination by BAP1. This was the case for both ASXL2^{DEU} and ASXL3^{DEU}, with kinetics comparable to ASXL1^{DEU} (Fig. 1e). These results establish that the DEUBAD domains in all human ASXL paralogs can stimulate BAP1 activity.

The BAP1/ASXL1 complex specifically deubiquitinates the Polycomb site

Besides mono-ubiquitination of H2A at K119 in Polycomb repression, H2A is also ubiquitinated at the K13/15 site by RNF168 in the early stages of the DNA double strand break response^{27,28}. Since K119 and K13/15 reside at distinct locations in the nucleosome (Supplementary Fig. 1c) we asked whether BAP1 could also deubiquitinate K13/15. We tested this by ubiquitinating oligonucleosomal H2A with full length RNF168 (Supplementary Fig. 1d) before providing the resulting conjugate as a substrate to the BAP1/ASXL1^{DEU} complex. While the activity was low on the K13/15 site, the complex robustly deubiquitinated the Polycomb site indicating a strong preference for this site over the K13/15 site (Fig. 1f). Since the N-terminal tail of H2A, that contains K13/15 and the C-terminal tail that contains K119, differ in sequence the low activity on the K13/15 site could simply reflect a structural incompatibility between the tail and the active site of BAP1. To investigate whether this is the case, we incubated BAP1 and the BAP1/ASXL1^{DEU} complex with N and C terminal peptides derived from H2A, ubiquitinated on either the K13 or K119, and measured hydrolysis. Peptides were obtained by solid phase peptide synthesis followed by chemical ubiquitination using thiolysine mediated ubiquitin conjugation²⁹. In both cases, either BAP1 alone or in complex with ASXL1^{DEU} could deubiquitinate the substrates. Moreover the enzyme was more efficient in hydrolyzing the K13 site on this peptide (Fig. 1g). These data show that the specificity of the BAP1/ASXL1 complex for the Polycomb site (K119) is not determined by the local environment of the scissile isopeptide bond, but at regions outside the ubiquitinated tail such as the nucleosome core.

BAP1 binds ASXL1^{DEU} similar to the UCH-L5/RPN13^{DEU} complex

The BAP1/ASXL1 complex has two closely related counterparts, the UCH-L5/RPN13 and UCH-L5/INO80G that are present in the proteasome and in INO80 chromatin remodeling complexes respectively. In these two complexes a DEUBAD domain is present in the regulatory proteins, RPN13 and INO80G, that binds to the C-terminal ULD domain of the UCH-L5. RPN13^{DEU} binding activates UCH-L5 via a combination of mild allosteric effects that increase UCH-L5's affinity for substrates. First RPN13 positions the active site cross-

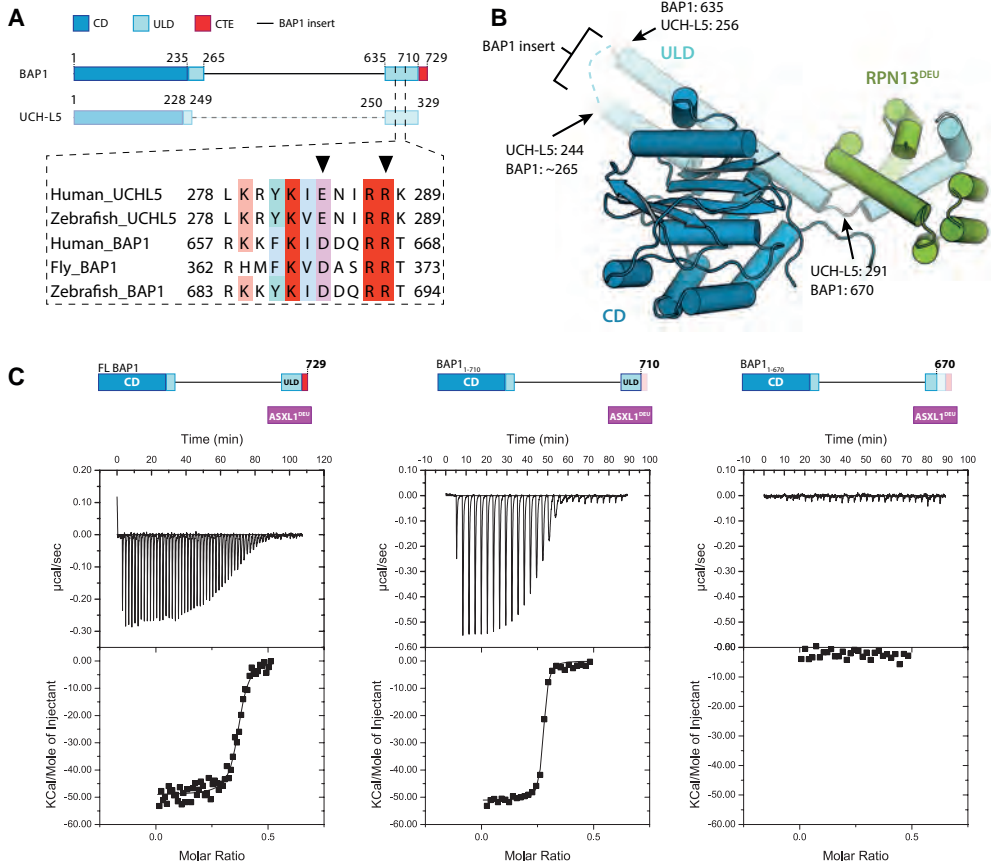


Figure 2 | The BAP1 ULD binds ASXL1^{DEU}. **A)** The BAP1 and UCH-L5 are highly similar in the catalytic domain and ULD. UCH-L5 does not contain the insert that BAP1 has as indicated by a dashed line. The ULD anchor is highly conserved in BAP1 and UCH-L5 (inset, ULD anchor residues indicated with triangle). **B)** Cartoon representation of the UCH-L5/RPN13^{DEU} structure (PDB: 4uel, UCH-L5 CD in blue, UCH-L5 ULD in light blue, RPN13^{DEU} in green) with labels indicating equivalent BAP1 positions. **C)** Isothermal titration calorimetry (ITC) assays. ASXL1^{DEU} binds the C-terminal ULD of BAP1 and the BAP1 CTE is not required for ASXL1^{DEU} binding.

over loop (CL) in an active conformation. The CL is a flexible loop close to the active site in UCH enzymes that limits enzymatic activity. RPN13^{DEU} binding furthermore precisely anchors the ULD domain to the catalytic domain of UCH-L5 using a highly conserved interface that is also present in BAP1 (Fig. 2a, inset). Since the ULD domain is close to the ubiquitin binding site, this positioning of the “ULD anchor” locks the ULD domain in a conformation that allows ubiquitin binding. This positioning also creates a small interface between ubiquitin and RPN13^{DEU} itself that gives an additional effect on UCH-L5 activation.

The sequence and functional similarity between the BAP1/ASXL1^{DEU} and UCH-L5/RPN13^{DEU} complexes prompted us to examine whether the BAP1/ASXL1 complex

functions in a similar fashion (Fig. 2a). We first characterized complex formation by deleting the predicted ASXL1^{DEU} binding site on BAP1, based on the crystal structure of the UCH-L5/RPN13^{DEU} complex (Fig. 2b). As expected this construct, BAP1_{1-670'} did not interact with ASXL1^{DEU} in isothermal titration calorimetry binding assays (ITC) and also not in gel filtration (data not shown). In contrast, WT BAP1 bound ASXL1^{DEU} with a K_d of 18 nM (Fig. 2c and Supplementary Table 2). These results indicate that BAP1 and UCH-L5 use the same region in the ULD to bind their activator. The ULD of BAP1 is largely similar to UCH-L5 except that it contains an approximately 20 amino acid C-terminal extension (CTE) (Fig. 2a). The CTE is not important for ASXL1^{DEU} binding though, since both full length BAP and BAP1₁₋₇₁₀ (construct lacking the CTE) could bind ASXL1^{DEU} with similar affinity (Fig. 2c and Supplementary Table 2).

Even though BAP1 and UCH-L5 use the same region to dock their activator, the ITC analysis indicated a notable difference between these complexes. While the UCH-L5/RPN13 complex is equimolar at 1:1, our ITC analysis suggests that the BAP1/ASXL1 complex is asymmetric and consists of two BAP1 molecules bound to one ASXL1^{DEU} molecule. This result is in agreement with a previous quantitative mass spectrometry study that also suggested a 2:1 stoichiometry for the BAP1/ASXL1 complex in cells¹⁵.

ASXL1^{DEU} increases BAP1's affinity for ubiquitin

ASXL1^{DEU} stimulates BAP1 by lowering the K_M on Ub-AMC (Supplementary Table 1). Therefore we tested whether ASXL1^{DEU} can activate BAP1 by increasing its affinity for ubiquitin. To this end, we analyzed the rate of Ub-AMC hydrolysis by BAP1 or the BAP1/ASXL1^{DEU} complex, in the presence of increasing concentrations of a novel non hydrolysable H2A-peptide ubiquitin conjugate. The conjugate was obtained using an azido-alkyne click reaction between Ub-75-propargyl (Ub-75-Prg) and azido ornithine followed by thorough purification to remove any traces of Ub-75-Prg which is a covalent DUB inhibitor³⁰. The resulting conjugate mimics substrates³¹ (Fig. 3a) and will therefore compete with Ub-AMC for binding to BAP1 leading to inhibition of Ub-AMC hydrolysis. While the conjugate inhibited BAP1 with an IC_{50} of approximately 45 μ M, the IC_{50} of the BAP1/ASXL1^{DEU} complex was more than 10 fold lower indicating that ASXL1^{DEU} induces a higher affinity of BAP1 to the conjugate (Fig. 3a and Supplementary Table 3). The H2A corresponding peptide without a conjugated ubiquitin molecule did not inhibit Ub-AMC hydrolysis at all, and ubiquitin alone had only a minor inhibitory effect on the rate of the BAP1/ASXL1^{DEU} complex (Supplementary Figs. 2a and 2b). The fact that an ubiquitin-conjugate can inhibit BAP1 to a greater extent than ubiquitin alone, illustrates how this DUB prefers binding its target (ubiquitin-conjugate) over its product (ubiquitin alone).

To validate this result in a more relevant setting we performed band shift assays with

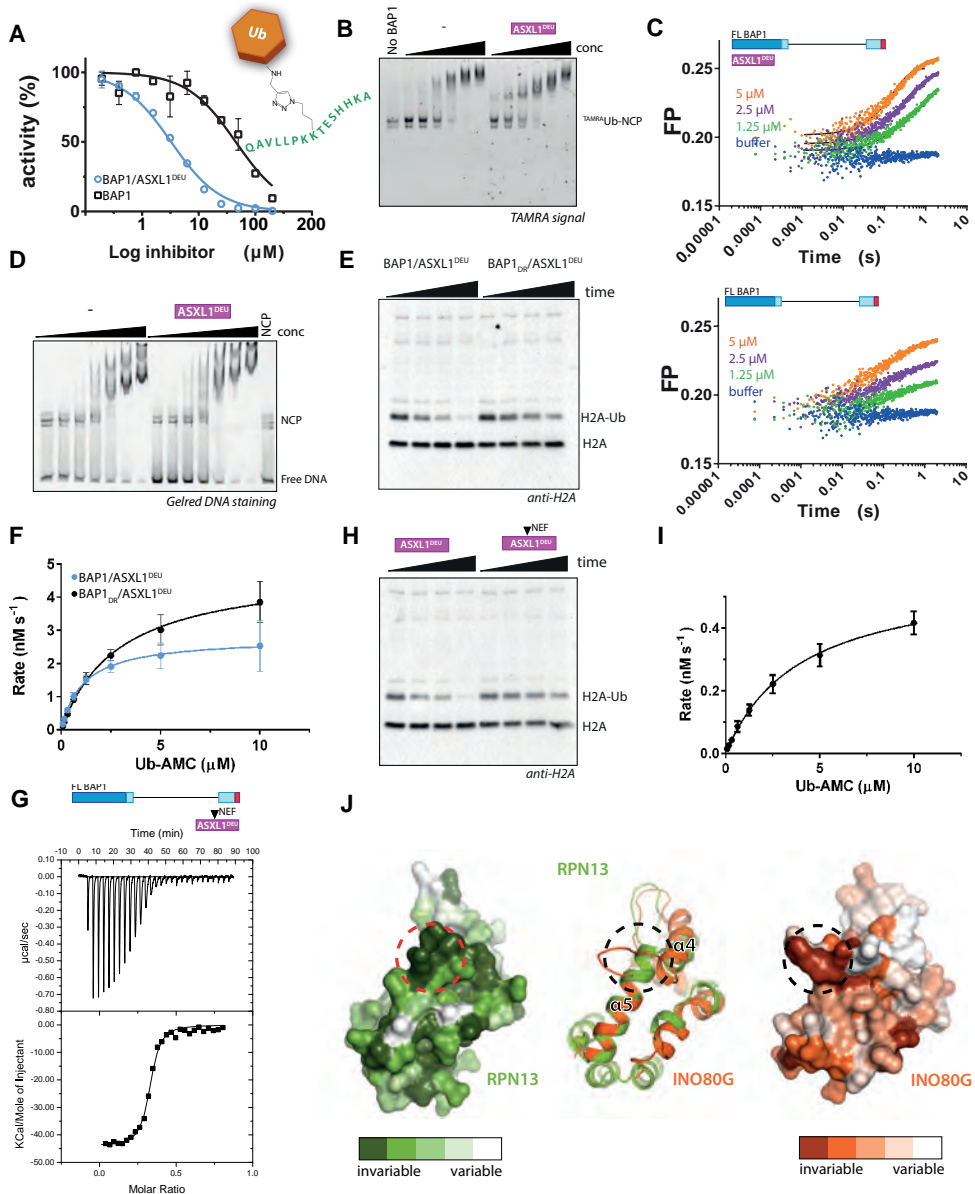


Figure 3 | ASXL1^{DEU} activates BAP1 by increasing its affinity for ubiquitin. **A)** BAP1 is inhibited more readily by the non-hydrolyzable ubiquitin conjugate in the presence of ASXL1^{DEU}. Inset: Schematic of the non-hydrolyzable H2A ubiquitin conjugate. Error bars, SD (n=2 independent experiments). **B)** In the presence of ASXL1^{DEU}, BAP1 has a higher affinity for monoubiquitinated NCPs than BAP1 alone in band shift assays (2-fold dilutions starting from 15 μM). **C)** Using stopped-flow fluorescence polarization binding assays we confirmed that the BAP1/ASXL1^{DEU} complex (top) binds better to monoubiquitinated nucleosomes than BAP1 alone (bottom). **D)** BAP1 and BAP1/ASXL1^{DEU} bind unmodified NCPs with similar affinities in band shift assays (2-fold dilutions starting from 15 μM). **E)** The BAP1 ULD anchor mutant (D663A/R667A, DR) is less active in H2A deubiquitination. **F)** BAP1^{DR}/ASXL1^{DEU} complex has a 3-fold weaker K_M than the WT complex (see also Table S1). Error bars, SD (n=3 independent experiments). **G)** ASXL1^{NEF} (N310A/E311K/F312A, NEF) binds BAP1 with similar affinity as WT ASXL1^{DEU} in ITC. **H and I)** ASXL1^{NEF} cannot activate BAP1 to the same extent

as WT ASXL1^{DEU} using mono-ubiquitinated H2A or Ub-AMC as a substrate. Error bars, SD (n=3 independent experiments). **J**) Surface representation of DEUBAD domains of RPN13 (left) and INO80G (right) indicate high conservation of a region (dotted circle) between helix 4 and 5 (middle: RPN13 green, INO80G orange).

reconstituted recombinant nucleosome core particles (NCPs), modified with N-terminally TAMRA labeled ubiquitin (^{TAMRA}Ub-NCP) using the E3 ligase RING1B/BMI1 (Supplementary Fig. 2c). In these assays the BAP1/ASXL1^{DEU} complex shifted ^{TAMRA}Ub-NCP more readily compared to BAP1 alone as indicated by the high molecular weight bands appearing already at low concentrations (Fig. 3b). This effect is mainly mediated through BAP1 since ASXL1^{DEU} alone did not bind ^{TAMRA}Ub-NCP (Supplementary Fig. 2d). We could confirm our result in a stopped-flow fluorescence polarization binding assay where the BAP1/ASXL1^{DEU} complex could bind to ^{TAMRA}Ub-NCP ($K_D = 4\mu\text{M}$) better than BAP1 alone of which we could not quantify the affinity constant (Figs. 3c and Supplementary 2e). Surprisingly, when we tested binding to unmodified nucleosomes, BAP1 and the complex could shift the NCPs equally well (Fig. 3d). Thus ASXL1^{DEU} specifically promotes the binding of the conjugated ubiquitin and not the nucleosome by itself.

As the region of BAP1 equivalent to the ULD anchor in UCH-L5 (see earlier) is highly conserved (Fig. 2a) we assessed whether it contributes to BAP1 activation. To test this we incubated an ULD anchor mutant of BAP1 (D663A/R667A referred to as DR) and WT complex with mono-ubiquitinated H2A and Ub-AMC. The ULD anchor mutant complex BAP1_{DR}/ASXL1^{DEU} was indeed slightly impaired in H2A deubiquitination and had a weaker K_M than the WT complex in Ub-AMC hydrolysis (Figs. 3e and 3f and Supplementary Table 1). Using the non-hydrolyzable ubiquitin-H2A conjugate (Fig. 3a), we found that the mutant complex had a weaker IC_{50} for the conjugate than the WT complex in Ub-AMC assays (Supplementary Fig. 2f and Supplementary Table 3). This suggests that like the UCH-L5/RPN13^{DEU} complex, ASXL1^{DEU} stabilizes the BAP1 ULD domain by anchoring it to the CD allowing more efficient substrate binding.

We next focused our attention on ASXL1^{DEU}. After analysis of a multiple sequence alignment of the ASX family we noticed a highly conserved “NEF” region that suggests it is important for ASXL1^{DEU} function (Supplementary Fig. 2g). To test this hypothesis we generated a triple mutant containing N310A, E311K and F312A (referred to as ASXL1_{NEF}^{DEU}). We first validated that ASXL1_{NEF}^{DEU} was not impaired in BAP1 binding using ITC ($K_D = 45\text{ nM}$) (Fig. 3g and Supplementary table 2). Then we tested activity against mono-ubiquitinated nucleosomes and found that this mutant was impaired in activating BAP1 compared to WT ASXL1^{DEU} (Fig. 3h). We quantified the activation effect using Ub-AMC as a substrate and noted a 3-fold weaker K_M but surprisingly also a 3-fold lower k_{cat} compared to WT (Fig. 3i and Supplementary Table 1) conforming that this region of the protein affects BAP1 activation.

To rationalize the effect of the ASXL1^{DEU} “NEF” mutant, we examined the crystal structure of the UCH-L5/RPN13^{DEU} complex bound to ubiquitin^{20,21}. In the structure, the RPN13 region equivalent to the “NEF” region stabilizes ubiquitin and thereby contributes to activation of UCH-L5 (Supplementary Fig. 2h). Thus it seems likely that ASXL1^{DEU} also uses this ubiquitin interface to stabilize ubiquitin binding of BAP1 and stimulate activity.

This region in DEUBAD domains in general seems to be important for their function. Analysis of the surface conservation in this region of the DEUBAD domains of UCH-L5 activator RPN13 or inhibitor INO80G, reveals that it is highly conserved within the RPN13 and INO80G proteins (Fig. 3j), but not between these two proteins. In contrast to RPN13^{DEU}, which facilitates ubiquitin binding, residues in this conserved region in INO80G block ubiquitin binding^{20,21}. The fact that in all DEUBAD domains, this region is highly conserved and of functional importance, points out that it is a critical site for BAP1/UCH-L5 regulation.

In summary, we have shown that ASXL1^{DEU} activates BAP1 by increasing the affinity for ubiquitin through a combination of mild effects including stabilization of the BAP1 ULD anchor. On the ASXL1^{DEU} side, the highly conserved “NEF” region contributes to the activation likely by stabilizing ubiquitin as in the UCH-L5/RPN13^{DEU} complex.

The BAP1 C-terminus is required for H2A deubiquitination activity

BAP1 is frequently mutated in a various tumor types. A subset of mutations in BAP1 result in frame-shifts that lead to premature stop-codons. In some cases, the catalytic domain is still intact suggesting that regions outside this domain are important for proper BAP1 functioning. Therefore we assessed the effect of H2A deubiquitination activity of BAP1 variants truncated at different points: BAP1₁₋₂₃₅ consisting of only the catalytic domain, BAP1₁₋₆₇₀, which has a disrupted ULD domain and BAP1₁₋₇₁₀, that lacks the C-terminal extension (CTE) of BAP1. While the WT BAP1/ASXL1^{DEU} complex was active in H2A deubiquitination, BAP1₁₋₂₃₅ and BAP1₁₋₆₇₀ had low activity towards H2A irrespective of the presence of ASXL1^{DEU} (Fig. 4a). This is in accordance with our binding data (Fig. 2c) that indicates that these constructs lack the ASXL1^{DEU} docking site. Surprisingly, BAP1₁₋₇₁₀ that only lacks the CTE compared to WT and still binds ASXL1^{DEU} similar to WT, had a low activity despite the presence of ASXL1^{DEU} (Fig. 4a). These results suggested that the BAP1 CTE is important for activity.

To exclude that the intrinsic catalytic activity was affected by the truncation mutants we tested their activity on the minimal substrate Ub-AMC. In contrast to the nucleosomal substrate, we found that all BAP1 variants were active on Ub-AMC, with BAP1₁₋₂₃₅ and BAP1₁₋₆₇₀ being even slightly more active than WT demonstrating that the intrinsic

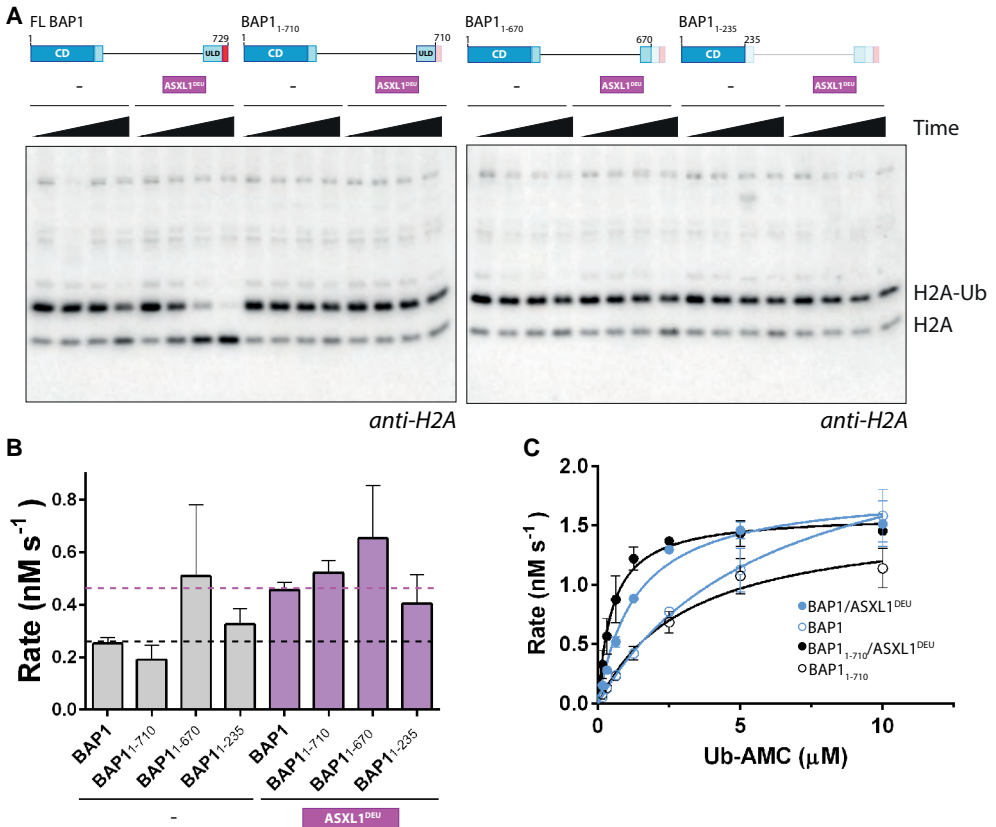


Figure 4 | The BAP1 C-terminal extension is required for H2A deubiquitination. A) Only WT BAP1 can be activated for H2A deubiquitination in oligonucleosomes (time points: 0, 1, 5, 25 min). **B)** All BAP1 variants are active on Ub-AMC. Purple bars represents rates in presence of ASXL1^{DEU}. Dotted black and purple lines highlight the rate of WT BAP1 or BAP1/ASXL1^{DEU} respectively. Error bars, SD (n=3 independent experiments). **C)** Like WT (blue) (Curves from Fig 1b), BAP1₁₋₇₁₀ (black) can be fully activated (reactions with ASXL1^{DEU} in filled circles) on the minimal substrate Ub-AMC. Error bars, SD (n=3 independent experiments).

activity was not compromised (Fig. 4b). On this model substrate, WT BAP1 and BAP1₁₋₇₁₀ were equally active in absence of ASXL1^{DEU}, and could be activated to the same extent in presence of ASXL1^{DEU} (Figs. 4b and 4c and Supplementary table 1). Apparently the CTE does not affect ASXL-dependent activity, but instead it has a substrate-specific role. The tail does not interfere with the intrinsic ability of BAP1 to be activated on the Ub-AMC substrate but is important for activity on the oligonucleosomal H2A substrate.

The BAP1 C-terminus auto-recruits BAP1 to nucleosomes

After establishing that the CTE is important on BAP1's natural substrate H2A we sought to determine the basis of this requirement. The nucleosomal substrate can be considered to consist of two functional parts; the globular core containing the DNA wrapped around the

histone octamer, and the ubiquitinated H2A tail protruding from this core (Fig. 5a). We interrogated the role of the BAP1 CTE by decomposing the nucleosomal substrate and only using a synthetic ubiquitinated H2A tail at K119 as a substrate. On this reduced substrate, both WT and BAP1₁₋₇₁₀/ASXL1^{DEU} complexes were equally active indicating (Fig. 5b) that the BAP1 CTE is not important at this region of the substrate.

To study how the CTE confers activity on the nucleosomal substrate core (Fig. 5a) we studied a multiple sequence alignment of this region. It contains a nuclear localization sequence³², is conserved across species and highly cationic (Fig. 5c). The presence of these conserved positive charges suggest they may participate in electrostatic interactions with the regions of the nucleosome core that tether BAP1 to the substrate. In this hypothesis, co-incubation of BAP1 with a peptide derived from the CTE would compete with the BAP1/ASXL1^{DEU} complex for nucleosome binding leading to decreased DUB activity. We tested this hypothesis, by incubating WT BAP1/ASXL1^{DEU} and BAP1₁₋₇₁₀/ASXL1^{DEU} with increasing concentrations of a synthetic peptide of the CTE. In absence of peptide, the WT BAP1/ASXL1^{DEU} complex, deubiquitinated H2A robustly as observed before (Fig. 5d). But indeed, in the presence of increasing concentrations of the peptide DUB activity was inhibited for the WT complex (Fig. 5d). The synthetic peptide did not inhibit the intrinsic DUB activity on Ub-AMC demonstrating that the observed effect is specific for nucleosomes (Fig. S3a). Interestingly, a scrambled peptide of the CTE also inhibited H2A deubiquitination, suggesting that not the actual sequence but most likely the charge composition is important for the inhibition (Supplementary Fig. 3b).

We then asked if charges on the nucleosome were required for the interaction. An increasing number of chromatin associated proteins are reported to require the acidic patch on nucleosomes for binding or proper functioning³³⁻³⁵. This acidic patch is formed at the interface between the H2A/H2B dimer and is prominently solvent exposed. Since the BAP1 CTE is positively charged at physiological pH, we wondered whether it uses the acidic patch to electrostatically recruit itself to nucleosomes in band shift assays. We found however, that BAP1 does not require the acidic patch for binding since it shifted WT NCPs and the acidic patch mutant of the NCPs (NCP-EA) in a similar fashion (Fig. 5e). This indicates that BAP1 binds to nucleosomes in a way that is distinct from other nucleosome binding proteins.

We then tested if the CTE was important for BAP1 recruitment to the nucleosome in a direct binding assay. In band shift assays, BAP1/ASXL1^{DEU} could shift the NCPs whereas BAP1₁₋₇₁₀/ASXL1^{DEU} complex was less capable of shifting the NCPs indicating again that the C-terminus is important for binding to nucleosomes (Fig. 5f). In short, these results are consistent with a model that the BAP1/ASXL1^{DEU} complex has two main binding components. The BAP1 CTE is required for binding to the NCP core, and presence of ASXL1^{DEU}

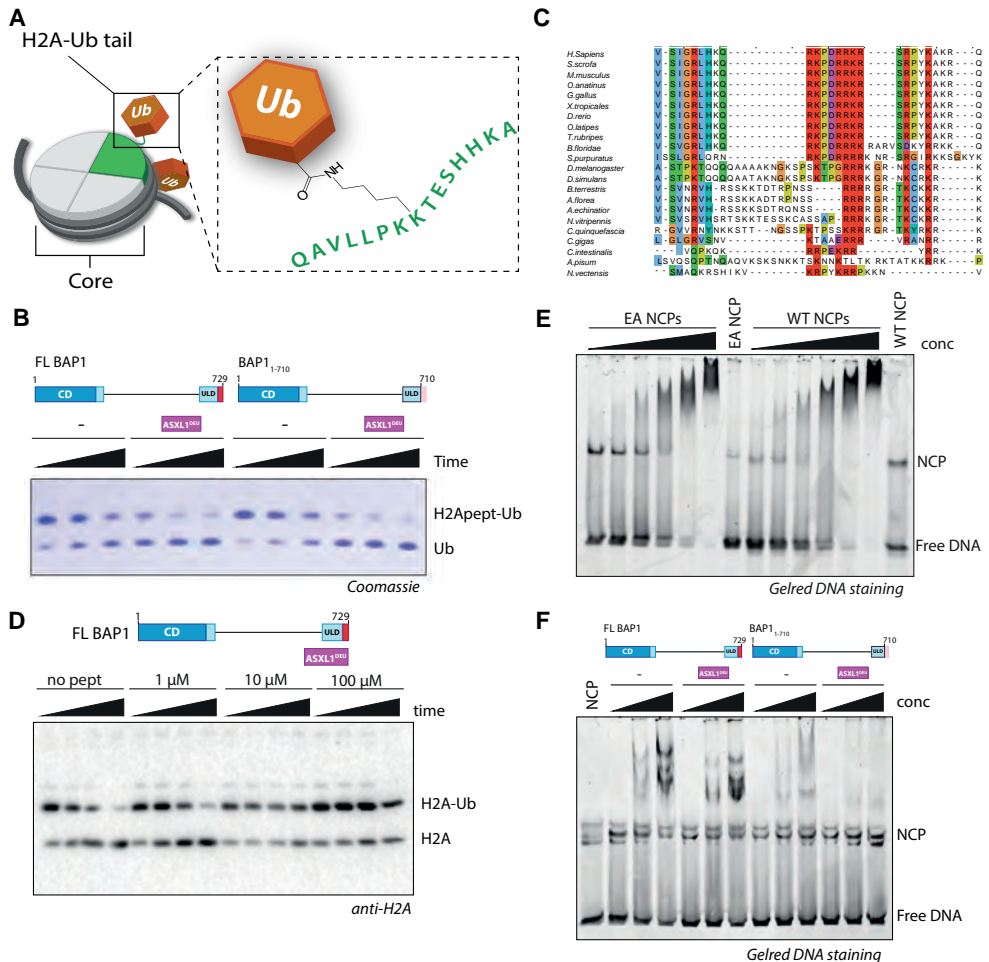


Figure 5 | The BAP1 C-terminal extension auto-recruits BAP1 to nucleosomes. A) The nucleosomal H2A substrate can be decomposed into two functional parts. **B)** While the BAP1₁₋₇₁₀/ASXL1^{DEU} complex is inactive on oligonucleosomes, it is as active as the WT complex on a minimal H2A substrate (time points: 5, 15, 30 min). **C)** The BAP1 tail is highly positively charged. **D)** A synthetic peptide of the BAP1 C-terminus inhibits activity of BAP1/ASXL1^{DEU} on oligonucleosomes (time points: 0, 1, 5, 25 min). **E)** BAP1 does not require the H2A/H2B acidic patch to bind the nucleosomes (2-fold dilutions starting from 15 μM). **F)** BAP1 that lacks its C-terminal tail is impaired in binding NCPs in band shift assays (1, 5, 10 μM of BAP1 variant).

increases BAP1's affinity for the ubiquitin moiety at the protruding H2A tail.

DISCUSSION

BAP1 is a critical tumor suppressor that is frequently mutated in human cancer. In this paper we describe that similar to the homologous UCH-L5/RPN13^{DEU} complex, the DEUBAD domains of ASXL1, ASXL2 and ASXL3 can activate BAP1 by increasing BAP1's affinity for ubiquitin through a combination of mild effects. We observed that activation by ASXL proteins is not sufficient for deubiquitination of BAP1's natural substrate H2A. This

requires the BAP1 C-terminal extension that binds to nucleosomes.

We propose a model where H2A deubiquitination by the BAP1/ASXL1^{DEU} complex consists of two key processes. The BAP1 CTE tethers BAP1 to the nucleosome core. This initial encounter-like complex is however unproductive due to BAP1's low affinity for the mono-ubiquitinated H2A tail in absence of an activator. In a second key process ASXL1^{DEU} can convert this complex into a productive one by increasing BAP1's affinity for ubiquitin (Fig. 6).

The mechanism by which ASXL1^{DEU} increases BAP1's affinity for ubiquitin is related to that of the UCH-L5/RPN13^{DEU} complex of which crystal structures were reported recently^{20,21}. RPN13^{DEU} activates UCH-L5 by decreasing the mobility of the ULD domain, a domain close to the ubiquitin binding site. By fixating it to the UCH-L5 CD via the ULD anchor, RPN13^{DEU} exposes the ubiquitin docking site on UCH-L5 thereby increasing the affinity for ubiquitin. RPN13^{DEU} also mildly contributes to UCH-L5 activation by directly contacting ubiquitin, and by positioning the active-site cross over loop (CL). The CL is a flexible loop close to the active site in UCH enzymes that limits enzymatic activity. Individually these effects are mild but combined they provide substantial regulation.

For BAP1 we observe similar effects. The ULD anchor has a mild effect on affinity, and the region on ASXL1^{DEU} that is equivalent to the region of RPN13^{DEU} that contacts ubiquitin also affects BAP1 activity. The effect of the latter is however stronger in ASXL1^{DEU} than in RPN13^{DEU}. This highlights that although the regulatory regions are similar in the UCH-L5/RPN13^{DEU} or BAP1/ASXL1^{DEU} complex, their relative individual contribution to activation may be different. The lack of conservation between the UCH-L5 and BAP1 CLs made it difficult to assess whether ASXL1^{DEU} also positions the BAP1 CL towards an active con-

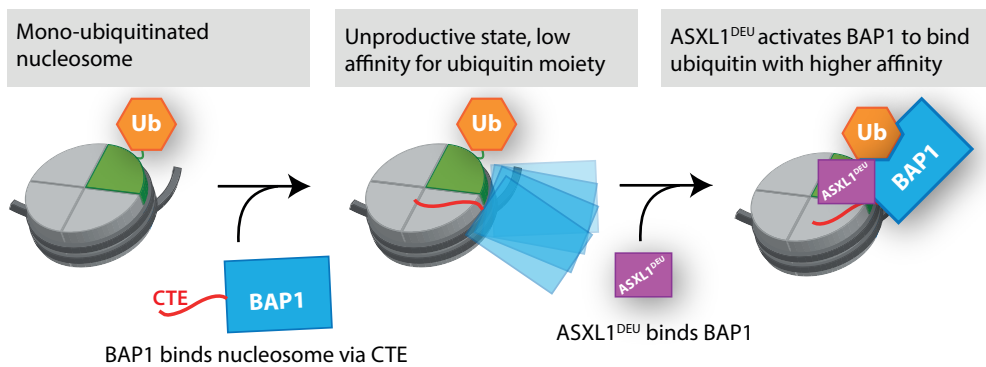


Figure 6 | Model for H2A deubiquitination by the BAP1/ASXL1 complex. BAP1 (blue) binds nucleosomes monoubiquitinated at K119 using its C-terminal extension (red). This complex has low DUB activity due to BAP1's low affinity for ubiquitin (orange). Binding of the DEUBAD domain of ASXL1 (purple) allosterically activates BAP1 by increasing its affinity for the ubiquitin moiety, driving the DUB reaction.

formation. Therefore we omitted this aspect from our analysis but we do not exclude that this may occur.

Our data suggest that the BAP1 CTE is an important component for nucleosome binding. Even though BAP1 is recruited to nucleosomes by various proteins in cells, it is possible that BAP1's relative orientation towards H2A-Ub in these complexes is suboptimal for substrate binding and catalysis. This could be the reason why the BAP1 CTE is required. In addition to the function ascribed to the BAP1 CTE in this study, others have shown that it also hosts a nuclear localization signal that can be ubiquitinated by UBE2O to mislocalize BAP1 to the cytoplasm^{32,36} underscoring the importance of this small region of BAP1. The multiple functions of the CTE also make analysis of its importance in cells difficult.

While ASXL1 and ASXL2 are known to interact with BAP1, ASXL3 was not. Our *in vitro* analysis indicates that also ASXL3 can bind and activate BAP1, which is not surprising in the light of the high sequence similarity between the DEUBAD domains in the ASXL family. It suggests that there may be a functional association between BAP1 and ASXL3 in cells and further cell based work is required to shed more light on this issue.

We found that in a nucleosomal context, the BAP1/ASXL^{DEU} complex is specific for H2A mono-ubiquitinated at the Polycomb site K119 and not on the DNA damage site K13/15. BAP1 has been suggested to play a role in DNA repair but its exact role is unclear. Our results indicate that it is unlikely that the BAP1/ASXL1 complex regulates the DNA damage response by deubiquitinating H2A at K13/15. The specificity for the Polycomb site may be governed by interfaces of the complex with the nucleosome. Therefore we also assessed whether BAP1 can bind the acidic patch on the nucleosome and found that the complex does not rely on this site for binding unlike other nucleosome binding proteins.

An unexpected finding was the stoichiometry of the BAP1/ASXL1 complex where one molecule of ASXL1 is present for two BAP1 molecules. DUB dimers are not unusual. The JAMM proteins RPN11 and BRCC36 both require hetero-dimerization with RPN8 and Abro1 or Abraxas respectively, but in these cases only the first protomer is active. It may also be possible that only one subunit is active in the BAP1/ASXL1 complex. It is conceivable that the BAP1 dimerization is a manifestation of selective pressures on BAP1 to be part of multi-protein complexes where one monomer functions as an assembly platform for other proteins. Future studies will be necessary to further examine the possible functional implications of the BAP1/ASXL1 stoichiometry.

BAP1 associates with many factors to form multi-protein complexes. One of the main outstanding questions is whether multiple mutually exclusive BAP1 complexes exist and whether BAP1 catalytic activity is required in all of these complexes. Perhaps BAP1 can

also serve as a scaffold in some of these complexes to recruit other chromatin modifiers. An important step in understanding the carcinogenesis in BAP1 deficiency will therefore rely on a thorough understanding of the different BAP1 complexes and the effects on BAP1 activity. Our comprehensive biochemical analysis of binding interfaces, activation mechanism and recruitment factors of the BAP1/ASXL1 complex provides a framework for future work on the possible role of these larger BAP1 complexes in tumorigenesis.

MATERIALS & METHODS

Protein expression and purification

His-tagged full length BAP1, BAP1₁₋₇₁₀, BAP1₁₋₆₇₀ and their mutants were expressed in sf21 insect cells using the Bac-to-Bac baculovirus expression system (Invitrogen) and purified by nickel affinity, anion exchange and size exclusion chromatography. Full length RNF168 was prepared as described previously²⁷. His-ASXL1^{DEU} (aa 238-390), GST-ASXL1₁₋₉₄, His-ASXL1₁₋₃₉₀, His-ASXL2^{DEU} (aa 261-380), His-ASXL3^{DEU} (aa 188-304) and HisSUMO-BAP1₁₋₂₃₅ were expressed in *E.coli*. These proteins were purified using nickel and/or GST affinity chromatography, followed by ion exchange chromatography and/or size exclusion chromatography. Nucleosome core particles were prepared as described previously using either the 147 or 167 bp widom601 DNA positioning sequence³⁷⁻³⁹.

Oligonucleosome DUB assays

Oligonucleosomes were purified from HEK 293T cells as described previously⁴⁰ and mono-ubiquitinated at Lys119 in a reaction mixture that also contained 500 nM Uba1, 2 μM UbcH5c, 2 μM RING1B/BMI1 and 7.5 μM Ubiquitin. For ubiquitination of H2A K13/15, 1 μM of full length RNF168 was used. The reaction took place for 1 hour in reaction buffer (25 mM HEPES pH 7.5, 150 mM NaCl, 2 μM ZnCl₂, 5 mM DTT, 5 mM ATP and 3 mM MgCl₂) at 30°C. Reactions were terminated by depleting ATP using Apyrase (Sigma-aldrich). The DUB reaction was performed by addition of 50-100 nM BAP1 variant or BAP1/ASXL1^{DEU} variant at 30°C. Prior to the reaction the BAP1/ASXL1 complexes were allowed to form on ice for 10-30 minutes. Reaction were terminated by the addition of SDS-PAGE protein loading buffer and analyzed by Western blotting using anti-H2A (07-146, Millipore).

Reconstitution of nucleosome core particles

Recombinant nucleosome core particles were prepared as described previously³³. Xenopus histones and 167 bp widom 601 strong positioning sequence were used to reconstitute the core particles.

Ub-AMC enzymatic assays

Enzyme activity was followed as release of fluorescent AMC from the quenched Ub-AMC substrate, providing a direct read-out of DUB activity. Michealis-Menten parameters were

determined using 1 nM of enzyme either with or without 1 μ M of ASXL1 variant while varying the substrate concentration. Complexes were allowed to form for 30 minute on ice prior to the reaction. Initial rates were plotted against substrate concentration and fitted to the Michealis-Menten model using non-linear regression in Prism 6. In single concentration experiments, 1 nM of enzyme was allowed to react with 1 μ M of substrate. Activity was quantified by calculating the initial rates. For the inhibition assays 500 pM enzyme and 2 μ M of Ub-AMC was used while titration the non-hydrolyzable ubiquitinated H2A peptide starting from 200 μ M with 2-fold dilutions. IC50 values were obtained by fitting the data to the “log inhibitor vs normalized response” model in Prism6.

Synthesis Non-hydrolyzable H2A-ubiquitin conjugate

For the synthesis of non-hydrolyzable H2A-ubiquitin conjugates, an H2A peptide was prepared with the target lysine mutated to azidonorvaline. This peptide was subsequently coupled to a modified form of ubiquitin which has its C-terminal glycine mutated to propargylamine (Ub-Prg)³⁰. Both polypeptides were obtain through linear full-length synthesis²⁹. Ub-Prg was coupled to the azide-functionalized peptide under 8M urea denaturing conditions using a Cu(I)-catalyzed alkyne-azide cycloaddition (CuAAC, click reaction) to afford a non-hydrolysable triazole linked peptide-ubiquitin conjugate. This conjugate was purified using C18 reverse phase HPLC and gelfiltration.

H2A-peptide conjugate hydrolysis assay

Native H2A-peptide ubiquitin conjugates were chemically synthesized as described previously^{29,41}. Twenty μ M of conjugate was incubate with 100 nM of enzyme or enzyme complex in reaction buffer (25 mM HEPES pH 7.5, 150 mM NaCl and 5 mM DTT and incubated at 30 degrees Celsius. Reactions were terminated by the addition of protein loading buffer and analyzed by SDS-PAGE.

Band-shift assays

Band-shift assays were performed using native gel electrophoresis on 4–12% Pre-Cast Tris-Glycine gels (Life Technologies), pre-run for at least 1 h at 125 V in Novex Tris-Glycine buffer at 4 degrees Celsius. NCPs or monoubiquitinated NCPs (both 100 nM) were incubated with increasing amounts of BAP1 or ASXL1 variant or BAP1/ASXL1 variant and the gel was run for 90 min at 125 V at 4 dregrees Celsius. BAP1/ASXL1 complexes were allowed to form for 10-30 minutes on ice prior to electrophoresis. Bands were visualized by DNA staining with GelRed or uing the TAMRA signal in a ChemiDoc XRS instrument (Biorad).

Isothermal Titration Calorimetry

ITC experiments were performed in a VP-ITC Microcal calorimeter at 25°C. All proteins

were dialyzed to ITC buffer (25 mM HEPES pH7.5, 150 mM NaCl, 10% glycerol, 0.5 mM TCEP) prior to the experiment. Using 10 or 5 μ l injections, 30 μ M ASXL1^{DEU} was titrated into 13 μ M of BAP1 variant. Data were fitted to a one-site binding model using the manufacturer's Origin software.

Stopped-flow fluorescent polarization binding assay

Pre-steady state binding events between BAP1 (C91A) or BAP1(C91A)/ASXL1^{DEU} and NCPs monoubiquitinated with ^{TAMRA}Ub (^{TAMRA}Ub-NCPs) were monitored in stopped-flow fluorescent polarization experiments. Varying concentrations of BAP1 or complex were injected together 20 nM (final concentration) ^{TAMRA}Ub-NCPs after which fluorescent polarization was followed during 10 s. Association binding traces were fitted to a one-phase association model in Prism6 to obtain k_{obs} . The k_{obs} values were plotted against protein concentration to estimate k_{on} , k_{off} and K_D .

Supplemental information

Detailed methods, supplementary figures and tables can be found in the supplementary information section.

ACKNOWLEDGEMENTS

We thank B8 members for discussions and critical reading of the manuscript. We thank Jürg Müller for kindly providing ASXL1, ASXL2 and BAP1 cDNA; Farid El Oualid and Raymond Kooij for providing ubiquitin reagents. This work was supported by European Research Council advanced grant 249997, NWO-TOP to TKS, and an ECHO grant (nr. 700.58.011) from the Netherlands Organization for Scientific Research Chemical Sciences (NWO-CW) to HO.

AUTHOR CONTRIBUTIONS

DDS designed, performed and analyzed all experiments and wrote the manuscript. DDS and WJD expressed and purified all proteins. RE performed ubiquitin-conjugate synthesis and HO supervised ubiquitin-conjugate research. TKS supervised research and wrote the manuscript.

REFERENCES

1. Carbone, M. et al. BAP1 and cancer. *Nat. Rev. Cancer* 13, 153–9 (2013).
2. Harbour, J. W. et al. Frequent mutation of BAP1 in metastasizing uveal melanomas. *Science* 330, 1410–3 (2010).
3. Bott, M. et al. The nuclear deubiquitinase BAP1 is commonly inactivated by somatic mutations and 3p21.1 losses in malignant pleural mesothelioma. *Nat. Genet.* 43, 668–72 (2011).
4. Testa, J. R. et al. Germline BAP1 mutations predispose to malignant mesothelioma. *Nat. Genet.* 43, 1022

- 5 (2011).
5. Wiesner, T. et al. Germline mutations in BAP1 predispose to melanocytic tumors. *Nat. Genet.* 43, 1018–21 (2011).
 6. Goldstein, A. M. Germline BAP1 mutations and tumor susceptibility. *Nat. Genet.* 43, 925–6 (2011).
 7. Peña-Llopis, S. et al. BAP1 loss defines a new class of renal cell carcinoma. *Nat. Genet.* 44, 751–9 (2012).
 8. Dey, A. et al. Loss of the tumor suppressor BAP1 causes myeloid transformation. *Science* 337, 1541–6 (2012).
 9. Kandath, C. et al. Mutational landscape and significance across 12 major cancer types. *Nature* 502, 333–9 (2013).
 10. Yu, H. et al. Tumor suppressor and deubiquitinase BAP1 promotes DNA double-strand break repair. *Proc. Natl. Acad. Sci. U. S. A.* 111, 285–90 (2014).
 11. Lee, H.-S., Lee, S.-A., Hur, S.-K., Seo, J.-W. & Kwon, J. Stabilization and targeting of INO80 to replication forks by BAP1 during normal DNA synthesis. *Nat. Commun.* 5, 5128 (2014).
 12. Eletr, Z. M. & Wilkinson, K. D. An emerging model for BAP1's role in regulating cell cycle progression. *Cell Biochem. Biophys.* 60, 3–11 (2011).
 13. Misaghi, S. et al. Association of C-terminal ubiquitin hydrolase BRCA1-associated protein 1 with cell cycle regulator host cell factor 1. *Mol. Cell. Biol.* 29, 2181–92 (2009).
 14. Ji, Z. et al. The forkhead transcription factor FOXK2 acts as a chromatin targeting factor for the BAP1-containing histone deubiquitinase complex. *Nucleic Acids Res.* 42, 6232–42 (2014).
 15. Baymaz, H. I. et al. MBD5 and MBD6 interact with the human PR-DUB complex through their methyl-CpG-binding domain. *Proteomics* 14, 2179–89 (2014).
 16. Scheuermann, J. C. et al. Histone H2A deubiquitinase activity of the Polycomb repressive complex PR-DUB. *Nature* 465, 243–7 (2010).
 17. Gaytán de Ayala Alonso, A. et al. A genetic screen identifies novel polycomb group genes in *Drosophila*. *Genetics* 176, 2099–108 (2007).
 18. Katoh, M. Functional and cancer genomics of ASXL family members. *Br. J. Cancer* 109, 299–306 (2013).
 19. Hoischen, A. et al. De novo nonsense mutations in ASXL1 cause Bohring-Opitz syndrome. *Nat. Genet.* 43, 729–31 (2011).
 20. Sahtoe, D. D. et al. Mechanism of UCH-L5 Activation and Inhibition by DEUBAD Domains in RPN13 and INO80G. *Mol. Cell* 57, 887–900 (2015).
 21. VanderLinden, R. T. et al. Structural Basis for the Activation and Inhibition of the UCH37 Deubiquitylase. *Mol. Cell* 57, 901–11 (2015).
 22. Sowa, M. E., Bennett, E. J., Gygi, S. P. & Harper, J. W. Defining the human deubiquitinating enzyme interaction landscape. *Cell* 138, 389–403 (2009).
 23. Clague, M. J. et al. Deubiquitylases from genes to organism. *Physiol. Rev.* 93, 1289–315 (2013).
 24. Sanchez-Pulido, L., Kong, L. & Ponting, C. P. A common ancestry for BAP1 and Uch37 regulators. *Bioinformatics* 28, 1953–6 (2012).
 25. Aravind, L. & Iyer, L. M. The HARE-HTH and associated domains: novel modules in the coordination of epigenetic DNA and protein modifications. *Cell Cycle* 11, 119–31 (2012).
 26. Dang, L. C., Melandri, F. D. & Stein, R. L. Kinetic and mechanistic studies on the hydrolysis of ubiquitin C-terminal 7-amido-4-methylcoumarin by deubiquitinating enzymes. *Biochemistry* 37, 1868–79 (1998).
 27. Mattioli, F. et al. RNF168 ubiquitinates K13-15 on H2A/H2AX to drive DNA damage signaling. *Cell* 150,

- 1182–95 (2012).
28. Gatti, M. et al. A novel ubiquitin mark at the N-terminal tail of histone H2As targeted by RNF168 ubiquitin ligase. *Cell Cycle* 11, 2538–44 (2012).
 29. El Oualid, F. et al. Chemical synthesis of ubiquitin, ubiquitin-based probes, and diubiquitin. *Angew. Chem. Int. Ed. Engl.* 49, 10149–53 (2010).
 30. Ekkebus, R. et al. On terminal alkynes that can react with active-site cysteine nucleophiles in proteases. *J. Am. Chem. Soc.* 135, 2867–70 (2013).
 31. Shanmugham, A. et al. Nonhydrolyzable ubiquitin-isopeptide isosteres as deubiquitinating enzyme probes. *J. Am. Chem. Soc.* 132, 8834–5 (2010).
 32. Ventii, K. H. et al. BRCA1-associated protein-1 is a tumor suppressor that requires deubiquitinating activity and nuclear localization. *Cancer Res.* 68, 6953–62 (2008).
 33. Mattioli, F., Uckelmann, M., Sahtoe, D. D., van Dijk, W. J. & Sixma, T. K. The nucleosome acidic patch plays a critical role in RNF168-dependent ubiquitination of histone H2A. *Nat. Commun.* 5, 3291 (2014).
 34. McGinty, R. K., Henrici, R. C. & Tan, S. Crystal structure of the PRC1 ubiquitylation module bound to the nucleosome. *Nature* 514, 591–6 (2014).
 35. Kalashnikova, A. A., Porter-Goff, M. E., Muthurajan, U. M., Luger, K. & Hansen, J. C. The role of the nucleosome acidic patch in modulating higher order chromatin structure. *J. R. Soc. Interface* 10(82) (2013).
 36. Mashtalir, N. et al. Autodeubiquitination Protects the Tumor Suppressor BAP1 from Cytoplasmic Sequestration Mediated by the Atypical Ubiquitin Ligase UBE2O. *Mol. Cell* 54, 392–406 (2014).
 37. Luger, K., Rechsteiner, T. J. & Richmond, T. J. Expression and purification of recombinant histones and nucleosome reconstitution. *Methods Mol. Biol.* 119, 1–16 (1999).
 38. Dyer, P. N. et al. Reconstitution of nucleosome core particles from recombinant histones and DNA. *Methods Enzymol.* 375, 23–44 (2004).
 39. Lowary, P. T. & Widom, J. New DNA sequence rules for high affinity binding to histone octamer and sequence-directed nucleosome positioning. *J. Mol. Biol.* 276, 19–42 (1998).
 40. Buchwald, G. et al. Structure and E3-ligase activity of the Ring-Ring complex of polycomb proteins Bmi1 and Ring1b. *EMBO J.* 25, 2465–74 (2006).
 41. Geurink, P. P., El Oualid, F., Jonker, A., Hameed, D. S. & Ovaa, H. A general chemical ligation approach towards isopeptide-linked ubiquitin and ubiquitin-like assay reagents. *ChemBiochem* 13, 293–7 (2012).

Supplemental Information table of contents

Figure S1	104
Figure S2	104
Figure S3	105
Supplemental tables	106
Supplemental experimental procedures	107

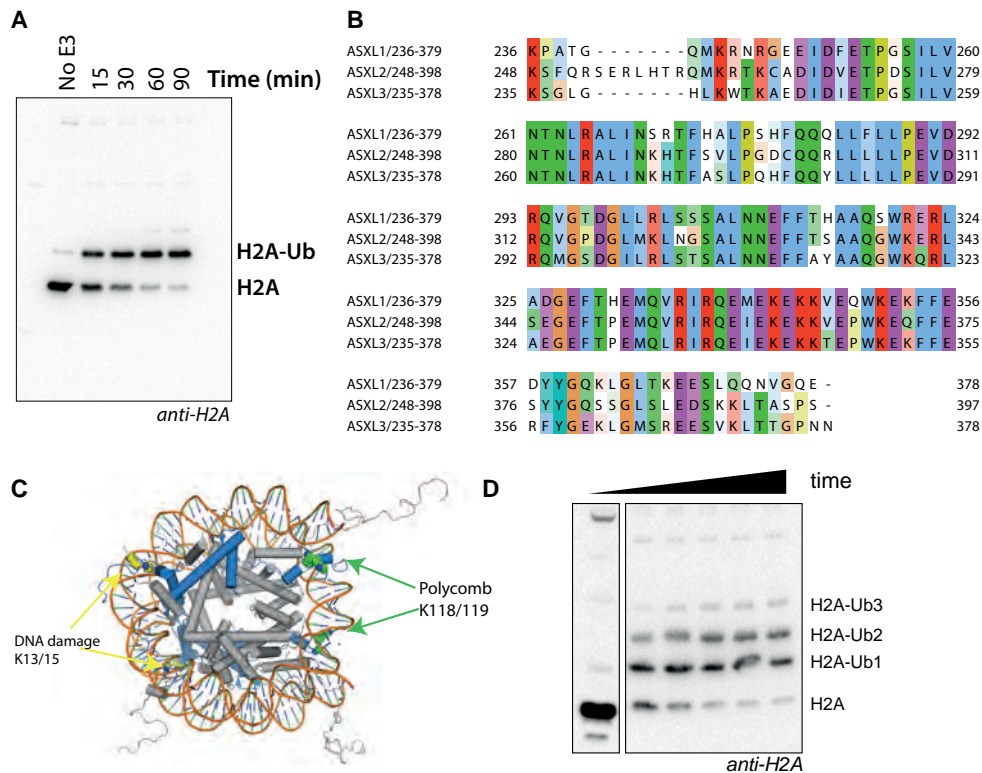
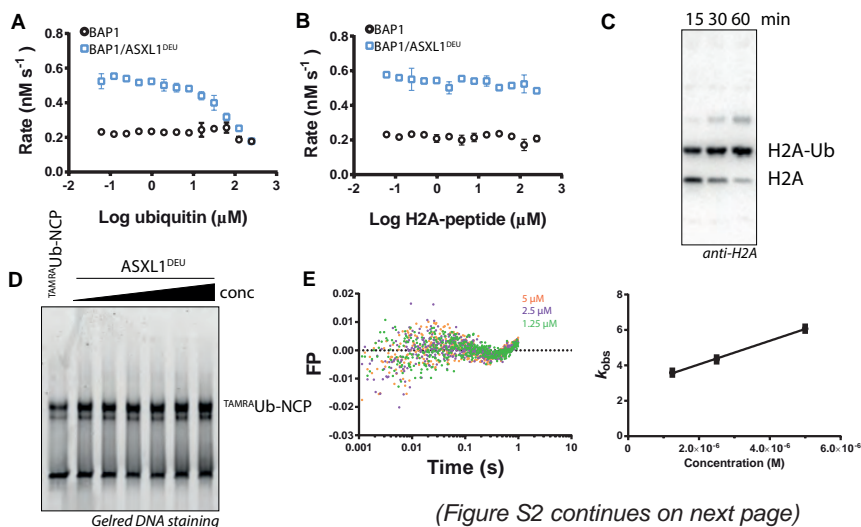


Figure S1 | ASXL DEUBAD domains stimulate H2A K119 deubiquitination by BAP1. A) Monoubiquitination of H2A K118/119 by full length Ring1b/Bmin. **B)** Multiple sequence alignment of the DEUBAD domains in ASXL1, ASXL2 and ASXL3. The sequence identity among the family members is >60%. **C)** The Polycomb (green spheres) and DNA damage (yellow spheres) ubiquitination sites on H2A (blue) are situated at distinct location in the nucleosome core particle (H2A in blue). **D)** Ubiquitination of lysine 13 and 15 by full length RNF168 (time points: 0, 15, 30, 45, 60, 90 min). Time point 0 was not adjacent to other time points on gel.



(Figure S2 continues on next page)

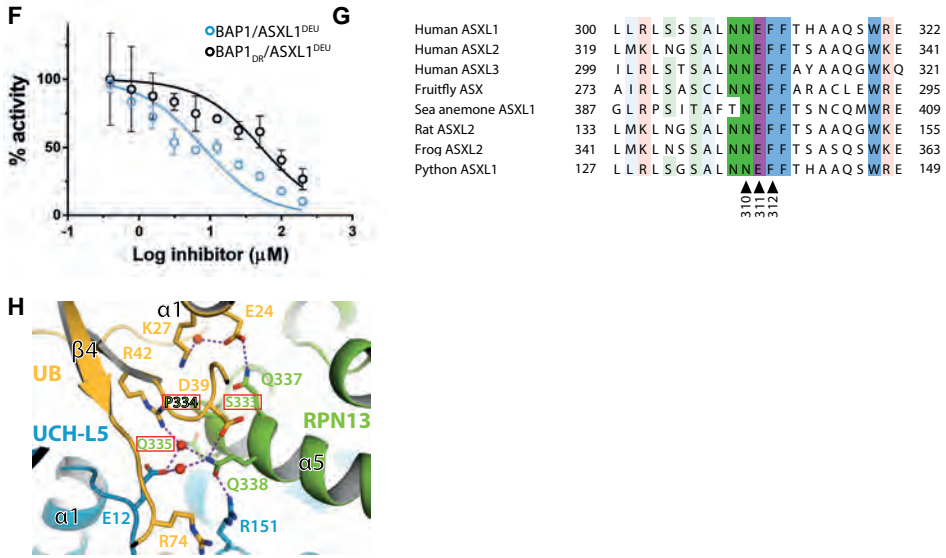


Figure S2 | Activation mechanism ASXL1^{DEU}. **A)** Ubiquitin alone does not inhibit BAP1 and mildly inhibits BAP1/ASXL1^{DEU} (blue). **B)** The C-terminal H2A peptide cannot inhibit BAP1 (black) nor the complex (blue). **C)** Monoubiquitination of H2A in nucleosome core particles with TAMRAUb by full length RING1B/BMI1. **D)** ASXL1^{DEU} cannot shift TAMRAUb-NCPs (concentration series is 2-fold dilution starting from 15 micromolar). **E)** Residuals and linear plot for binding of BAP1/ASXL1^{DEU} to TAMRAUb-NCPs in stopped-flow fluorescent polarization binding assays gives an approximate K_d of 4 micromolar. BAP1 alone data could not be fitted. **F)** BAP1^{DR}/ASXL1^{DEU} (black) has a higher IC₅₀ than the WT complex (blue) when inhibited by a non-hydrolyzable H2A-ubiquitin conjugate in Ub-AMC assays. **G)** The DEUBAD domains in the ASXL family are highly conserved around the "NEF" region. **H)** In the structure of UCH-L5 (blue) in complex with RPN13^{DEU} (green) and ubiquitin (yellow), the region equivalent to the ASXL1^{DEU} "NEF" region in RPN13^{DEU} (residues in boxes) contact ubiquitin.

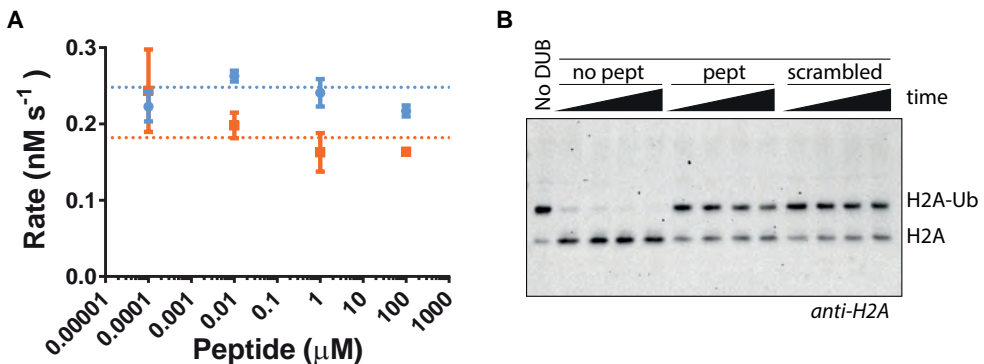


Figure S3 | A BAP1 CTE derived peptide does not inhibit intrinsic catalysis. **A)** The intrinsic enzymatic activities of full length BAP1 (orange) and BAP1₁₋₇₁₀ (blue) are not affected by various concentrations of the BAP1 C-terminal peptide in an Ub-AMC assay. Dotted lines represent the rate in absence of peptide. **B)** A scrambled peptide of the BAP1 C-terminus is also able to inhibit the activity of the complex. Time points (7.5, 15, 22.5, 30min). Concentration peptides was 100 μM.

SUPPLEMENTAL TABLES

Table 1 | Ub-AMC Enzyme kinetics parameters

	k_{cat} (s ⁻¹)			K_M (μM)			k_{cat}/K_M (M ⁻¹ s ⁻¹) * 10 ⁵
BAP1	2,5	±	0,2	5,9	±	1,1	4,2
BAP1/ASXL1 ^{DEU}	1,8	±	0,1	1,3	±	0,2	13,9
BAP1 ₁₋₇₁₀	1,6	±	0,1	3,1	±	0,6	5,2
BAP1 ₁₋₇₁₀ /ASXL1 ^{DEU}	1,6	±	0,1	0,5	±	0,1	32
BAP1/ASXL1 _{NEF} ^{DEU}	0,6	±	0,03	3,9	±	0,4	1,5
BAP1 _{DR} /ASXL1 ^{DEU}	4,6	±	0,3	2,9	±	0,4	16

Table 2 | ITC parameters binding experiments

Cell	Syringe	K_D (nM)	ΔH (kcal/mol)	$T\Delta S$ (kcal/mol)	N
BAP1	ASXL1 ^{DEU}	18	-49	-38	0.37
BAP1 ₁₋₇₁₀	ASXL1 ^{DEU}	5	-51	-40	0.27
BAP1 ₁₋₆₇₀	ASXL1 ^{DEU}	n/a	n/a	n/a	n/a
BAP1	ASXL1 _{NEF} ^{DEU}	46	-44	-34	0.32

Table 3 | IC₅₀ values for inhibition assays

	IC ₅₀ (μM)		
BAP1	45	±	0,1
BAP1/ASXL1 ^{DEU}	3,3	±	0,02
BAP1 _{DR} /ASXL1 ^{DEU}	52	±	0,1

SUPPLEMENTAL EXPERIMENTAL PROCEDURES

Plasmids and cloning

Full length cDNA's for BAP1 (uniprot Q92560), ASXL1 (uniprot Q8IXJ9) and ASXL2 (uniprot Q76L83) were kindly provided by Dr. Jürg Müller. cDNA for the ASXL3 DEUBAD domain (uniprot Q9C0F0) was purchased as a codon optimized gBlock (Integrated DNA Technologies). All constructs were cloned into expression vectors of the NKI Ligation Independent Cloning Suite¹. Full length BAP1, BAP1₁₋₇₁₀ and BAP1₁₋₆₇₀ were cloned into pFastBac-NKI-his-3C-LIC vector; BAP1₁₋₂₃₅ into pET-NKI-strepII-3C-LIC; ASXL1^{DEU}, ASXL2^{DEU}, ASXL3^{DEU} and ASXL1₁₋₃₉₀ into pET-NKI-his-3C-LIC (carbenicilin); and finally ASXL1^{HH} into pGEX-NKI-3C-LIC. All clones were verified by DNA sequencing.

Protein expression and purification

Full length BAP1, BAP1₁₋₇₁₀, BAP1₁₋₆₇₀, full length Ring1b/Bmi1 and their variants were expressed as His-tagged fusion constructs in Sf9 cells for 48-72 hours at 27°C, whereas His-ASXL1^{DEU} (aa 238-390), His-ASXL2^{DEU} (aa 261-380), His-ASXL3^{DEU} (aa 188-304), His-ASXL1₁₋₃₉₀, GST-ASXL1^{HH} (1-94), StepII-BAP1₁₋₂₃₅ and their variants were expressed in *Escherichia coli*. For bacterial expression, cell were grown to an OD of 0.6 at 37°C before inducing expression with 0.5 mM IPTG at 25°C for 4-6 hours. All cells were lysed by either bead beating or sonication using lysis buffer (50 mM Tris pH 8.0, 200 mM NaCl, 50 mM Imidazole pH 8.0, 0.5 mM TCEP) supplemented with complete EDTA-free protease inhibitor cocktail (Roche).

For the insect cell expressed constructs, cleared lysates were incubated with chelating sepharose beads (GE Healthcare) pre-charged with Ni²⁺. After washing with >15 column volume (CV) lysis buffer and elution with elution buffer (20 mM Tris pH 8.0, 150 mM NaCl, 500 mM Imidazole pH 8.0, 10% Glycerol and 0.5 mM TCEP), the sample was purified in anion exchange chromatography using Poros HQ resin (Applied Biosystems). A linear salt gradient from 0-75% buffer B (20 mM Tris pH 8.0, 1 M NaCl, 5% Glycerol, 0.5 mM TCEP) was used to elute the protein from the column that was previously equilibrated in buffer A (20 mM Tris pH 8.0, 50 mM NaCl, 5% Glycerol, 0.5 mM TCEP). As a final step, the sample was fractionated on a Superose6 (GE Healthcare) size exclusion chromatography (SEC) column for full length BAP1 and BAP1₁₋₇₁₀ or on a Superdex 200 SEC column for BAP1₁₋₆₇₀ in gel filtration buffer (10 mM HEPES pH 7.5, 150 mM NaCl, 10% Glycerol and 0.5 mM TCEP).

The BAP1 catalytic domain was purified using StrepTactin beads (GE Healthcare). After washing the beads with <10CV lysis buffer, protein was eluted with Strep elution buffer (20 mM Tris pH 8.0, 150 mM NaCl, 10% Glycerol, 2.5 mM Desthiobiotin and 0.5 mM TCEP). This was followed by a final SEC step using a Superdex 75 (GE Healthcare) equilibrated in

gel filtration buffer.

Cleared lysates of ASXL constructs were purified using His-tag affinity chromatography using chelating sepharose beads (GE Healthcare) pre-charged with Ni²⁺. After washing with >10 column volume (CV) lysis buffer and elution with elution buffer (20 mM Tris pH 8.0, 100 mM NaCl, 500 mM Imidazole pH 8.0, 10% Glycerol and 0.5 mM TCEP), the sample was purified in anion exchange chromatography using Poros HQ resin (Applied Biosystems) for the DEUBAD domains. A linear salt gradient from 0-75% buffer B (20 mM Tris pH 8.0, 1 M NaCl, 5% Glycerol, 0.5 mM TCEP) was used to elute the protein from the column that was previously equilibrated in buffer A (20 mM Tris pH 8.0, 50 mM NaCl, 5% Glycerol, 0.5 mM TCEP). For the ASXL1^{HH} and ASXL1₁₋₃₉₀ constructs, a cation exchange step using a Poros HS (Applied Biosystems) was introduced instead of the anion exchange step. Here, a linear salt gradient from 0-75% buffer B (20 mM Bis-Tris pH 6.5, 1 M NaCl, 5% Glycerol, 0.5 mM TCEP) was employed to elute the protein from the column that was previously equilibrated in buffer A (20 mM Bis-Tris pH 6.5, 50 mM NaCl, 5% Glycerol, 0.5 mM TCEP). The final step was SEC using a Superdex75 (GE Healthcare) column equilibrated in gel filtration buffer.

Full length RING1B/BMI1-his was lysed in 50 mM Tris pH8.0, 500 mM NaCl, 50 mM Imidazole pH 8.0, 10% Glycerol, 2 μM ZnCl₂ and 0.5 mM TCEP. The cleared lysate was incubated with chelating sepharose beads (GE Healthcare) pre-charged with Ni²⁺. After washing with >10 column volume (CV) lysis buffer and elution with elution buffer (50 mM Tris pH8.0, 500 mM NaCl, 500 mM Imidazole pH 8.0, 10% Glycerol, 2 μM ZnCl₂ and 0.5 mM TCEP). Hereafter, the sample was fractionated on a Superdex200 SEC column (GE Healthcare) in 10 mM HEPES pH 7.5, 400 mM NaCl, 10% Glycerol, 2 μM ZnCl₂ and 0.5 mM TCEP. Full length RNF168 was purified as described before². After SEC, all samples were concentrated using AMICON Ultra concentration columns (Millipore) to 2-20 mg/ml and flash frozen in liquid nitrogen.

Ub-AMC enzymatic assays

Enzyme activity was followed as the release of fluorescent AMC from the quenched Ub-AMC substrate, providing a direct read-out of DUB activity³. Ub-AMC was synthesized as described previously⁴. The purified Ub-AMC was dissolved in pure DMSO. The residual amount of DMSO left in the enzymatic reaction was never higher than 6%. Kinetic parameters were determined using 1 nM of enzyme while varying the substrate concentration in 30 μl reactions using reaction buffer (25 mM HEPES pH 7.5, 150 mM NaCl, 5 mM DTT and 0.05% Tween-20) at 25°C. Reactions took place in black 384-well non-binding surface low flange plates (Corning). In the single concentration experiments, 1 nM of enzyme was allowed to react with 1 μM of substrate and activity was quantified by calculating the initial rates. Experiments were performed in a Pherastar (BMG Labtechnologies) plate reader using

350 nm and 450 nm excitation and emission wavelengths respectively. Measurements were taken every 10 s for 10 minutes. Fluorescence and velocities were related using an AMC standard curve. The initial rates were plotted against substrate concentration and fitted to the Michealis-Menten model using non-linear regression in Prism 6. Three different independent experiments were performed with at least two different enzyme preparation.

For the inhibition assays, increasing concentrations of the non-hydrolyzable H2A ubiquitin conjugates were incubated with 500 pM enzyme and 2 μ M of substrate. Data were normalized by setting the no-inhibitor control at 100% activity. Inhibition data were fitted to a “log inhibitor vs. normalized response” model to obtain values for the IC₅₀ value in Prism 6.

Synthesis non-hydrolyzable H2A-Ub conjugates

The H2A derived peptide was obtained through standard linear Fmoc-based peptide synthesis on WANG resin. The target lysine in the peptide (K119) was substituted for Azidonorvaline (incorporated as Fmoc-azidonorvaline). Ubiquitin with a C-terminal propargyl (Ub-Prg) was obtained as described previously⁵. The Tris triazole ligand (tris(1-(O-ethylcarboxymethyl)-1H-1,2,3-triazol-4-ylmethyl)amine) used in the click reactions was synthesized as previously described⁶.

For the reaction to be successful it is important that the source of Cu(I) is pure and free of oxidized byproduct, Cu(II). CuBr was obtained in 99% purity and was a green/brown powder indicating traces of Cu(II). Cu(II)Br was suspended 10% v/v in high purity (glacial) acetic acid. This suspension was vigorously stirred under nitrogen overnight. After stirring overnight the suspension was filtered and the off-white residue separated from the greenish solution. The solid was washed with ethanol and dried under high vacuum. The obtained off-white powder was stored under inert atmosphere.

Both the functionalized H2A peptide and Ub-Prg dissolved in DMSO at 50 mg/ml and heated to facilitate solubilization. The peptide was dissolved in DMSO at 50 mg/ml and heated in case it failed to dissolve. Ub-Prg was dissolved in DMSO at 50 mg/ml and heated to make a proper solution. To 1 ml of 8M Urea (0.1M Phosphate Buffer pH 8), was added 100uL of Ub-Prg solution and 100 uL of peptide solution. After mixing the peptide and the ubiquitin the click solution was prepared.

A fresh solution of CuBr was prepared (20 mg/ml in Acetonitrile) and a stock solution of ligand (50 mg/ml in Acetonitrile) were used. 19.2 uL of CuBr solutions was added to 30uL of ligand solution. The Cu/Ligand solutions was then added in 5 equal steps to the

reaction mixture, each addition being vortexed and left for a few minutes before adding another 10uL of Cu/Ligand mix. The progression of the reaction was checked using LC-MS. After completion of the reaction 50uL of a 0.5M EDTA pH 7 solution was added to quench the reaction and dissolve remaining Cu(II) species. As a final step, The reaction mixture was applied directly to reversed phase HPLC for purification. Fractions were analysed for presence of product, pooled and lyophilized.

H2A-peptide-ubiquitin hydrolysis assays

Native ubiquitin conjugates were synthesized as described previously^{4,7}. Reactions were performed in reaction buffer (see above) at 30 degrees Celsius using 20 μ M of substrate and 50 nM of enzyme. Time points were taken and the reactions were terminated by the addition of protein loading buffer before analysis by SDS-PAGE. The experiments were performed at least three independent times.

Stopped-flow fluorescent polarization binding assays

Pre-steady state binding events between inactive mutants (C91A) of BAP1 or BAP1/ASXL1^{DEU} and NCPs monoubiquitinated with TAMRA-ubiquitin at K118/119 (^{TAMRA}Ub-NCP) by Ring1b/Bmi1 were monitored in stopped-flow fluorescent polarization experiments. The experiments were performed on a TgK Scientific stopped-flow system (model SF-61DX2) equipped with a photomultiplier tube R10699 (Hamamatsu). Monochromatic light at 544 nm and a 570 nm cutoff filter were used for excitation and readout, respectively. The light was polarized using a calcite prism for the incident beam and dichroic sheet polarizers in front of each of two photo-multiplier detectors arranged in a T-configuration.

The experiments were performed in stopped-flow binding buffer (25 mM HEPES pH 7.5, 150 mM NaCl, 0.05% Tween-20 and 0.5 mM TCEP) at 20°C. For the association 20 nM of ^{TAMRA}Ub-NCP (final concentration) and various concentrations of BAP1 or BAP1/ASXL1^{DEU} were injected in equal volumes and rapidly mixed after which FP signal was followed during 10 s. For each concentration 3 injections were averaged to improve signal. Association binding traces were fitted to a one-phase association model in Prism6 to obtain k_{obs} . The k_{obs} values were plotted against protein concentration to estimate k_{on} , k_{off} and $-K_D$. BAP1 association traces did not come close to saturation and were therefore not fitted.

Nucleosome core particle preparation

Recombinant nucleosome core particles were prepared as described previously⁸. Xenopus histones and 167 bp widom 601 strong positioning sequence were used to reconstitute the core particles.

Band shift assays

Band-shift assays were performed using native gel electrophoresis on 4–12% Pre-Cast

Tris-Glycine gels (Life Technologies), pre-run for at least 1 h at 125 V in Novex Tris-Glycine buffer at 4 degrees Celsius. NCPs or monoubiquitinated NCPs (both 100 nM) were incubated with increasing amounts (typically seven 2-fold dilutions starting from 15 μ M final concentration) of BAP1 or ASXL1 variant or BAP1/ASXL1 variant and the gel was run for 90 min at 125 V at 4 degrees Celsius. BAP1/ASXL1 complexes were allowed to form for 10-30 minutes on ice prior to electrophoresis. Bands were visualized by DNA staining with GelRed in a ChemiDoc XRS instrument (Biorad). The experiments were performed at least two times with different batches of NCPs.

Surface conservation DEUBAD domains

Twenty or more sequences across all eukaryotic lineages containing both UCH-L5 and RPN13 or INO80G were aligned using the MAFFT algorithm⁹ with default settings. PBD codes for the DEUBAD domains are 4uem and 4uf5. The structures of the DEUBAD domains were superimposed using pdbeFOLD¹¹.

SUPPLEMENTAL REFERENCES

1. Luna-Vargas, M. P. A. *et al.* Enabling high-throughput ligation-independent cloning and protein expression for the family of ubiquitin specific proteases. *J. Struct. Biol.* **175**, 113–119 (2011).
2. Mattioli, F. *et al.* RNF168 ubiquitinates K13-15 on H2A/H2AX to drive DNA damage signaling. *Cell* **150**, 1182–95 (2012).
3. Dang, L. C., Melandri, F. D. & Stein, R. L. Kinetic and mechanistic studies on the hydrolysis of ubiquitin C-terminal 7-amido-4-methylcoumarin by deubiquitinating enzymes. *Biochemistry* **37**, 1868–79 (1998).
4. El Oualid, F. *et al.* Chemical synthesis of ubiquitin, ubiquitin-based probes, and diubiquitin. *Angew. Chem. Int. Ed. Engl.* **49**, 10149–53 (2010).
5. Ekkebus, R. *et al.* On terminal alkynes that can react with active-site cysteine nucleophiles in proteases. *J. Am. Chem. Soc.* **135**, 2867–70 (2013).
6. Holger B. Kramer, J. M. C. & B. G. D. Tristriazole ligand for use in the Cu-Catalyzed [3+2] azide-alkyne cycloaddition on protein surfaces (doi:10.1038/nprot.2007.462). *Nature protocol exchange* (2007). at <<http://www.nature.com/protocolexchange/protocols/374>>
7. Geurink, P. P., El Oualid, F., Jonker, A., Hameed, D. S. & Ovaas, H. A general chemical ligation approach towards isopeptide-linked ubiquitin and ubiquitin-like assay reagents. *Chembiochem* **13**, 293–7 (2012).
8. Mattioli, F., Uckelmann, M., Sahtoe, D. D., van Dijk, W. J. & Sixma, T. K. The nucleosome acidic patch plays a critical role in RNF168-dependent ubiquitination of histone H2A. *Nat. Commun.* **5**, 3291 (2014).
9. Katoh, K. & Toh, H. Recent developments in the MAFFT multiple sequence alignment program. *Brief. Bioinform.* **9**, 286–98 (2008).
10. Ashkenazy, H., Erez, E., Martz, E., Pupko, T. & Ben-Tal, N. ConSurf 2010: calculating evolutionary conservation in sequence and structure of proteins and nucleic acids. *Nucleic Acids Res* **38**, W529–33 (2010).
11. Krissinel, E. & Henrick, K. Secondary-structure matching (SSM), a new tool for fast protein structure alignment in three dimensions. *Acta Crystallogr. D. Biol. Crystallogr.* **60**, 2256–68 (2004).

chapter | FIVE

Characterization of the oligomeric state of the BAP1/ASXL1 complex

Danny D. Sahtoe, Willem J. Van Dijk and Titia K. Sixma

*Division of Biochemistry and Cancer genomics center
Netherlands Cancer Institute, Plesmanlaan 121, 1066CX, Amsterdam, the Netherlands*

ABSTRACT

The deubiquitinating enzyme (DUB) BAP1 is a critical tumor suppressor that is activated by ASXL1 to remove ubiquitin from Histone 2A (H2A) K119 during Polycomb gene repression. The BAP1/ASXL1 complex consists of two BAP1 molecules but only one ASXL1 molecule. The functional consequences of this asymmetric stoichiometry are not understood. In this study, we characterize the oligomeric state of the BAP1/ASXL1 complex and investigate its possible relevance for DUB activity. We find that the full length BAP1 alone forms large oligomers via its C-terminal ULD domain and that truncation of this domain shifts the oligomeric state to a monomer dimer equilibrium. A single ASXL1 binds to a ULD domain and stabilizes BAP1 as dimer, to the 2:1 state. In this heterotrimeric BAP1/ASXL1 complex one ASXL1 molecule can stimulate both copies of BAP1 to deubiquitinate H2A. These results provide a basis for further studies on the role of BAP1 oligomeric states in enzymatic activity.

INTRODUCTION

BRCA-1 associated protein 1 (BAP1) is an important deubiquitinating enzyme (DUB) with tumor suppressor activity that is mutated in a wide variety of tumors^{1,2}. In these tumors both somatic and germ line mutations of BAP1 are found³⁻⁵ with individuals possessing germline mutations in BAP1 being predisposed to the BAP1 cancer syndrome⁶. In general BAP1 mutants in cancer are associated with poor prognosis and high tumor aggressiveness⁷. How BAP1 disruption contributes to tumorigenesis is not known.

Recent studies have revealed that BAP1 has important roles in key nuclear processes such as DNA repair, DNA replication and the regulation of gene expression^{4,8-12} and these are countered by an army of deubiquitinating enzymes (DUBs). In *Drosophila* BAP1 participates in gene regulation by being part of the evolutionarily conserved Polycomb Repressive DUB¹³ genetic studies identified more than 15 different PcG proteins that are required to repress homeotic (HOX). Polycomb gene repression is characterized by the mono-ubiquitination of H2A at K119 by the E3 ligase RING1B/BMI1¹⁴. BAP1 is responsible for the deubiquitination of mono-ubiquitinated H2A at K119. For this function BAP1 is activated by Polycomb protein ASXL1 and this deubiquitination event contributes to gene repression¹³.

BAP1 belongs to the UCH family of DUBs together with UCH-L1, UCH-L3 and UCH-L5. All these enzymes contain an N-terminal UCH domain whereas BAP1 and UCH-L5 also contain an C-terminal ULD domain. In UCH-L5 the ULD domain directly follows the UCH domain, but in BAP1 a 350 aa insert is present between its UCH and ULD domains. The ULD domains have important roles. In UCH-L5 the C-terminal helices of this domain bind the DEUBAD domain of activator RPN13, which subsequently restricts the mobility of the ULD to increase UCH-L5's affinity for ubiquitin¹⁵. This mechanism is conserved in the BAP1/ASXL1 complex, with the DEUBAD domain of ASXL1 employing a similar mechanism to increase BAP1's affinity for ubiquitin (Sahtoe et al, chapter 4). In addition to ASXL1, efficient H2A deubiquitination also requires recruitment of the complex to nucleosomes by the BAP1 C-terminal extension (CTE) (Sahtoe et al, chapter 4).

Studies on the stoichiometry of BAP1 have revealed a surprising asymmetry, the complex consists of two BAP1 molecules in complex with one ASXL1 molecule¹⁶. This is surprising since the homologous UCH-L5/RPN13 complex is equimolar, consisting of one UCH-L5 molecule bound to one RPN13 molecule¹⁵. Nonetheless UCH-L5 has previously been suggested to form functionally important higher order oligomers. Based on its crystal structure and biochemical analysis¹⁷⁻²⁰ it was proposed that UCH-L5 forms an inactive tetramer, via its ULD domain, that could be disrupted by RPN13 binding and thus activate the enzyme^{17,19}. However, this finding has never been confirmed in solution. For BAP1 it

is currently unknown whether the protein can form oligomers in isolation, and what the functional significance of the asymmetric BAP1/ASXL1 complex could be. For example, to deubiquitinate H2A a number of requirements need to be satisfied. BAP1 has to be recruited to the nucleosome by the CTE, BAP1 needs to bind ASXL1 and perform actual catalysis. How these functions are distributed over the subunits in the asymmetric complex is unclear.

5

In this study, we characterize the oligomeric states of BAP1 and the BAP1/ASXL1 complex. We demonstrate that BAP1 in isolation forms higher order oligomers driven by its ULD domain. Disruption of the ULD domain abrogates oligomer formation but instead promotes a monomer-dimer equilibrium, that is stabilized into the dimer state by binding of ASXL1. Using Ub-AMC assays we find that BAP1 truncation mutants that are deficient in higher order oligomerization, are probably not affected in enzymatic activity, in absence of ASXL1. Furthermore, we show that in the BAP1/ASXL1 complex, both BAP1 molecules are capable of H2A deubiquitination.

RESULTS

BAP1 can form dimers

To understand the functional consequences of the asymmetry of the BAP1/ASXL1^{DEU} complex, we first characterized the oligomeric states of BAP1 (MW=80 kDa) and ASXL1^{DEU} (MW=17 kDa) separately. We expressed full length (FL) BAP1 in insect cells and purified the protein to homogeneity. We noticed that in the final size exclusion chromatography (SEC) step BAP1 eluted from the column as a broad peak (Figure 1A) with a molecular weight of more than 440 kDa based on SEC calibration curves. Because the MW of a BAP1 monomer is 80 kDa, we conclude that our BAP1 sample forms a range of oligomers. Interestingly, the BAP1/ASXL1^{DEU} complex eluted from SEC-MALLS in a peak with an MW of 145 kDa (Figure 1B), in line with previous studies showing that it is not a stoichiometric 1:1 complex. The shift in oligomeric state when BAP1 is in complex with ASXL1^{DEU} suggests that ASXL1^{DEU} abolishes the propensity of BAP1 to oligomerize and favors a dimeric BAP1 form ASXL1^{DEU} itself was a monomer in MALLS analysis (Figure 1C).

Crystal structure and biophysical analyses have indicated that UCH-L5 can dimerize and tetramerize via its ULD (Figure 1D), but the biological significance of this phenomenon is unclear. We wondered whether the BAP1 C-terminal ULD could also mediate BAP1 oligomerization, and therefore we truncated BAP1 at residue 670 and expressed this variant in insect cells. This construct lacks the equivalent region in UCH-L5 that mediated tetramerization in the crystal structure¹⁷. In contrast to FL BAP1, the BAP1₁₋₆₇₀ variant (73 kDa), eluted as two peaks and at much lower molecular weight from SEC instead of one broad peak (Figure 1E). This suggests that this C-terminal ULD indeed mediates BAP1

oligomerization. Using MALLS we could show that these two peaks represent a monomer-dimer equilibrium (Figure 1E). The region responsible for the dimerization interface lies outside the BAP1 catalytic domain since this catalytic domain alone did not dimerize, but instead eluted as a single peak, with a mass equivalent to a monomer in MALLS analysis (Figure 1F). Deletion of the BAP1 CTE only, did not change the oligomeric state (data not shown).

To assess whether BAP1 oligomerization affects enzymatic activity, we analyzed the enzyme kinetics of different BAP1 constructs using the minimal substrate ubiquitin-7-amido-4-coumarin (Ub-AMC). In these assays BAP1₁₋₆₇₀ and the BAP1 catalytic domain (BAP1₁₋₂₃₅) had similar activity (Figure 1G). In comparison to FL BAP1, both constructs were more active. This difference was mainly mediated by k_{cat} and left K_M unaffected. We suspect that the effect in the truncation variants, is likely due to protein stability effects rather than an intrinsic difference in activity mediated by oligomeric state, since BAP1₁₋₆₇₀ and BAP1₁₋₂₃₅ are more stable than FL BAP1 during expression and purification.

In summary, we show that BAP1 forms a range of oligomers mediated by its C-terminal ULD region. ASXL1^{DEU} binding reorganizes the oligomeric state and activates the enzyme.

Functional analysis of BAP1/ASXL1^{DEU} asymmetry

Several questions arise from the observed asymmetry in the BAP1/ASXL1^{DEU} complex, especially regarding the task of each BAP1 molecule in H2A deubiquitination. First, are both BAP1 molecules functionally equivalent? Which BAP1 molecule binds ASXL1^{DEU}, and, is the BAP1 molecule that binds ASXL1^{DEU} also the molecule that is activated by ASXL1^{DEU} to deubiquitinate H2A (activation *in cis*). Or does ASXL1^{DEU} bind one molecule of BAP1 and activate the other (activation *in trans*) (Figure 2A)?

We have recently shown that the C-terminal extension (CTE) of BAP1 is necessary for binding to the nucleosome (Sahtoe et al, chapter 4). Since there are also two CTE's in the complex the number of options is even larger. Analogously to the activation, we can ask if the BAP1 that binds the nucleosome via the CTE is also the BAP1 molecule that performs the catalysis (nucleosome binding *in cis*) or instead, does one CTE binds the nucleosome and the other BAP1 molecule perform catalysis (nucleosome binding *in trans*) (Figure 2A)?

We investigated these possible scenarios by mixing different BAP1 variants and testing H2A DUB activity using purified oligonucleosomes that we mono-ubiquitinated at H2A K119. This allows reconstitution of specific "mixed" complexes and separation of functions for each BAP1 monomer in H2A deubiquitination reactions. For example mixing an excess of a FL BAP1 variant with an active site C91A mutation with a BAP1 variant

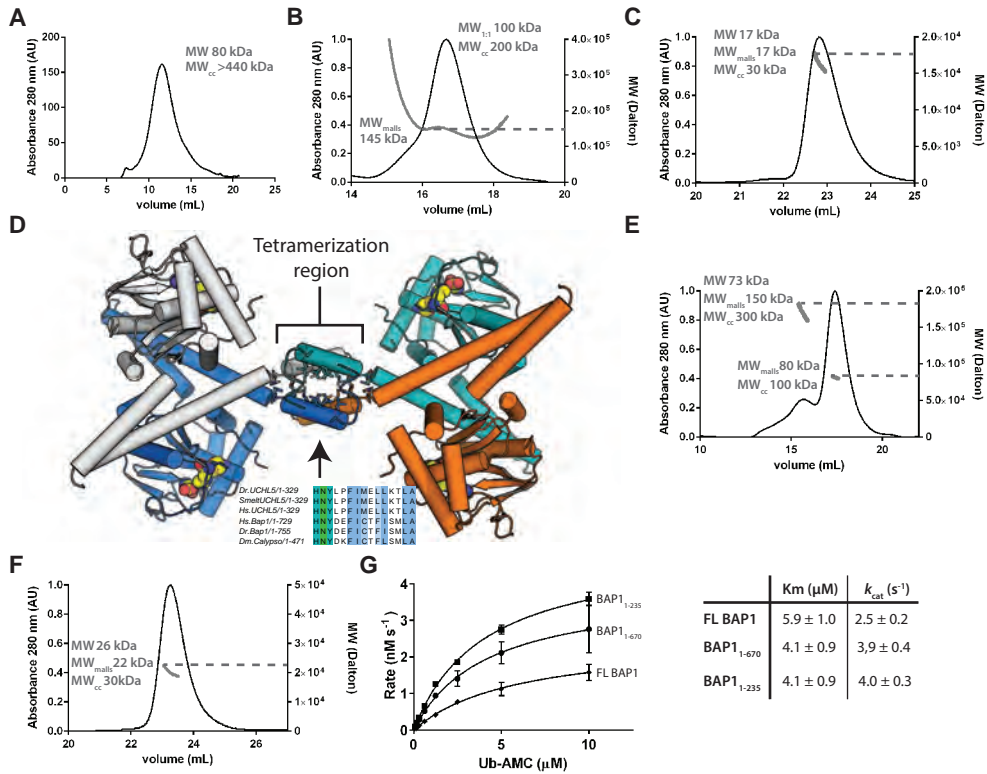


Figure 1 | Analysis oligomeric state BAP1/ASXL1. **A**) BAP1 elutes as a broad peak from size exclusion chromatography (SEC). The molecular weight of BAP1 based on calibration curve (MW_{cc}) is 440 kDa. Throughout this figure “MW” represents the molecular weight of a monomer, “MW_{cc}” the molecular weight based on the SEC calibration curve for globular shaped proteins, and “MW_{malls}” the molecular weight as measured by MALLS. **B**) The BAP1/ASXL1^{DEU} complex is not a 1:1 complex as shown by MALLS. **C**) ASXL1^{DEU} is monomeric with a MW of 17 kDa. **D**) Crystal structure of full length UCH-L5 (3ihr) shows tetramer that is mediated via a tetramerization region (arrow). **E**) Disruption of the region equivalent to the UCH-L5 tetramerization region in BAP1, shifts the BAP1 oligomer observed in FL to a monomer-dimer equilibrium as shown by MALLS. **F**) The BAP1 catalytic domain is monomeric in MALLS. **G**) The BAP1 catalytic domain and BAP1₁₋₆₇₀ are more active than WT BAP1 (Error bars, SD).

that cannot bind ASXL1^{DEU} and cannot bind the nucleosome (BAP1₁₋₆₇₀), would favor the formation of a BAP1_{C91A}-BAP1₁₋₆₇₀/ASXL1^{DEU} complex. In this complex ASXL1^{DEU} can only bind to FL BAP1_{C91A} since the other variant does not have an ASXL1^{DEU} binding site. Similarly nucleosome binding could only be conferred by FL BAP1_{C91A} since it is the only subunit with a CTE. Since this BAP1₁₋₆₇₀ variant is normally inactive on H2A (Sahtoe et al, chapter 4), any H2A deubiquitination activity would necessarily come from the BAP1₁₋₆₇₀ variant since the active site cysteine of the FL is mutated. This would indicate that ASXL1^{DEU} activates BAP1₁₋₆₇₀ *in trans*. We could indeed detect an increased DUB activity upon mixing of BAP1₁₋₆₇₀ with a 20 fold excess of BAP1_{C91A} and ASXL1^{DEU} suggesting that ASXL1^{DEU} mediated activation and nucleosome binding can both occur *in trans* (Figure 2B,

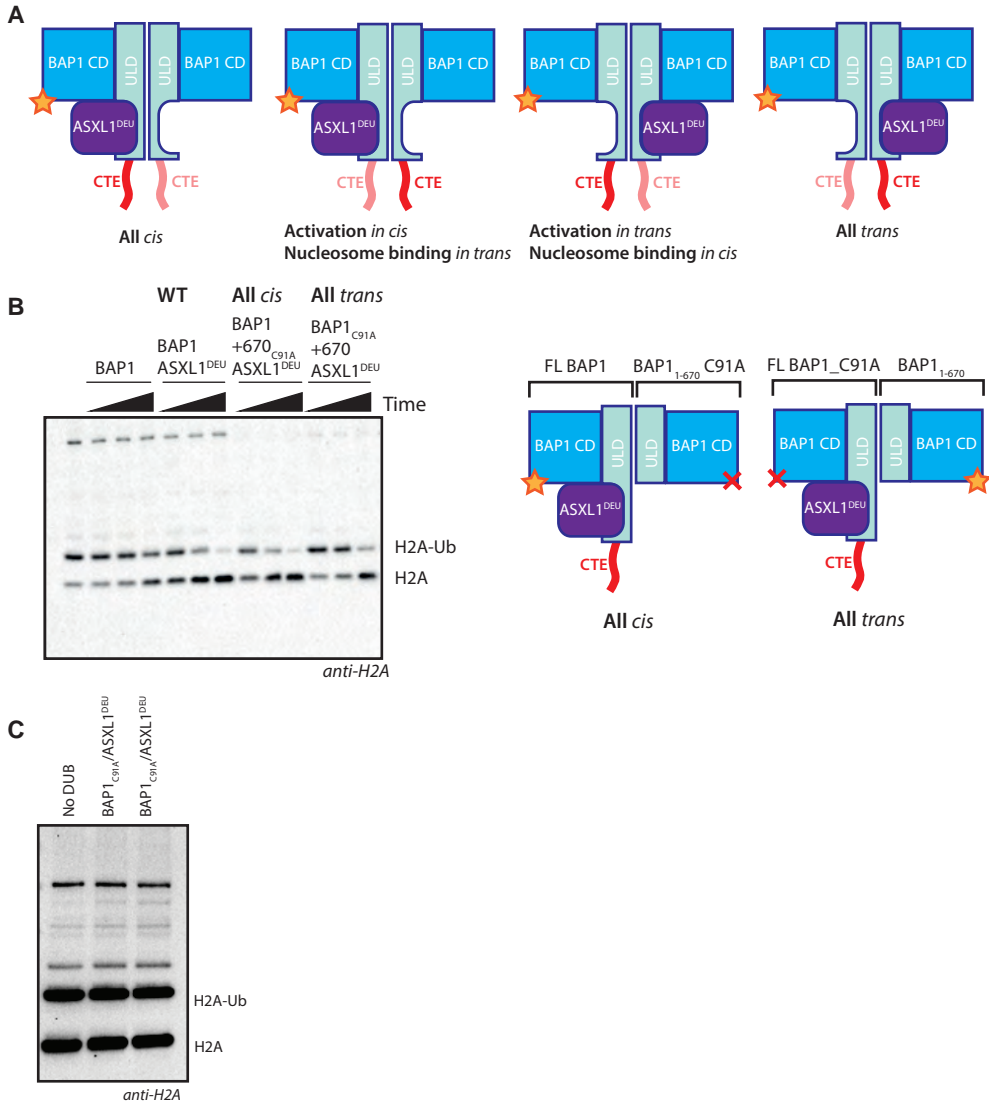


Figure 2 | Functional analysis BAP1/ASXL1 stoichiometry in H2A deubiquitination. A) Possible scenarios of ASXL1^{DEU} activation and nucleosome binding with respect to the BAP1 molecule that performs the DUB reaction (yellow star). The CTE that does not bind the nucleosome is faded. **B)** Left; Anti-H2A blot showing that both BAP1 molecules are capable of deubiquitinating H2A although WT and “all cis” complexes more active than the “in trans” complexes. Time points: 1, 5 and 25 min. Right; schematic depiction of reconstituted heterotrimeric mutant BAP1 complexes used in Figure 2A. Red cross represents the inactivate C91A mutants. **C)** Two preparations of BAP1C91A/ASXL1^{DEU} are not active on the substrate even after 25 minutes at 2 μM.

lanes 11-13) . This activity was not as effective however as the WT (Figure 2B, lanes 5-7) or all cis (Figure 2B, lanes 8-10) complexes.

After establishing that BAP1 activation by ASXL1^{DEU} as well as nucleosome binding can occur *in trans*, we wondered how this compared to “all *cis*” activity. To test this we mixed WT BAP1 with a 20-fold excess of a BAP1₁₋₆₇₀ variant containing an active site mutant (C91A) enabling the formation of a BAP1_{670,C91A}-BAP1/ASXL1^{DEU} complex. In this complex, any observed activity should be *in cis* as BAP1₁₋₆₇₀C91A does not have an active site, cannot bind ASXL1^{DEU} and lacks the CTE. This complex variant had similar activity to WT and was thus more active than the “all *trans*” variant. This may suggest that the physiological relevant activity mode is to have both activation by ASXL1^{DEU} and nucleosome binding *in cis*. The FL BAP1_{C91A}/ASXL1^{DEU} complexes by themselves were devoid of DUB activity when incubated with the substrate for 25 minutes at concentrations of 2 μM (Figure 2C).

In summary, our results suggest that both BAP1 molecules in the BAP1/ASXL1^{DEU} complex can be activated by ASXL1^{DEU} and bind to nucleosome. *In cis* activation and binding however seems to be more efficient suggesting that this is the primary mode of H2A deubiquitination.

DISCUSSION

Previous studies indicated that the BAP1/ASXL1 complex is asymmetric consisting of two BAP1 molecules and one ASXL1 molecule. In this study we characterized the oligomeric state of the BAP1/ASXL1^{DEU} complex and its possible relevance for H2A deubiquitination activity and find that *in vitro* both molecules can have H2A deubiquitination activity although only one BAP1 molecule is bound by ASXL1^{DEU}.

We showed that similar to the crystal structure of UCH-L5¹⁷, BAP1 can form high MW oligomers mediated by its C-terminal ULD domain. Disruption of this region redistributes the oligomers to a monomer-dimer equilibrium. For UCH-L5, the tetramerization was proposed to inhibit the enzyme since in this arrangement, the ubiquitin binding sites were blocked. Since the UCH-L5 activator, RPN13, binds to the tetramerization region, activation was suggested to merely prevent tetramerization. Since these UCH-L5 tetramers have not been observed in solution^{17,19,20} each of the catalytic domains was blocking the other's ubiquitin (Ub, it is not clear how important they are functionally). Moreover, deletion of the tetramerization region does not activate UCH-L5 to the same extent as RPN13, indicating that loss of tetramerization per se does not explain the activation of the enzyme. RPN13 instead mediates allosteric activation by positioning of the UCH-L5 cross-over loop and ULD domain^{15,20}.

Our results on the increased activity of BAP1 truncation mutants, that cannot oligomerize anymore, on the minimal substrate Ub-AMC suggested that unlike in UCH-L5, BAP1 oligomerization could inhibit enzyme activity (Figure 1G). Several observations indicate

that this is unlikely though. First the observed lower activity is at least partially due to the fact that FL BAP1 was expressed at lower levels and prone to time-dependent inactivation during purification. This is underscored by the fact that the difference between FL BAP1 and the truncation mutants is in k_{cat} . This value is very sensitive to the fraction of active enzyme in a mixture, and thus suggests that FL BAP1 is simply less stable than the truncation mutants. Second, if truncation of FL BAP1 would be enough for activation, the activation effect observed in the truncation mutants should affect the K_M of the BAP1/ASXL1^{DEU} complex (since ASXL1^{DEU} activates K_M) rather than k_{cat} .

Addition of ASXL1^{DEU} stabilized the BAP1 oligomer towards a 2:1 complex. By mixing different BAP1 variants we obtained results that suggest that both BAP1 variants in the complex can deubiquitinate H2A. This is interesting because of the inherent asymmetry in a 2:1 complex. Of special interest, is the observed *in trans* H2A deubiquitination. In this activity mode, the BAP1 molecule that does not bind the nucleosome and that does not bind ASXL1^{DEU} can be stimulated to deubiquitinate H2A albeit with lower efficiency than WT complexes and *in cis* activity. A question regarding the *all trans* activity mode is how binding of ASXL1 on one BAP1 molecule can stimulate the other BAP1 molecule. We speculate that ASXL1 may achieve this by increasing the affinity for ubiquitin through indirect stabilization of the ULD domain of the active BAP1 subunit. Enzyme kinetics experiments of the *in trans* complex could partially resolve this question by revealing whether the activation is on K_M .

Our variant BAP1/ASXL1^{DEU} complexes were reconstituted by mixing one BAP1 variant with an excess of another BAP1 molecule. This would ensure the incorporation of two BAP1 molecules of different type in one complex. Even though we have no direct evidence for the actual formation of such complexes via direct binding assays, the fact that we observed increased activity of the FL BAP1_{C91A}-BAP1₁₋₆₇₀/ASXL1^{DEU} complex compared to BAP1₁₋₆₇₀/ASXL1^{DEU}, strongly indicates that such complexes form. This is because BAP1₁₋₆₇₀ can only associate with ASXL1^{DEU}, and, can only be bound to nucleosomes in presence of an ASXL1^{DEU} binding region and CTE respectively, both of which BAP1₁₋₆₇₀ lacks. These elements can only be provided by complex formation of BAP1₁₋₆₇₀ with a FL BAP1 variant, in this case BAP1_{C91A}. Nonetheless additional direct controls are necessary for definitive proof of formation of such mixed complexes.

For the sake of simplicity we assumed a division of labor between the two BAP1 molecules with respect to nucleosome binding, ASXL1 binding and catalysis. It is however possible that both monomers contribute equally to H2A deubiquitination. What the relevance could be of the 2:1 stoichiometry remains to be discovered. Our results suggest that it does not generate a strict partition of functions (i.e. one BAP1 molecule performing catalysis and the other nucleosome binding). In fact, because the “*all cis*” activity mode

displayed activity close to WT, it is likely that one BAP1 molecule in the WT performs all H2A deubiquitination related functions. A possibility could be that the other BAP1 molecule then functions as an assembly platform for other proteins in one of the many multi-protein complexes that BAP1 is thought to form.

EXPERIMENTAL PROCEDURES

5

Molecular biology and antibodies

FL BAP1 and its variant except for the BAP1 CD were cloned into the pFastbac vector of the NKI LIC suite²¹ or pFastbac HTa (Invitrogen). BAP1 CD was cloned into the his-SUMO vector of the NKI LIC suite. ASXL1^{DEU} was cloned into the pET-NKI-his vector of the NKI LIC suite. Histone H2A in oligonucleosomes was visualized by western blotting using rabbit anti-H2A (07-146, Millipore).

Protein expression and purification

All BAP1 variants except for the catalytic domain BAP1 were expressed in insect cells using the Bac-to-Bac expression system (Invitrogen). BAP1 CD and ASXL1^{DEU} were expressed in *E. coli* using the pET expression system.

For all constructs, cells were resuspended in lysis buffer (50 mM Tris pH 8.0, 200 mM NaCl, 50 mM Imidazole pH 7.5, 0.5 mM TCEP) supplemented by complete EDTA-free protease inhibitor tablets (Roche) and lysed by sonication. Lysates were cleared by centrifugation and subsequently incubated with chelating sepharose beads (GE Healthcare) pre-charged with Ni²⁺ for 30 minutes after which beads were washed with typically 20CV of lysis buffer. The proteins were eluted using elution buffer (20 mM Tris pH 8.0, 150 mM NaCl, 500 mM Imidazole pH 7.5, 10% glycerol and 0.5 mM TCEP) and diluted 2-3 times before applying the sample to a Poros Q (GE Healthcare) anion exchange chromatography column equilibrated in 20 mM Tris pH 8.0, 50 mM NaCl, 5% glycerol and 0.5 mM TCEP. Samples were eluted by a linear salt gradient from 0% buffer B to 75% buffer B over 7-10CV, with buffer B containing 20 mM Tris pH 8.0, 1000 mM NaCl, 5% glycerol and 0.5 mM TCEP.

For BAP1CD and ASXL1^{DEU} the affinity tag was cleaved overnight with either SENP or 3C protease while dialyzing against 20 mM Tris pH 8.0, 150 mM NaCl, 10% glycerol and 0.5 mM TCEP. Uncleaved protein, SENP or 3C were captured using a reverse purification step on the affinity resin.

The final purification step for all proteins was a size exclusion chromatography (SEC) in 10 mM HEPES pH 7.5, 150 mM NaCl, 10% glycerol and 0.5 mM TCEP. FL BAP1 was purified on a Superose 6, BAP1₁₋₆₇₀ on a Superdex 200 and BAP1CD and ASXL1^{DEU} on a Superdex 75 SEC column (all GE Healthcare). Proteins were concentrated to 2-20 mg/ml

using AMICON concentration columns and flash-frozen in aliquots using liquid nitrogen for storage at -80 degrees Celsius.

Multi angle laser light scattering (MALLS)

MALLS experiments were performed on a Mini-Dawn light scattering detector (Wyatt Technology) coupled to a Superose 6, Superdex 200 10/30 or Superdex 75 10/30 column equilibrated in 25 mM HEPES pH 7.5 150 mM NaCl, 10% glycerol and 0.5 mM TCEP at 4 degrees Celsius. Refractive index and light scattering detectors were calibrated against toluene and BSA. Molecular weights were calculated using the manufacturer's Astra software.

Oligonucleosome deubiquitination assay

Oligonucleosomes were purified from HEK293T cells as described previously²² and mono-ubiquitinated at K119 using 3 μ M of the ubiquitin E3 ligase Ring1b/Bmi1 in a reaction that also contained 500 nM E1, 2 μ M UbcH5c and 7.5 μ M ubiquitin at 30 degrees Celsius for 90 minutes. The reaction was terminated by ATP depletion using the ATPase Apyrase (Sigma). DUB reactions were performed in 10 μ l reaction using 7.5 μ l of the ubiquitinated oligonucleosomes and 100 nM of DUB or DUB complex. DUB complexes were preincubated on ice for at least 15 min prior to addition of substrate. For reactions where different BAP1 variants were mixed, 2 μ M of excess of one DUB variant was used (indicated) while the other variant was kept at 100 nM. In these "mixed" reactions 2 μ M of ASXL1^{DEU} was used instead of 100 nM. DUB reactions were terminated by the addition of SDS-PAGE loading buffer before analysis by western blotting.

Ubiquitin-AMC enzyme kinetics assay

Enzyme activity was followed as the release of fluorescent AMC from the quenched Ub-AMC substrate, providing a direct read-out of DUB activity. Michealis-Menten parameters were determined using 1 nM of enzyme variant while varying the substrate concentration. Initial rates were plotted against substrate concentration and fitted to the Michealis-Menten model using non-linear regression in Prism 6.

REFERENCES

1. White, A. E. & Harper, J. W. Cancer. Emerging anatomy of the BAP1 tumor suppressor system. *Science* **337**, 1463–4 (2012).
2. Carbone, M. *et al.* BAP1 and cancer. *Nat. Rev. Cancer* **13**, 153–9 (2013).
3. Peña-Llopis, S. *et al.* BAP1 loss defines a new class of renal cell carcinoma. *Nat. Genet.* **44**, 751–9 (2012).
4. Dey, A. *et al.* Loss of the tumor suppressor BAP1 causes myeloid transformation. *Science* **337**, 1541–6 (2012).

5. Harbour, J. W. *et al.* Frequent mutation of BAP1 in metastasizing uveal melanomas. *Science* **330**, 1410–3 (2010).
6. Testa, J. R. *et al.* Germline BAP1 mutations predispose to malignant mesothelioma. *Nat. Genet.* **43**, 1022–5 (2011).
7. Kandath, C. *et al.* Mutational landscape and significance across 12 major cancer types. *Nature* **502**, 333–9 (2013).
8. Misaghi, S. *et al.* Association of C-terminal ubiquitin hydrolase BRCA1-associated protein 1 with cell cycle regulator host cell factor 1. *Mol. Cell. Biol.* **29**, 2181–92 (2009).
9. Yu, H. *et al.* The ubiquitin carboxyl hydrolase BAP1 forms a ternary complex with YY1 and HCF-1 and is a critical regulator of gene expression. *Mol. Cell. Biol.* **30**, 5071–85 (2010).
10. Yu, H. *et al.* Tumor suppressor and deubiquitinase BAP1 promotes DNA double-strand break repair. *Proc. Natl. Acad. Sci. U. S. A.* **111**, 285–90 (2014).
11. Ji, Z. *et al.* The forkhead transcription factor FOXK2 acts as a chromatin targeting factor for the BAP1-containing histone deubiquitinase complex. *Nucleic Acids Res.* **42**, 6232–42 (2014).
12. Lee, H.-S., Lee, S.-A., Hur, S.-K., Seo, J.-W. & Kwon, J. Stabilization and targeting of INO80 to replication forks by BAP1 during normal DNA synthesis. *Nat. Commun.* **5**, 5128 (2014).
13. Scheuermann, J. C. *et al.* Histone H2A deubiquitinase activity of the Polycomb repressive complex PR-DUB. *Nature* **465**, 243–7 (2010).
14. Wang, H. *et al.* Role of histone H2A ubiquitination in Polycomb silencing. *Nature* **431**, 873–8 (2004).
15. Sahtoe, D. D. *et al.* Mechanism of UCH-L5 Activation and Inhibition by DEUBAD Domains in RPN13 and INO80G. *Mol. Cell* **57**, 887–900 (2015).
16. Baymaz, H. I. *et al.* MBD5 and MBD6 interact with the human PR-DUB complex through their methyl-CpG-binding domain. *Proteomics* **14**, 2179–89 (2014).
17. Burgie, S. E., Bingman, C. a, Soni, A. B. & Phillips, G. N. Structural characterization of human Uch37. *Proteins* 649–654 (2011). doi:10.1002/prot.23147
18. Yao, T. *et al.* Proteasome recruitment and activation of the Uch37 deubiquitinating enzyme by Adrm1. *Nat. Cell Biol.* **8**, 994–1002 (2006).
19. Jiao, L. *et al.* Mechanism of the Rpn13-induced activation of Uch37. *Protein Cell* **5**, 616–30 (2014).
20. VanderLinden, R. T. *et al.* Structural Basis for the Activation and Inhibition of the UCH37 Deubiquitylase. *Mol. Cell* **57**, 901–11 (2015).
21. Luna-Vargas, M. P. A. *et al.* Enabling high-throughput ligation-independent cloning and protein expression for the family of ubiquitin specific proteases. *J. Struct. Biol.* **175**, 113–119 (2011).
22. Buchwald, G. *et al.* Structure and E3-ligase activity of the Ring-Ring complex of polycomb proteins Bmi1 and Ring1b. *EMBO J.* **25**, 2465–74 (2006).

chapter | SIX

6

General discussion

Deubiquitinating enzymes (DUBs) are key components of the ubiquitin-system. These enzymes hydrolyze the ubiquitin adducts and therefore control all processes affected by ubiquitination. To properly carry out this function their activities are tightly regulated by several factors in cells. Since the ubiquitin-system is often disrupted in human disease, DUBs hold a promise as “druggable” components of the system. A clear and detailed understanding of DUB function at the molecular level and in cellular context is required for the development of therapeutics. In this thesis, we described the different regulatory layers that exist for DUBs and investigated the molecular details of the regulation of the closely related DUBs UCH-L5 and BAP1.

DEUBAD domain regulation of BAP1 and UCH-L5

In chapters 3 and 4 we described how the enzymatic activities of the related DUBs UCH-L5 and BAP1 are modulated by DEUBiquitinase ADaptor (DEUBAD) domains present in their cognate regulatory proteins¹. Activity modulation by these domains takes place mainly at the level of substrate binding rather than at the level of catalysis as observed for other DUBs^{2,3}. Mechanistically the activation of UCH-L5 and BAP1 follow similar strategies. In both cases, the DEUBAD domains activate the DUB using a combination of mild allosteric effects. Our structural analysis indicates that UCH-L5 activity modulation is made possible by the intrinsic flexibility of structural elements such as the active-site cross over loop (CL) and the ULD domain. In absence of a regulatory protein, this flexibility generates a wide range of conformations of which some severely limit enzyme activity while others promote enzyme activity. It is likely that this conformational plasticity has been exploited in cells by the evolution of the DEUBAD domains of RPN13 and INO80G, which lock the ULD domain in conformations that either allow or block ubiquitin binding. While ULD domain conformation is affected by both RPN13 and INO80G, we observe that the conformation of the CL is only affected by RPN13 that directly binds and positions it. Mutational analysis indicated that disruption of this interface resulted in a weaker K_m suggesting that, like the ULD anchor mutant, stabilization of the CL by RPN13, increases ubiquitin binding. Interestingly however, we found that CL mutant complexes bind ubiquitin with the same affinity as WT complexes suggesting that the CL does not affect substrate binding but rather actual catalysis (k_{cat}). Further studies are required to elucidate the role of the CL in UCH enzyme catalysis.

The activation effects that we observe for BAP1 and, especially, UCH-L5, are not as dramatic as observed in other DUBs. In the latter set of DUBs, virtually no enzymatic activity is observed in isolation but they can be dramatically activated, in some cases several orders of magnitude, by activators. The milder activation of UCH-L5 and BAP1 in the presence of their cognate DEUBAD domains suggests that under physiological conditions additional factors may be present that further stabilize the active state of the DUB to yield full activity.

The requirement of multiple additional factors for full enzymatic activity has been well established for certain biochemical reactions. The mono-ubiquitination of the DNA sliding clamp PCNA for example by the Rad6/Rad18 complex is greatly enhanced when PCNA is loaded onto DNA by a sliding clamp loading complex, compared to the situation where PCNA is not loaded onto DNA. This example stresses the importance of studying complete “holoenzyme” complexes where all components that drive the reaction are present in the reaction mixture. Such activity enhancing factors may also exist for UCH-L5 and BAP1. Our minimal UCH-L5/RPN13 complex for example does not hydrolyze its natural substrate, K48 polyubiquitin chains. For this activity UCH-L5 needs to be embedded within the 19S proteasomal regulatory particle⁴. Future studies on UCH-L5 activity in the proteasome should be directed towards understanding this requirement by identifying stable (sub) complexes capable of chain hydrolysis.

While challenges still exist for UCH-L5's role in the proteasome, our structural analysis of the UCH-L5/INO80G complex, and the identification of a single point mutant that alleviates UCH-L5 inhibition, can provide novel insights into the still mysterious role of UCH-L5 in INO80 chromatin remodeling complexes. UCH-L5 is inhibited in these complexes, but both complex formation with INO80G and UCH-L5's catalytic activity are required to drive DNA end resection, suggesting that strict temporal regulation of UCH-L5 inhibition exists that ensures that the inhibition is alleviated when UCH-L5's DUB activity is required in the pathway⁵. Besides clarifying these issues, our point mutant can provide a unique opportunity to de-couple proteasome and INO80 related functions of UCH-L5 since this mutant is predicted to leave proteasome-associated function of UCH-L5 unaffected. In general, mutants identified *in vitro* that can de-couple different functions are instrumental for studying the functional relevance of certain steps in a reaction.

In contrast to the UCH-L5/RPN13 complex, the BAP1/ASXL1 DEUBAD complex is active on its natural substrate, H2A mono-ubiquitinated at K119⁶. We show in chapter 4 that this is made possible by the BAP1 C-terminal extension (CTE), an element unique to BAP1 and absent in UCH-L5. Whereas DUBs often require external factors to recruit substrates, the BAP1 CTE is one of the examples where the DUB itself can also recognize the target (nucleosome). This target recognition comes on top of the generic ability of DUBs to recognize ubiquitin and thereby increases the specificity for the substrate. Substrate specificity is a remarkable characteristic of the BAP1/ASXL1 complex as it can only deubiquitinate H2A ubiquitinated at K119 and not K13/15, the DNA damage response modification. BAP1 has a not fully understood role in DNA repair⁷, but our analysis rules out that the DEUBAD domain of ASXL1 can stimulate deubiquitination of K13/15 by BAP1. In cells other factors may exist though, that could confer K13/15 DUB activity to BAP1. How the specificity is achieved is unclear, but since the BAP1 CTE is involved in nucleosome binding, it seems

plausible that it has a role in determining specificity.

Even though the BAP1/ASXL1 is active on its natural substrate, it is however unclear if this activity reflects “holoenzyme” activity or whether additional factors exist that can further activate BAP1. This DUB is present in large multi-protein complexes with proteins such as, OGT, HCF-1, YY1, ASXL2, FOXK2, UBE2O, MBD5/6, KDM1A/B, where its catalytic activity is required to regulate gene expression programs^{8–12}. It is conceivable that in these complexes, some of the BAP1 partners can further stimulate its activity in addition to the stimulation by ASXL1.

6

The BAP1/ASXL1^{DEU} and UCH-L5/RPN13^{DEU} complexes share many features, but a major significant difference is the stoichiometry of the complex with the DEUBAD domain protein. While UCH-L5/RPN13^{DEU} is stoichiometric at 1:1, the BAP1/ASXL1^{DEU} complex consists of two BAP1 molecules in complex with one ASXL1^{DEU} molecule. The results obtained in chapter 5 suggest that both BAP1 molecules can be activated by ASXL1^{DEU} to deubiquitinate H2A. The presence of multiple DUB-like proteins in complexes occurs often in the JAMM class of DUBs. These DUBs are heterodimers consisting of an active and inactive JAMM DUB where the inactive variant stabilizes the active DUB and functions as a scaffold for the binding of additional proteins^{13–15}. Even though the relevance of the asymmetric stoichiometry of the BAP1/ASXL1^{DEU} complex is unclear, it is possible that one BAP1 variant similarly functions as an assembly platform for other proteins. Another possible explanation could be that the binding of one complex would facilitate the deubiquitination of both H2A proteins present in one nucleosome simultaneously, although it is questionable why this could be beneficial. A major focus in investigating the relevance of the BAP1/ASXL1^{DEU} stoichiometry for function would be to identify mutants that result in an obligate 1:1 BAP1/ASXL1^{DEU} complex and see how this affects BAP1 function.

Conserved architecture of DUB complexes

A curious aspect of a series of multi-protein DUB complexes is that they are present in a set of slightly different variants that play roles in separate pathways. The first example of this are the UCH-DEUBAD domain complexes studied in this thesis. Here, BAP1/ASXL1, UCH-L5/RPN13 and UCH-L5/INO80G form a UCH-DEUBAD DUB module that have roles in three very different cellular processes^{4,6,13–15}. This situation also occurs in other DUB families. In the USP family, USP1 and its most closely related paralogs USP12 and USP46 are all activated by proteins containing WD40 type β -propellers. All three DUBs are activated by UAF-1, and, USP12 and USP46 are moreover further activated by WDR20, a protein similar to UAF1^{16–18}. Some DUBs of the JAMM family exist in large architecturally similar molecular assemblies. BRCC36 is the catalytic subunit of the BRCA1-A and BRISC complexes^{19,20} and the DUBs CSN5 and RPN11 are present in the COP9 signalosome and proteasome

regulatory particle respectively^{21,22}. Many of the subunits are conserved across these four different complexes, suggesting that they share common regulatory themes. Even though the presence of multiple homologs is very common in eukaryotes, they often evolve to bind very different proteins and perform different functions.

In this light, the co-evolution of entire sets of molecular architectures, that occurred multiple times, for the DUBs discussed above is remarkable. It suggests that these molecular architectures exist because they are highly useful for cells and can be easily integrated into different pathways. This is further underscored by the elongation initiation factor 3 complex (eIF3) that regulates translation. This complex is devoid of DUB activity but shares its molecular architecture with the four JAMM complexes mentioned above²³.

DUBs regulatory mechanism are diverse

On a very basic biochemical level, DUB regulation can be defined as forces acting on actual catalysis (k_{cat}) or substrate binding (K_M or K_D). In chapter 2 we illustrate how these two regulatory modes manifest themselves in cells. We find that the manner by which the k_{cat} and K_M of DUBs are regulated are highly individual and diverse, suggesting that the regulatory modes are precisely tailored for each DUB. The diversity itself opens up avenues for future targeted therapy that is not directed towards active sites of DUBs but towards regulatory sites. This may be useful since active sites of DUBs are often highly conserved raising concerns regarding the specificity of active site inhibition. Crystal structure analysis would aid in the pursuit of therapies targeting regulatory sites, since it will reveal the details of the relevant complexes and thus serve as starting points for the development of inhibitors of specific protein-protein interactions. Together with the potentially powerful structure-based drug design methods, emerging fragment-based drug design methods will make all current and future structures invaluable sources of information²⁴.

A fundamental question in the DUB field is why so many DUBs are subject to tight regulation. A prevailing idea is that DUBs require tight regulation because they are relatively unspecific enzymes. This is because they are specialized in recognizing ubiquitin and can therefore potentially deubiquitinate the vast numbers of ubiquitinated proteins in a cell. Regulation, hence, aims at either providing specificity via recruitment factors and/or catalytic activation to DUBs. Stimulation of DUBs with low activity, is necessary since these enzymes display very low catalytic efficiencies (in the order of $10^3 \text{ M}^{-1} \text{ s}^{-1}$) when studied in isolation on minimal substrates²⁵. Interestingly, this is several orders of magnitudes lower than the average catalytic efficiencies ($10^5 \text{ M}^{-1} \text{ s}^{-1}$) found for other enzymes²⁶ and well below that of diffusion limited enzymes ($10^8\text{-}10^9 \text{ M}^{-1} \text{ s}^{-1}$)²⁶. This low activity may support a scenario that some DUBs were “actively” kept in a low activity state during evolution to protect cells from harmful unspecific deubiquitination. Tight co-

evolution of regulatory proteins hence evolved to provide sufficient activity modulation and specificity to allow deubiquitination of relevant substrates. It would be informative to know the catalytic properties of the ancestral DUB from which the “low activity” DUBs are derived, as has been done for other protein families^{27,28}. If this ancestral DUB was catalytically more proficient than extant DUBs, it would suggest that the extant DUBs were evolutionarily downgraded supporting the idea that DUB regulation emerged as a consequence of too high activity towards ubiquitin conjugates. Studying these aspects of DUB enzymology may result in a general better understanding of ubiquitin biology.

In summary our analyses of the regulation of the UCH class DUBs UCH-L5 and BAP1, two essential DUBs that are deregulated in multiple medical conditions, have highlighted remarkable allosteric regulatory modes that are associated with large conformational changes. These different conformations reflect the activity states of the DUBs, providing opportunities for the development of allosteric therapeutics. This work will provide a framework for future structural and cell based studies on these enzymes.

References

1. Sanchez-Pulido, L., Kong, L. & Ponting, C. P. A common ancestry for BAP1 and Uch37 regulators. *Bioinformatics* **28**, 1953–6 (2012).
2. Keusekotten, K. *et al.* OTULIN antagonizes LUBAC signaling by specifically hydrolyzing Met1-linked polyubiquitin. *Cell* **153**, 1312–26 (2013).
3. Cohn, M. A. *et al.* A UAF1-containing multisubunit protein complex regulates the Fanconi anemia pathway. *Mol. Cell* **28**, 786–97 (2007).
4. Yao, T. *et al.* Proteasome recruitment and activation of the Uch37 deubiquitinating enzyme by Adrm1. *Nat. Cell Biol.* **8**, 994–1002 (2006).
5. Nishi, R. *et al.* Systematic characterization of deubiquitylating enzymes for roles in maintaining genome integrity. *Nat. Cell Biol.* (2014). doi:10.1038/ncb3028
6. Scheuermann, J. C. *et al.* Histone H2A deubiquitinase activity of the Polycomb repressive complex PR-DUB. *Nature* **465**, 243–7 (2010).
7. Yu, H. *et al.* Tumor suppressor and deubiquitinase BAP1 promotes DNA double-strand break repair. *Proc. Natl. Acad. Sci. U. S. A.* **111**, 285–90 (2014).
8. Dey, A. *et al.* Loss of the tumor suppressor BAP1 causes myeloid transformation. *Science* **337**, 1541–6 (2012).
9. Misaghi, S. *et al.* Association of C-terminal ubiquitin hydrolase BRCA1-associated protein 1 with cell cycle regulator host cell factor 1. *Mol. Cell. Biol.* **29**, 2181–92 (2009).
10. Ji, Z. *et al.* The forkhead transcription factor FOXK2 acts as a chromatin targeting factor for the BAP1-containing histone deubiquitinase complex. *Nucleic Acids Res.* **42**, 6232–42 (2014).
11. Baymaz, H. I. *et al.* MBD5 and MBD6 interact with the human PR-DUB complex through their methyl-CpG-binding domain. *Proteomics* **14**, 2179–89 (2014).
12. Mashtalir, N. *et al.* Autodeubiquitination Protects the Tumor Suppressor BAP1 from Cytoplasmic Sequestration Mediated by the Atypical Ubiquitin Ligase UBE2O. *Mol. Cell* **54**, 392–406 (2014).

13. Yao, T. *et al.* Distinct modes of regulation of the Uch37 deubiquitinating enzyme in the proteasome and in the Ino80 chromatin-remodeling complex. *Mol. Cell* **31**, 909–17 (2008).
14. Qiu, X.-B. *et al.* hRpn13/ADRM1/GP110 is a novel proteasome subunit that binds the deubiquitinating enzyme, UCH37. *EMBO J.* **25**, 5742–53 (2006).
15. Hamazaki, J. *et al.* A novel proteasome interacting protein recruits the deubiquitinating enzyme UCH37 to 26S proteasomes. *EMBO J.* **25**, 4524–36 (2006).
16. Cohn, M. a, Kee, Y., Haas, W., Gygi, S. P. & D'Andrea, A. D. UAF1 is a subunit of multiple deubiquitinating enzyme complexes. *J. Biol. Chem.* **284**, 5343–51 (2009).
17. Cohn, M. A. *et al.* A UAF1-containing multisubunit protein complex regulates the Fanconi anemia pathway. *Mol. Cell* **28**, 786–97 (2007).
18. Kee, Y. *et al.* WDR20 regulates activity of the USP12 x UAF1 deubiquitinating enzyme complex. *J. Biol. Chem.* **285**, 11252–7 (2010).
19. Cooper, E. M. *et al.* K63-specific deubiquitination by two JAMM/MPN+ complexes: BRISC-associated Brcc36 and proteasomal Poh1. *EMBO J.* **28**, 621–31 (2009).
20. Sobhian, B. *et al.* RAP80 targets BRCA1 to specific ubiquitin structures at DNA damage sites. *Science* **316**, 1198–1202 (2007).
21. Cope, G. A. *et al.* Role of Predicted Metalloprotease Motif of Jab1 / Csn5 in Cleavage of Nedd8 from Cul1. *Science (80-)*. **298**, 608–611 (2002).
22. Worden, E. J., Padovani, C. & Martin, A. Structure of the Rpn11-Rpn8 dimer reveals mechanisms of substrate deubiquitination during proteasomal degradation. *Nat. Struct. Mol. Biol.* **21**, 220–7 (2014).
23. Enchev, R. I., Schreiber, A., Beuron, F. & Morris, E. P. Structural insights into the COP9 signalosome and its common architecture with the 26S proteasome lid and eIF3. *Structure* **18**, 518–27 (2010).
24. Lounnas, V. *et al.* Current progress in Structure-Based Rational Drug Design marks a new mindset in drug discovery. *Computational and Structural Biotechnology Journal* **5**, (2013).
25. Faesen, A. C. *et al.* The differential modulation of USP activity by internal regulatory domains, interactors and eight ubiquitin chain types. *Chem. Biol.* **18**, 1550–61 (2011).
26. Bar-Even, A. *et al.* The moderately efficient enzyme: Evolutionary and physicochemical trends shaping enzyme parameters. *Biochemistry* **50**, 4402–4410 (2011).
27. Thornton, J. W., Need, E. & Crews, D. Resurrecting the ancestral steroid receptor: ancient origin of estrogen signaling. *Science* **301**, 1714–1717 (2003).
28. Harms, M. J. & Thornton, J. W. Evolutionary biochemistry: revealing the historical and physical causes of protein properties. *Nat. Rev. Genet.* **14**, 559–71 (2013).

Addendum

&

Summary
Samenvatting
Curriculum Vitae
PhD portfolio
List of publications
Dankwoord

Summary

The covalent attachment of the small protein ubiquitin to target proteins, ubiquitination, is a major type of modification in cells. This modification can have a vast array of outcomes that allow cells to tightly control processes. Ubiquitination is reversed by deubiquitinating enzymes (DUBs) allowing these enzymes to regulate all processes affected by ubiquitination. Because of this powerful property, they themselves need to be kept in check by a variety of regulatory mechanisms that exist in cells.

In **chapter 2** we describe the currently known mechanisms of DUB regulation. These mechanisms are diverse and can be exerted from outside the DUB, by external factors or post-translational modifications, or from within DUBs by domains specialized in recruiting targets or activating the catalysis. The different types of regulation do not stand on their own though, but instead cooperate. This is exemplified by the fact that many DUBs are subject to multiple types of regulation simultaneously.

A particular type of DUBs that are regulated are ubiquitin C-terminal hydrolases (UCH) family. These enzymes are all characterized by an catalytic UCH domain responsible for the catalytic activity. The family members UCH-L5 and BAP1 also contain an additional ULD domain at their C-termini that is thought to be important for their regulation. For both proteins, the regulation is thought to be performed by proteins containing DEUBiquitinase ADaptor (DEUBAD) domains. BAP1 and UCH-L5 play important roles in basic cellular processes such as DNA repair and gene regulation and are mutated in several cancers.

UCH-L5 presents a remarkable case of DUB regulation since it can be activated by the DEUBAD domain of RPN13 but inhibited by the DEUBAD domain of INO80G. In **chapter 3** we show how this regulation works. Using crystal structure and functional analyses we demonstrate that RPN13 activates UCH-L5 by increasing the affinity for substrates through correct positioning of the ULD domain and active site cross over loop. Conversely, INO80G inhibits UCH-L5 by dramatically decreasing the affinity for substrates and achieves this by blocking the ubiquitin binding site via large conformational changes.

In **chapter 4** we investigate the mechanism of H2A deubiquitination by the BAP1/ASXL1 complex, a complex homologous to the UCH-L5/RPN13 complex. We show that the BAP1/ASXL1 complex specifically deubiquitinates the Polycomb site (K119) and is inactive on the DNA damage site (K13/15). Like RPN13, the DEUBAD domain of ASXL1 activates BAP1 H2A deubiquitination by increasing the affinity for the ubiquitinated substrate. Activation of BAP1 by the DEUBAD domain of ASXL1 is however not the only requirement to deubiquitinate nucleosomal H2A. This also requires the C-terminal extension of BAP1 that binds to nucleosomes.

An interesting feature of the BAP1/ASXL1 complex is that it is an asymmetric complex consisting of two molecules of BAP1 and one molecule of ASXL1. Moreover BAP1 itself forms homo-oligomers. In **chapter 5** we characterize the oligomeric state of BAP1 and the BAP1/ASXL1^{DEU} complex and examine the consequence of different oligomerization states on the enzymatic activity. We find that the C-terminal two helices of BAP1 promote higher order oligomerization and that ASXL1^{DEU} prevents this by promoting a 2:1 BAP1/ASXL1^{DEU} complex. We further show that in this complex both BAP1 molecule can be activated to deubiquitinate H2A despite the presence of only one ASXL1^{DEU} molecule.

We end with a general discussion presented in **chapter 6** where we place our findings in a broader context.



Samenvatting

De covalente modificatie van eiwitten met het kleine eiwit ubiquitine, genaamd ubiquitineren, is één van de meest voorkomende types modificaties in cellen. Ubiquitineren heeft een breed scala aan gevolgen en wordt door cellen gebruikt om processen te reguleren. Ubiquitineren wordt ongedaan gemaakt door de-ubiquitineringsenzymen (DUB's). Hierdoor zijn deze enzymen in staat om alle processen die betrokken zijn bij ubiquitineren te reguleren. Vanwege deze belangrijke functie, worden DUB's zelf ook streng gecontroleerd door talloze regulatiemechanismen die in cellen voorkomen.



In **hoofdstuk 2** beschrijven we de huidige bekende mechanismen van DUB-regulatie. Deze mechanismen zijn divers en kunnen uitgeoefend worden op DUB's van buiten het enzym door post-translationele modificatie, of vanuit het enzym zelf door bijvoorbeeld domeinen die gespecialiseerd zijn in het rekruteren van substraten, of door domeinen die katalyse direct kunnen stimuleren. De verschillende typen regulaties werken echter niet afzonderlijk van elkaar, maar kunnen samenwerken. Dit principe komt tot uiting door het feit dat veel DUB's gelijktijdig onderhevig zijn aan meerdere regulatietypes

Een bepaalde familie van DUB's die gereguleerd wordt is de ubiquitine C-terminale hydrolase familie. De aanwezigheid van een UCH-domein die verantwoordelijk is voor de katalytische activiteit karakteriseert deze enzymen, Familieleden UCH-L5 en BAP1 bevatten daarnaast ook nog een ULD-domein aan hun C-termini die als belangrijk wordt geacht voor hun regulering. Van beide enzymen wordt vermoed dat ze worden gereguleerd door eiwitten die DEUBiquitinase ADaptor (DEUBAD) domeinen bevatten. BAP1 en UCH-L5 zijn vaak gemuteerd in kanker en hebben belangrijke rollen in basale cellulaire processen zoals het herstellen van DNA-schade en genregulatie.

UCH-L5 is een speciaal geval van DUB-regulatie omdat het zowel geactiveerd kan worden, door het DEUBAD-domein van RPN13, als geremd kan worden, door het DEUBAD-domein van INO80G. In **hoofdstuk 3** laten we zien hoe deze regulering werkt. Met behulp van kristalstructuur en functionele analyses tonen we aan dat RPN13 UCH-L5 enerzijds activeert door de substraataffiniteit te verhogen via het correct positioneren van het ULD-domein en de active-site cross-over loop. INO80G remt UCH-L5 anderzijds, door de affiniteit voor substraten drastisch te verlagen en bereikt dit door het blokkeren van ubiquitine binding via grote, conformatie veranderingen.

In **hoofdstuk 4** onderzoeken we het mechanisme van H2A de-ubiquitineren door het BAP1/ASXL1-complex, een complex dat homoloog is aan het UCH-L5/RPN13-complex. We tonen aan dat het BAP1/ASXL1-complex specifiek de Polycomblocatie de-ubiquitineert (K119), en niet actief is op de DNA-schadelocatie (K13/15). Het DEUBAD-domein van ASXL1 activeert BAP1, net zoals bij RPN13, door de affiniteit voor substraten te ver-

hogen. Activatie van BAP1 door het DEUBAD-domein van ASXL1 is echter niet de enige voorwaarde om nucleosomaal H2A te de-ubiquitineren. Hiervoor is ook de C-terminale extensie van BAP1 nodig die nucleosoombinding mogelijk maakt.

Een interessante eigenschap van het BAP1/ASXL1-complex is dat het een asymmetrisch complex is bestaande uit twee BAP1-moleculen en één ASXL1-molecuul. BAP1 is bovendien zelf ook in staat om homo-oligomeren te vormen. In **hoofdstuk 5** karakteriseren we de oligomerische toestand van BAP1 en het BAP1/ASXL1-complex, en onderzoeken we de mogelijke gevolgen van de oligomerische toestand voor de enzymatische activiteit. We laten zien dat BAP1-oligomerisering wordt veroorzaakt door de twee C-terminale helixen van BAP1, en dat ASXL1 de neiging tot oligomerisering tegengaat door een 2:1 verhouding BAP1/ASXL1-complex te vormen. We laten verder zien dat in dat complex beide BAP-moleculen geactiveerd kunnen worden om H2A te de-ubiquitineren ondanks de aanwezigheid van slechts één ASXL1-molecuul.

We sluiten af met een algemene discussie in **hoofdstuk 6**, waar we onze bevindingen in een bredere context plaatsen.

Curriculum Vitae

Danny Dinesh Sahtoe werd geboren op 11 mei 1986 in Den Haag. In 2004 behaalde hij zijn VWO diploma aan het Atlas college te Rijswijk waarna hij in hetzelfde jaar begon aan de Bachelor opleiding biomedische wetenschappen aan de universiteit van Leiden. Als onderdeel hiervan deed hij onder begeleiding van Dr. Peter Bredenbeek een korte onderzoeksstage naar de rol van RNA stem-loop structuren in gele koorts virus infectie. Na het behalen van zijn Bachelor of Science in 2007 begon hij aan de master biomolecular science aan de vrije universiteit van Amsterdam. Tijdens deze periode deed hij stage-onderzoek naar de SUMOylering van transcriptiefactoren in de groep van Dr. David Baker aan het Leids universitair medisch centrum, en naar het mechanisme van PCNA ubiquitineren in de onderzoeksgroep van Prof.dr. Titia Sixma. Na voltooiing van zijn master in 2009 begon hij eveneens onder supervisie van Prof.dr. Titia Sixma aan zijn promotieonderzoek over deubiquitinerings enzymen op de afdeling Biochemie aan het Nederlands kanker instituut. De resultaten van dat onderzoek staan beschreven in dit proefschrift.



PhD portfolio

Summary of PhD training and teaching

Name PhD student: Danny Dinesh Sahtoe
 Erasmus MC Dept.: Genetics
 Research School: Onderzoekschool Oncologie Amsterdam
 PhD period: 2009-2015
 Promotor/Supervisor: Prof. dr. Titia K. Sixma

1. PhD training

Courses:

2011	OOA course, signal transduction, Amsterdam, the Netherlands
2012	British Crystallography Association, Summer school, Didcot, UK
2012	CCP4 crystallography study weekend, Warwick, UK
2014	Writing and presenting in biomedicine course, Amsterdam

Seminars and workshops:

2009-2015	NKI Research club seminars, Amsterdam (oral presentations)
2009-2015	Weekly division research meeting (oral presentations)
2009-2015	International NKI seminars, lunchmeetings with speakers
2015	Cancer genomics center annual meeting, Utrecht (oral presentation)

(Inter-)national conferences:

2009:	Annual meeting NWO studiegroep nucleïne-zuren, eiwitten en lipiden, Veldhoven
2010:	Rubicon ubiquitin meeting, Girona, Spain
2011:	The ubiquitin family, Cold spring harbor, United States
2012:	Annual meeting NWO studiegroep nucleïne-zuren, eiwitten en lipiden, Veldhoven (poster)
2013:	Annual meeting NWO studiegroep nucleïne-zuren, eiwitten en lipiden, Veldhoven (poster)
2014:	Benzon ubiquitin meeting, Copenhagen, Denmark (poster)
2015:	FOM Dutch biophysics meeting, Veldhoven

2. Teaching

Student intern supervision:

2012:	Supervision Master student
2013:	Supervision Bachelor student
2014:	Supervision Master student

Demonstrations:

2013:	Demonstration computational crystallography for Master and Bachelor students
2014:	Demonstration computational crystallography for Master and High-school students

List of publications

Mark P.A. Luna-Vargas, Evangelos Christodoulou, Andrea Alfieri, Willem J. van Dijk, Magda Stadnik, Richard G. Hibbert, **Danny D. Sahtoe**, Marcello Clerici, Valeria De Marco, Dene Littler, Patrick H.N. Celie, Titia K. Sixma, Anastassis Perrakis. *Enabling high-throughput ligation-independent cloning and protein expression for the family of ubiquitin specific proteases*. 2011, Journal of Structural Biology 175(2)113-119.

Francesca Mattioli, Michael Uckelmann, **Danny D. Sahtoe**, Willem J. van Dijk and Titia K. Sixma. *The nucleosome acidic patch plays a critical role in RNF168-dependent ubiquitination of histone H2A*. 2014, Nature Communications 5, 3291.

Danny D. Sahtoe, Willem J. van Dijk, Farid El Oualid, Reggy Ekkebus, Huib Ovaa and Titia K. Sixma. *Mechanism of UCH-L5 activation and inhibition by DEUBAD domains in RPN13 and INO80G*. 2015, Molecular Cell 57(5) 887-900.

Danny D. Sahtoe and Titia K. Sixma. *Layers of DUB regulation*. 2015, Trends in Biochemical Sciences 40(8)456-467.

Danny D. Sahtoe, Willem J. van Dijk, Reggy Ekkebus, Huib Ovaa and Titia K. Sixma. *BAP1/ASXL1 recruitment and activation for H2A Deubiquitination*. Manuscript submitted.



Dankwoord

Ik wil de mensen die hebben bijgedragen aan de voltooiing van mijn proefschrift hier bedanken. Ten eerste **Titia**. Bedankt dat ik in jouw lab heb mogen werken en voor de goede samenwerking. Ik heb enorm veel geleerd van jou en van de wetenschappelijke discussies.

Pim, bedankt voor je inzet en voor de velen preps die we hebben gedaan. Mede dankzij jou is dit proefschrift tot stand gekomen. **Patrick, Sasha** and **Tassos**, the wise men of B8, you have been a wealth of knowledge and I want to thank you for your help throughout the years.

I enjoyed working with all the people in the lab. First I want to thank the “old” B8 generation. **Fra, Judith, Rick, Kash, Alex** and **Mark**, thanks for advice and guidance in the early days of my PhD. **MC**, you have been a great mentor. I also want to thank you together with **Franzoos, Jens, Anas** and **Nicolas** for the good times outside of the lab. **Michael**, you are also in that list. Also thanks for being my paranimf and keep it up.

Flora, ik ben nu bijna weer net zo slim als jij, bedankt en veel succes. **Shreya** and **Robbert**, all the best with your PhD. **Herrie, Magda, John**, and **Tatjana**, together with Pim you are the engines of the lab, thanks for your efforts. **Robbie** and **Elli**, thanks for the help and advice with crystallography and refinement. **Willem**, bedankt voor het beantwoorden van mijn celbio vragen en veel succes. **Andrea**, many thanks for your illustrator tips and tricks, all the best. **Yoshi, Thanga, Nassos, Doreth, Luca** and **Bart**, all the best and good luck. **Caroline**, bedankt voor al je office managing. **Thijn** and the group members, **Jacqueline, Vincent, Joppe, Lucas, Mathijs, Markus, Sjoerd** and **Lisa**, keep up the awesome science.

I also want to thank the ubiquitin chemists **Huib, Paul, Farid, Reggy, Remco, Raymond** and **Darjath** for the good collaboration and your contributions.

Arun, bedankt dat je mijn paranimf bent. **Saadh**, bedankt voor het proeflezen ;). Ik wil verder nog de hele **Sahtoe-Rampersad** dynastie en de familie **Ramdass** bedanken voor jullie interesse in mijn werk, hopelijk is het nu ietsjes duidelijker.

Mijn grootste dank gaat uit naar het thuisfront, **Mama, Papa** en **Diana**.

Danny

